Dissertation zur Erlangung des Doktorgrades
der Fakultät für Chemie und Pharmazie
der Ludwig-Maximilians-Universität München

A high-throughput compatible cell-free protein fragment complementation assay monitoring viral protein interactions

Felicia Maria Wagner

aus

München, Deutschland

2012

Erklärung

Diese Dissertation wurde im Sinne von § 7 der Promotionsordnung vom 28. November 2011 von Herrn Prof. Ulrich Koszinowski betreut und von Herrn Prof. Karl-Peter Hopfner von der Fakultät für Chemie und Pharmazie vertreten.

Eidesstattliche Versicherung

Diese Dissertation wurde eigenständig und ohne unerlaubte Hilfe erarbeitet.

München, 19.07.2012

_____

Felicia Wagner

Dissertation eingereicht am 19.07.2012

1. Gutachter:	Prof. Dr. K.-P. Hopfner
2. Gutachter	Prof. Dr. U.H. Koszinowski

Mündliche Prüfung am 26.09.2012

Table of contents

Zusammenfassung

In gesunden Menschen führt eine Infektion mit dem humanen Cytomegalievirus (HCMV), wenn überhaupt, lediglich zu milden Symptomen. Jedoch stellt die anschließende lebenslange Latenz, Neuinfektionen oder die Reaktivierung aus der Latenz in immunsupprimierten Individuen ein schwerwiegendes Problem für das öffentliche Gesundheitswesen dar. Besonders betroffen sind dabei AIDS- und Transplantat-Patienten, sowie der sich entwickelnde Fötus, in denen ein Ausbruch einer CMV-Infektion zu einem lebensbedrohlichen Krankheitsbild führen kann. Da derzeit noch kein Impfstoff zur Verfügung steht, werden CMV-Infektionen medikamentös behandelt. Alle auf dem Markt befindlichen CMV-Medikamente sind gegen die virale Polymerase gerichtet und bringen das Problem der Langzeittoxizität und auftretender Resistenz mit sich. Aus diesen Gründen besteht großes Interesse an neuen anti-CMV Medikamenten, die gegen andere virale Zielstrukturen gerichtet sind. Essentielle virale Protein-Protein Interaktionen könnten solche potentiellen Targets darstellen.

Im Rahmen dieser Arbeit wurde ein Hochdurchsatzscreen etabliert, um Inhibitoren für die Interaktion zwischen den HCMV Proteinen pUL50 und pUL53 zu finden. Die Proteine interagieren direkt miteinander und sind Bestandteil eines Komplexes, der für den Kernaustritt des viralen Capsids essentiell ist. Der Hochdurchsatzscreen basierte dabei auf der Technik des Proteinfragment Complementations Assays (PCA), in dem zwei inaktive Proteinteile eines Reporterenzyms, in diesem Fall der N- und C-terminale Teil der TEM-1 β-lactamase von *E.coli*, an die entsprechenden interagierenden Proteine fusioniert werden. Die Interaktion der Proteine führt zur räumlichen Nähe der Reporterfragmente, die zur Faltung und Rekonstitution der Aktivität führt. Im Falle der Anwesenheit eines Inhibitors dieser Interaktion wird die aktive Form nicht oder nur vermindert gebildet. Um möglichst viele potentielle Inhibitoren kostengünstig und ohne Rücksicht auf zelltoxische Nebeneffekte testen zu können, wurden die Fusionsproteine in *E.coli* exprimiert, aufgereinigt und im Test von 4,000 chemischen Verbindungen kombiniert. Dabei wurden zwei strukturell verwandte Leitsubstanzen als direkte Inhibitoren der Interaktion von pUL50/pUL53 *in vitro* identifiziert.

Zusätzlich wurde ein weiterer spezifischer PCA, der die Interaktion der essentiellen HCMV Proteine pUL94/pUL99 im PCA System darstellt etabliert, um in späteren Hochdurchsatzscreens einen spezifischen Inhibitor für die sekundäre Umhüllung von HCMV identifizieren zu können.

Zusammenfassend berichtet die vorliegende Arbeit über die Etablierung eines neuen *in vitro* Proteinfragment Complementations Assays welcher sich als schnell, extrem spezifisch und deshalb geeignet für Hochdurchsatzscreens zeigte. Dieser Assay ist generell anwendbar und resultierte bereits in der Identifizierung einer Leitstruktur für die Inhibition des Kernaustrittskomplexes von HCMV.

Summary

Infection of healthy individuals with human cytomegalovirus (HCMV) is only associated with mild symptoms. However, the subsequently established life-long latency, primary infections or reactivation from latency in immunocompromised individuals demonstrate a severe public health problem. In particular, in patients with AIDS and transplant recipients as well as in the developing foetus, HCMV infections can cause fatal disease. Since there is still no vaccine available, human CMV infections are controlled by antiviral therapy. All currently licensed anti-CMV drugs target the viral polymerase and are accompanied by problems like long-time toxicity and the occurrence of resistance. Therefore, there is a major interest in new anti-CMV drugs affecting other viral targets. Essential viral protein-protein interactions could demonstrate such potential drug targets.

In this work, a high-throughput screen was established to identify inhibitors for the interaction of the HCMV proteins pUL50 and pUL53. The proteins directly bind to each other and are part of a complex which is crucial for the process of nuclear capsid egress. The high-throughput screen was thereby based on the technique of protein fragment complementation assay (PCA) in which two inactive fragments of a reporter protein, in this case the N- and C-terminal part of TEM-1 β-lactamase of *E.coli*, are fused to the corresponding interacting proteins. Interaction of the proteins leads to proximity of the reporter fragments, followed by proper folding and reconstitution of the reporter activity. In case of the presence of an inhibitor of the protein interaction the active reporter is not reconstituted or formed to a lower amount. In order to test many potential inhibitors in a cost effective way and regardless to cytotoxic side effects the fusion proteins were expressed in *E.coli*, purified and combined in a screen of 4,000 chemical compounds. Thereby, two structurally related lead compounds were identified as direct inhibitors of the pUL50/pUL53 interaction *in vitro*.

In addition, a further specific PCA monitoring the interaction of the essential HCMV proteins pUL94/pUL99 was established aiming a future high-throughput screening to identify specific inhibitors of the secondary envelopment of HCMV.

Collectively, the presented work reports about the establishment of a novel *in vitro* protein fragment complementation assay which appeared to be fast, extremely specific and therefore suitable for HTS. This assay is generally applicable and already resulted in identification of a lead structure for inhibition of the nuclear egress complex of HCMV.

1. Introduction

1.1 The family of *herpesviridae*

The family of *herpesviridae* (*gr.* herpein = creep) was initially classified by the unique architecture of the virion (see 1.1.1). To date, based on this morphological taxonomy, more than 200 herpesviruses have been identified in vertebrates including several human pathogens. The common feature of all herpesviruses is that in lytic infection their capsids assemble in the nucleus, whereas maturation and formation of infectious progeny takes place in the cytoplasm. Another general characteristic for all herpesviruses is the ability to establish a life long latency in the host. During latency no infectious viral particle can be detected. In the cells harbouring latent virus, viral genomes are maintained in a circular form and only a minimal viral gene expression takes place ensuring genome persistence.

On the basis of biological criteria such as host range, length of replication cycle and cell tropism, herpesviruses are classified into α-, β- and γ-herpesvirus subfamilies.

α-herpesviruses, with the most prominent members Herpes Simplex Virus 1 (HSV-1), HSV-2 and Varicella-Zoster Virus (VZV), are characterized by a broad host range and a short replication cycle with sensory ganglia as main target of infection. In contrast, long reproductive cycle, a broad cell tropism but strict species specificity qualifies the subfamily of β-herpesviruses including the genera of cytomegaloviruses (HCMV), muromegalovirus (MCMV) as well as the human herpesvirus 6 and human herpesvirus 7. γ-herpesviruses, where Kaposi-sarcoma-associated herpesvirus (KSHV) and Epstein-Barr virus (EBV) are the human representatives, infect preferentially cells of the lymphatic system, like T- and B-cells. However, the duration of their replication cycle varies drastically between species.

1.1.1 Virion structure

In general, a herpes virion contains a linear double-stranded DNA core in an icosahedral capsid, enveloped by an amorphous-appearing proteinaceous material called tegument layer, which is enclosed by a lipid bilayer embedding several viral glycoproteins (Figure 1). Mature herpesvirus particles (virions) vary in size from 120 to 260 nm depending on the thickness of their tegument and the state of the envelope.

The mature HCMV virion is 150-200 nm in diameter, and composed of a 100 nm large icosahedral capsid that is filled with a linear 230 kbp double-stranded DNA genome coding for approximately 200 genes (Streblow, 2006). Besides viral structural proteins, the tegument harbours viral and cellular mRNAs which can be translated immediately upon virus entry (Bresnahan and Shenk, 2000). A lytic HCMV infection produces three types of viral particles:

Infectious particles, non-infectious enveloped particles (NIEPs), which contain a capsid but no genome, and dense bodies (DBs), which are enveloped but lacking capsid and genome.

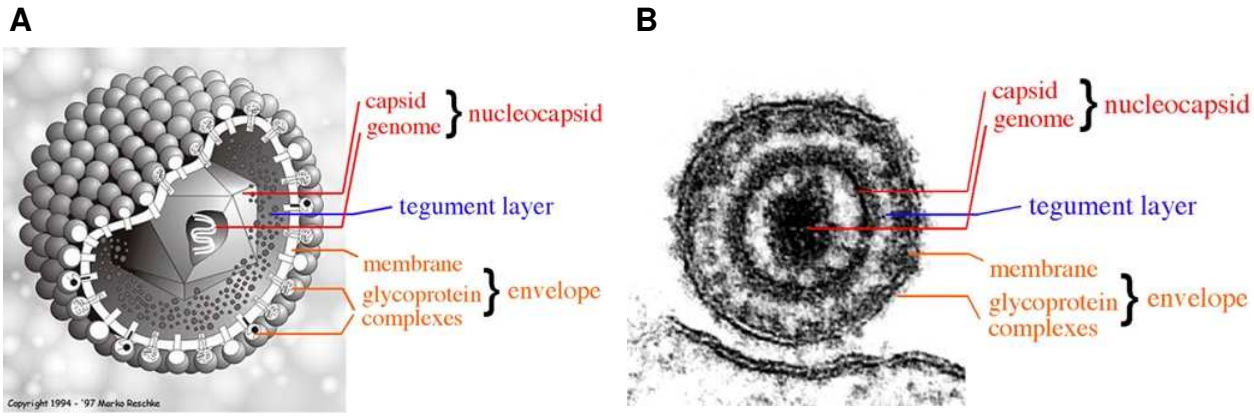

Figure 1: Virion structure of herpesviruses. **(A)** Schematic representation of a herpesvirus particle consisting of an icosahedral capsid encasing the viral genome, the surrounding tegument layer which is enveloped by the viral membrane in which different glycoproteins are embedded (Copyright Marko Reschke, University of Marburg). **(B)** Herpesviral particle detected by electron microscopy (Klupp et al., 2004).

1.1.2 Herpes virus replication cycle

Herpesvirus infection of a host cell starts by interaction of glycoproteins embedded in the viral envelope with receptors on the cellular surface (Spear and Longnecker, 2003). Entry then occurs by fusion of the plasma membrane with the virion envelope by an unknown mechanism and tegument constituents and the capsid are released into the cytoplasm (Figure 2). The capsid is transported along microtubules to the nuclear pores (Sodeik, Ebersold, and Helenius, 1997) where it docks and releases the viral DNA into the nucleus. Transcription of the viral genome occurs in consecutive phases resulting in immediate-early, early and late mRNAs. The latter mainly code for structural components like capsid- and tegument-constituents, which are translated in the cytoplasm and some are transported to the nucleus where the first part of the assembly process takes place. The viral genome replication leads to concatomeric DNA, which is cleaved into unit-length genomes upon packaging into the pre-formed capsids. These mature nuclear capsids (nucleocapsids) then need to be transported to the cytosol. In an early step of this transport process, called nuclear egress, the nucleocaspids bud at the inner nuclear membrane to get into the perinuclear space, thereby acquiring an envelope derived from the inner leaflet of the nuclear membrane. In a following step the primary envelope fuses with the outer leaflet of the nuclear membrane, resulting in loss of the primary envelope. In all herpesviruses the nuclear egress is governed by two viral proteins belonging to the UL31 and the UL34 family (see 1.3.2.1).
Naked capsids translocate into the cytoplasm, where they acquire their final tegument. Tegumented virus particles are assumed to be targeted to vesicles of the Golgi-apparatus

where they are finally enveloped (Sanchez et al., 2000). It is still unclear how tegumented particles reach the site of secondary envelopment and how viral glycoprotein assembly takes place, however it is suggested that proteins belonging to the UL11 and the UL16 family as well as their specific interaction are involved (chapter 1.3.1.2). Re-enveloped particles are retained in the vesicles and transported via the secretory pathway, where they fuse with the plasma membrane to release the virus particle into the extracellular compartment.

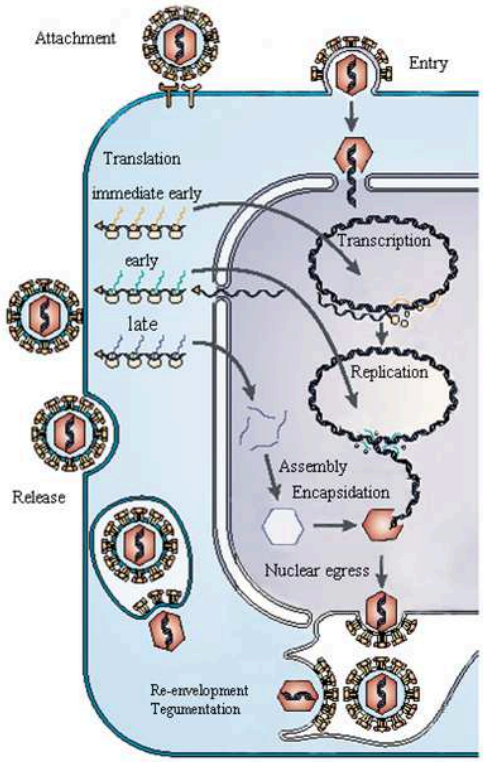

Figure 2: Replication cycle of herpeviruses
The virion absorbs via viral glycoproteins at special receptors on the cell surface. Fusion of the viral and cellular membrane is initiated and the viral capsid (red hexagons) is released into the cytoplasm and transported to the nuclear pores. The viral genome is released into the nucleus where it circularizes.
Three classes of viral genes (immediate-early, early and late) are transcribed chronologically and translated into proteins. Late proteins (blue) assemble to capsids, which incorporate newly synthesized viral DNA. DNA-filled capsids (nucleocapsids) leave the nucleus by budding at the inner nuclear membrane in the perinuclear space. Primary envelopment is lost by fusion with the outer nuclear membrane and capsids are released into the cytoplasm where final envelopment occurs by budding into special vesicles. The virion is released by exocytosis (Coen and Schaffer, 2003).

1.2 Human cytomegalovirus (HCMV)

Cytomegalovirus is an ubiquitous human β-herpesvirus, its systematic name is human herpesvirus type 5. Its common name was proposed by Weller in 1957 (Craig et al., 1957) to reflect both virus-induced cytopathic effects (syncytia formation resulting in large, multinucleated cells) and the role of the virus in congenitally acquired cytomegalic inclusion disease. HCMV can be found in 40% to 90% of human populations worldwide and is the most prevalent congenital transmitted virus. β-herpesviruses show high species specificity. Hence, human herpesviruses belonging to this subfamily are not suitable for studying the entire spectrum of their infection biology. Therefore closely related viruses of mice and guinea pigs and monkeys serve as animal model. Murine cytomegalovirus (MCMV) is the best studied animal model for HCMV showing significant similarities in their biology and

pathogenesis of infection, subsequent disease development and the establishment of latency (Brune, 2011; Hudson, 1979; Reddehase, Podlech, and Grzimek, 2002).

1.2.1 Clinical relevance

In immunocompetent individuals primary infection with HCMV is mostly asymptomatic resulting in a lifelong latent infection of the host. Reactivation of latency under certain conditions can be observed with or without clinical symptoms.

In contrast, HCMV is a highly relevant pathogen in individuals with innate, acquired or therapeutically induced immune deficiencies. In connately infected children who acquired the infection from their mother primary infected during pregnancy, HCMV induces cytomegalic inclusion disease. There is a remarkable variation between the phenotype of the resulting HCMV disease between the different patient groups, depending on the type of their underlying disease and the strength of the immunosuppression. In AIDS patients HCMV disease leads to retinitis and gastrointestinal ulcers (Jacobson et al., 1988), whereas in bone marrow/stem cell transplant or solid organ transplant patients it can result in pneumonitis, enteritis and viremia (Fishman and Rubin, 1998; Miller et al., 1986; Rubin, 2001). Around 2.5% of all newborns are infected with HCMV and 10% of infected children are already affected at birth, further 10% to 15% develop the symptoms later including severe neurological defects affecting the auditory system and/ or mental retardation (Harris et al., 1984; Neuberger et al., 2006; Ornoy and Diav-Citrin, 2006; Raynor, 1993; Rivera et al., 2002). In newborns, congenital CMV infection is the most common cause of non-hereditary hearing loss (Morton and Nance, 2006).

1.2.1.1 Vaccines

The major driving force behind the efforts to develop a HCMV vaccine is definitively the problem of the congenital HCMV infection. Although antiviral therapy in newborns with neurologic involvement shows some benefit in prevention of hearing deteriorations (Kimberlin et al., 2003), the success of the therapy is limited and the toxicity of available antiviral drugs are of concern. The economic costs of the society in caring for neurodevelopmental disability of children caused by congenital HCMV infection are a compelling argument for the Institute of Medicine to assign a vaccine to prevent CMV the highest priority (Stratton, 2001). Efforts were made over more than thirty years; however, no HCMV vaccine appears to be approaching imminent licensure up-to-date. The adaptive immune response, including humoral and T-cell mediated effector mechanisms, plays an important role in establishment of a long-lasting immunity, which serves to control HCMV reactivation and serious HCMV disease (Crough and Khanna, 2009). Trials with live, attenuated HCMV vaccines like the

laboratory-adapted clinical isolate, the Towne strain, resulted in neutralizing antibodies, as well as CD4+ and CD8+ T lymphocyte responses, which provided some protective impact on HCMV disease (Plotkin et al., 1994). However, a protection against infection, disease or reactivation was not assured. This was assumed to be caused by an over-attenuation resulting in an inadequate immune response following vaccination (Jacobson et al., 2006). Yet, the molecular basis of this apparent attenuation is still unclear. There are attempts going on in improvement of the immunogenicity of the Towne strain, but the concerns about potential risks of establishing a latent or persistent HCMV infection hindered the progress of live-attenuated vaccine studies. This stimulated the development of other vaccination strategies such as subunit or DNA vaccines. However, the HCMV vaccine development field still suffers from the lack of clarity specifying which HCMV features are indispensable and have to be included in the vaccine to result in a protective immunity (Schleiss, 2008).

1.2.1.2 Antiviral therapy of HCMV

Due to the lack of a vaccine, antiviral drugs for the treatment of HCMV infection and disease are of great importance but there are only a limited number of drugs which are licensed to date (reviewed in (Lischka and Zimmermann, 2008)). Still the designated gold standard is the nucleoside analog Ganciclovir (GCV) or its oral prodrug Valganciclovir (VGCV) (both Figure 3), respectively, which are selectively monophosphorylated by the viral kinase pUL97. Subsequently, they are converted by cellular kinases to triphosphate which targets the viral DNA polymerase. Its incorporation into the newly synthesized viral DNA strand leads to strand breaks and to substantial slow down of viral DNA synthesis. The same mode of action shows the broad-spectrum antiviral cidofovir (Figure 3) with the exception, that no initial phosphorylation step is required. Foscarnet (Figure 3) is a further HCMV drug targeting the DNA polymerase. It is a pyrophosphonate analog that directly binds to the pyrophosphonate binding site of the viral polymerase, thus preventing cleavage of the terminal pyrophosphate group of the growing DNA strain by product inhibition.

Although Acyclovir (not shown) or its oral prodrug Valacyclovir (VACV, Figure 3) have primarily been developed for the suppression of Herpes Simplex Virus (HSV), prophylactic use of VACV also showed the potency to reduce the incidence of HCMV disease (Lowance et al., 1999). Their mechanism of action is similar to GCV, however, it is a less efficient substrate for pUL97 than for HSV thymidine kinase. Therefore, VACV lacks sufficient potency to be used for the treatment of active infection and has only been approved for prophylaxis.

Fomivirsen (FOM) (not shown) is an antisense drug with a 21-nucleotide sequence complementary to the immediate early region 2 of CMV messenger ribonucleic acid. It is locally used in AIDS patients to treat cytomegalovirus retinitis.

The currently available drugs have considerable helped in the management of HCMV disease in immunocompromised patients. However, their use is limited due to toxicity, poor oral bioavailability, modest efficacy, and development of virus-drug resistance. Especially in the case of drug resistance, the drugs suffer from the fact that all except fomivirsen target the DNA polymerase, leading to cross-resistance, resulting in an urgent need of new drug targets.

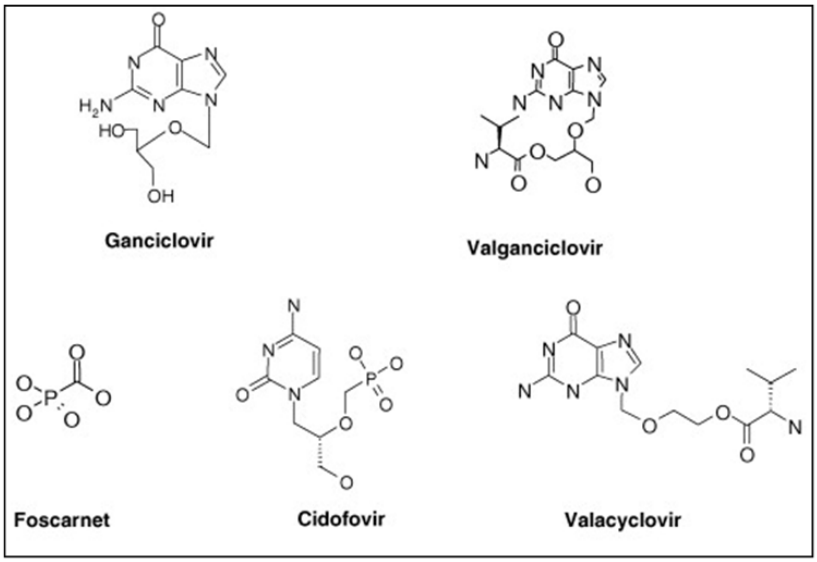

Figure 3: Chemical structures of approved anti-HCMV drugs. (Lischka and Zimmermann, 2008).

1.2.1.3 Current strategies in anti-HCMV drug development

There are several potential targets for pharmaceutical inhibition in the viral replication cycle, as virus attachment and entry, viral gene expression and DNA replication or in the steps of virus assembly and egress.

In a recent investigation for HCMV specific drugs (Melnik, Garry, and Morris, 2011) therapeutic peptides were studied targeting glycoprotein B (gB). gB is a highly conserved essential HCMV protein**,** that specifically promotes fusion of the viral envelope with the host cell. It was already shown in previous studies that synthetic peptides corresponding to or overlapping with these regions in viral fusion proteins sometimes serve as viral entry inhibitors (Akkarawongsa et al., 2009; Lambert et al., 1996; Sainz et al., 2006). These peptides have potential in the treatment of pregnant women as they show no statically significant toxicity.

Artesunate (ART), a semi-synthetic derivative of the natural product artemisinin, applies as a promising candidate in treatment of HCMV infections. It is in use in treating of severe malaria

(Adjuik et al., 2004; Gomes et al., 2008), but its antiviral activity against HCMV *in vivo* and *in vitro* could also be shown (Efferth et al., 2002; Kaptein et al., 2006). Though the antiviral mode of action of ART is not yet completely elucidated, the mechanism of inhibition seems to be unique as it interferes with HCMV at the very early stage of viral replication (Chou et al., 2011) likely by inhibition of pro-viral cell signalling process (Efferth et al., 2002; Efferth et al., 2008).

Recent targeted approaches for anti-HCMV drug development mainly concentrated on two promising novel drug targets: the viral terminase complex and the viral protein kinase pUL97. The terminase is a two-subunit enzyme that catalyzes cleavage and packaging of viral DNA (Bogner, 2002). Several different substances targeting this enzyme were discovered (e.g. BDRCRB, GW275175X, and BAY38-4766, AIC246) but due their inactivation *in vivo*, most of them did not reach phase II clinical trials (Lischka and Zimmermann, 2008). Only the 3,4-dihydro-quinazoline-4-yl-acetic acid derivative AIC246, which was shown to target the pUL56 subunit of the terminase (Goldner et al., 2011), was undergoing phase II evaluations and now enters clinical phase III.

Maribavir is a benimidazole-ribonucleoside derivative which targets the viral serine/threonine kinase pUL97, an enzyme that is involved in viral DNA synthesis and nuclear egress. Resistant strains also showed mutations in the UL27 gene, encoding a protein of unknown function. It was a very promising candidate with a favourable clinical safety profile and already entered phase III clinical trials. Since maribavir failed in a decisive phase III clinical trials, it is uncertain, if this drug will ever be licensed (ViroPharma, 2009a; ViroPharma, 2009b).

1.3 Approaches in drug development

In general, there are two different strategies in the process of drug discovery/development. The first, called rational drug design, requires the knowledge of the structure of either the basic molecule of a specific inhibitor (ligand based drug design) or of the three dimensional structure of the biological target (structure assisted drug design), which is obtained through methods such as x-ray crystallography or NMR. Most of the currently available anti-HCMV drugs mentioned in the previous chapter resulted from the ligand based approach, because their structures descend from the polymerase substrate. One example for structure-assisted drug design in the field of virology is the design of SARS-protease inhibitors. After the prediction of the structure by homology modelling (Anand et al., 2003) there was effort put into the design of inhibitory compounds (Yang et al., 2005). Rational drug design is a very hypothesis driven approach and once a compound is claimed *in silico,* it needs experimental

validation. Hit rates are expected to be low, but once it identifies a candidate it can be very effective to drastically shorten the discovery and optimisation process.

The other strategy in the process of drug discovery is high-throughput screening (HTS), wherein large libraries of chemicals are tested for their ability to inhibit a specific target (target-based) or variegate a distinct phenotype (phenotype-based). Whereas in the phenotype-based approach the substances are applied and analyzed in the context of living cells or tissue, in the target-based approach the effect of the test substances on the defined molecular target is investigated directly. Enzymes, protein-protein interactions or protein-DNA interactions can serve as defined biochemical targets. The effect of the substances on the target is displayed in HTS by assays like binding, enzyme activity or yeast two-hybrid (Y2H) based assays. For readout mostly biochemical methods can be applied, where a signal is measured as change in colour intensity, fluorescence or luminescence signal.

1.3.1 Protein-protein interactions as potential drug targets

Sustained investigations into protein-protein interactions have revealed their key role in regulating a wide range of cellular processes. Not surprisingly, many human diseases can be traced to abnormal protein-protein interactions involving endogenous proteins, proteins from pathogens or both (Ryan and Matthews, 2005). A variety of different approaches has been used to inhibit specific protein-protein interactions with the goal of developing therapies for different human diseases. Antibodies that block protein-protein interactions or sequester different members of a protein complex represent a strategy, because they tend to bind their target with high specificity and affinity. However, due to their large size, antibodies are not well suited to intracellular targets. Oligo-peptide inhibitors are a much smaller alternative, which can be very successful interfering with protein-protein interaction, though they suffer from instability *in vivo*. Therefore, the prospect of using small molecules to block interactions is attractive circumventing these pharmacological problems; however, this was also viewed with much scepticism considering biochemical aspects. It was expected that it would be difficult to specifically target interaction sites by a small molecule, which can be large and quite hydrophobic. However, progress in small molecule design and screening made this approach far more feasible (Pagliaro et al., 2004; Zhao and Chmielewski, 2005).

A prerequisite for the development of therapeutics against protein-protein interactions in disease is the basic understanding of complex formation by the targeted proteins. Knowledge about interaction partners or sites give are more detailed view on the comprehensive picture facilitating the decision for the later target and strategy of therapeutic development.

1.3.2 Essential intraviral protein interactions of HCMV as potential drug-targets

HCMV is the largest of the human herpesviruses composed of a 230 kbp DNA genome with a predicted coding capacity from 160 to more than 200 open reading frames (Murphy et al., 2003a; Murphy et al., 2003b). Cytomegalovirus genes can be grouped into two broad categories; those essential for replication in cell culture (core genes) and those dispensible for virus replication. BAC mutagenesis studies indicated 45 ORFs essential for viral replication in fibroblasts (Dunn et al., 2003). The infectious viral particle was shown to comprise of as many as 71 proteins (Varnum et al., 2004). Much of what is currently known about the intraviral protein-protein interactions of HCMV has been investigated by yeast-two hybrid analysis (Fossum et al., 2009; Phillips and Bresnahan, 2011b; To et al., 2011; Wood et al., 1997). Furthermore, a set of core interactions could be identified conserved throughout all herpesvirus subfamilies (Fossum et al., 2009; and see next chapters).

1.3.2.1 The pUL50/pUL53 interaction in the process of nuclear egress

The nuclear envelope of eukaryotic cells is composed of a double lipid-bilayer, the embedded nuclear pore complexes and an underlying nuclear lamina network. After assembly, nucleocapsids have to overcome the physical barrier of nuclear membranes and lamina because their size with around 120 nm exceeds the tolerated magnitude of transport machinery associated to the nuclear pore complexes (~39 nm) (Pante and Kann, 2002), generally mediating the transport between nucleus and cytoplasm. Therefore, herpesviruses developed a special mechanism for the nuclear capsid export akin to that which was recently elucidated for large RNP granules during synaptic Wnt signalling (Speese et al., 2012). In the first step of nuclear egress, capsids bud at the inner nuclear membrane into the perinuclear space by acquiring an envelope (Darlington and Moss, 1968). In this process two viral proteins that form a complex at the nuclear envelope, referred to as the nuclear egress complex (NEC), have been shown to be crucial (Figure 4A). Throughout the alpha, beta, and gamma herpesviruses, highly conserved homologs of these two proteins are found to form an NEC at the nuclear rim in all studied cases (Bubeck et al., 2004; Fuchs et al., 2002; Gonnella et al., 2005; Lake and Hutt-Fletcher, 2004; Lotzerich, Ruzsics, and Koszinowski, 2006; Reynolds et al., 2001; Yamauchi et al., 2001) and are assigned to the pUL34 and pUL31 herpesviral protein families. The corresponding representatives of these two proteins in HCMV are called pUL50 and pUL53 and have been categorized as essential for virus replication (Dunn et al., 2003; Yu, Silva, and Shenk, 2003). pUL50 and its homologs in the pUL34 protein family are type II C-terminally anchored membrane proteins, which reside primarily at the nuclear envelope (Shiba et al., 2000) and are expressed in the early to late phase of infection. Proteins of the pUL31 family, including pUL53, are expressed late in

infection and harbour an N-terminal nuclear localization signal (Lotzerich, Ruzsics, and Koszinowski, 2006). In absence of its partner pUL53 is localized in the nucleosol but upon co-expression of pUL50, pUL53 is recruited to the nuclear rim (Dal Monte et al., 2002). It was shown that pUL50 directly interacts with pUL53 (Milbradt, Auerochs, and Marschall, 2007; Sam et al., 2009) as it is also observed for their homologous proteins in MCMV, HSV, PrV and Epstein-Barr virus (Bubeck et al., 2004; Fuchs et al., 2002; Gonnella et al., 2005; Lake and Hutt-Fletcher, 2004; Lotzerich, Ruzsics, and Koszinowski, 2006; Reynolds et al., 2001; Yamauchi et al., 2001). Binding sites of heterodimerization were predicted as small linear motifs in the proteins (Figure 4B) (Lotzerich, Ruzsics, and Koszinowski, 2006; Sam et al., 2009). The complex is supposed to be involved in lamina destabilization (Reynolds, Liang, and Baines, 2004). Remarkably, in cells stably co-expressing the pUL31 and pUL34 of PrV, the NEC is capable of remodelling the nuclear membrane to form vesicles resembling the primary enveloped particles during infection in absence of any other viral protein (Klupp et al., 2007). It is postulated that lamina distortion is dependant on the phosphorylation of nuclear lamins (Lotzerich, Ruzsics, and Koszinowski, 2006; Muranyi et al., 2002; Sanchez and Spector, 2002). A recruitment of kinases is ascribed to pUL50 and pUL53 during the process of nuclear egress. In particular, it was shown that pUL50 and also its MCMV homolog pM50 is interacting with the cellular protein kinase C and re-localizes it to the nuclear lamina (Milbradt, Auerochs, and Marschall, 2007; Muranyi et al., 2002). Furthermore, pUL50 interacts with the cellular protein p32, a multifunctional lamina constituent, which itself binds to the viral protein kinase pUL97 (Marschall et al., 2005). Thus, the pUL50/pUL53 complex is supposed to serve as a docking station for cellular and viral proteins in order to disrupt the nuclear lamina meshwork. Members of the pUL31 protein family seems to have also another function in an upstream step of capsid maturation and packaging of viral DNA as it was described for MCMV pM53 functions, but which is independent from the interaction with the pM50 (Popa et al., 2010) (Pogoda et al., 2012, in revision).

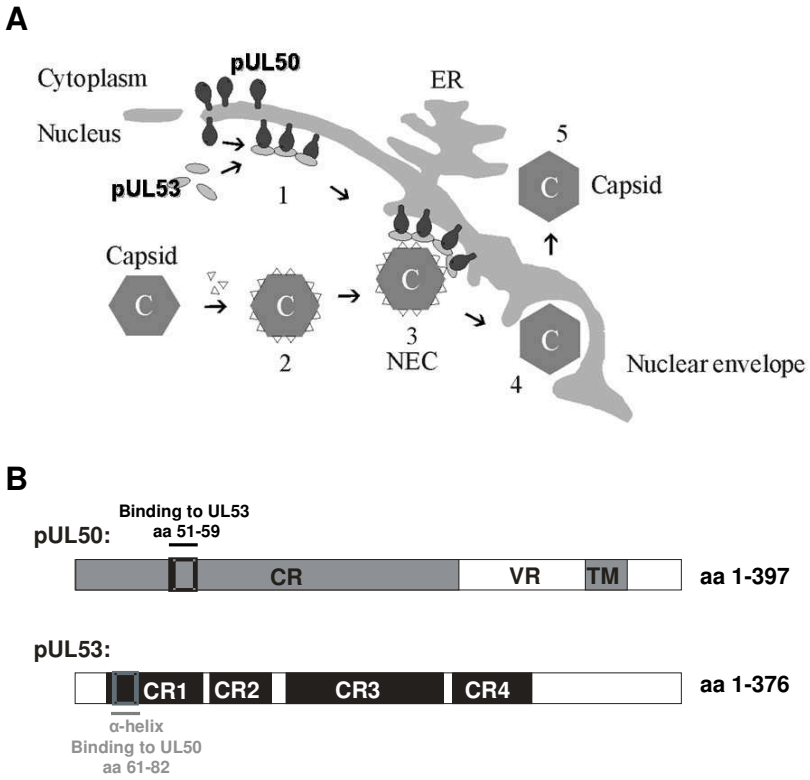

Figure 4: The HCMV pUL50 and pUL53 proteins. (A) Model of the nuclear egress process of viral capsids. HCMV capsids assemble and are packed with viral DNA in the nucleus (C). pUL50 and pUL53 interact at the inner nuclear membrane (1) and act as docking station for nuclear capsids (2) with tegument proteins (triangles) as adapter proteins. This configuration forms the nuclear egress complex (NEC) (3). The capsids bud at the nuclear membrane (4) before they are released into the cytoplasm (5) (Figure kindly provided by Margit Schnee). **(B)** Schematic representation of pUL50 and pUL53 of HCMV. pUL50 contains an N-terminal conserved region (CR) and a predicted transmembrane helix near to its C-terminus (TM) separated by a variable region (VR). pUL53 consists of four conserved regions (CR1-4). The predicted binding sites are located near to the N-termini of both proteins (open black and grey boxes).

1.3.2.2. The pUL94/pUL99 (pp28) interaction in the process of secondary envelopment

After fusion with the outer leaflet of the nuclear membrane viral particles loose their primary envelope and enter the cytoplasm as naked capsids. A complex network of protein-protein interactions is responsible to aid acquisition of the final tegument proteins and the final (secondary) envelope. However, due to intricacy and redundancy between different herpesvirus systems, the mechanism of the tegumentation and the secondary envelopment is still not completely elucidated. As the result of the final step of secondary envelopment of tegumented viral particles the infectious particles are formed by budding into Golgi-derived vesicles.

The highly abundant pUL99 (pp28) tegument protein (Baldick and Shenk, 1996; Landini et al., 1987; Martinez and St Jeor, 1986), which is encoded by the UL99 ORF of HCMV (belonging to the conserved UL11 protein family of herpesviruses), is a 190-aa myristoylated

phosphoprotein (Chee et al., 1990), which was shown to be expressed in virus replication with early-late kinetics (Jones and Lee, 2004). During infection, it accumulates on cytoplasmatic faces of nuclear and Golgi apparatus-derived membranes (Homman-Loudiyi et al., 2003; Sanchez et al., 2000). In further studies it was shown to play a crucial role in the process of final envelopment (Britt et al., 2004; Silva et al., 2003); pUL99-deficient HCMV mutants were not able to produce infectious virus and were shown to generate cytoplasmic, DNA-containing, tegument-associated capsids, but the capsids failed to acquire an envelope. pUL99 was shown to interact with tegument protein pUL94 (Liu et al., 2009), a member of the conserved pUL16 protein family of herpesviruses. This interaction can also be found for the MCMV homologs pM99 and pM94 (Maninger et al., 2011) as well as for their α-herpesvirus homologs pUL11 and pUL16 (Loomis et al., 2001; Yeh, Meckes, and Wills, 2008). Recently, Phillips and Bresnahan (Phillips and Bresnahan, 2011a) demonstrated that pUL99 is essential for HCMV and confirmed its crucial role in secondary. The same was shown for the MCMV homolog pM94 (Maninger et al., 2011). Null phenotypes of pUL94 or pM94 showed a defect in secondary envelopment without influence on any preceding viral replication steps. Furthermore, the null-phenotype of pUL94 exhibited aberrant localization of the interaction partner pUL99. This suggested a directing function of pUL94 for pUL99 to the site of secondary envelopment (Meckes, Marsh, and Wills, 2010; Phillips and Bresnahan, 2011a). This notion was recently accredited by the observation that a failure in the pUL94/pUL99 interaction lead to abberant localization of both proteins and a complete block in production of infectious virus (Phillips et al., 2012).

Moreover, pUL94 and its homologs have nuclear and cytoplasmic localization and are tightly virion associated (Meckes, Marsh, and Wills, 2010). This leads to the hypothesis, that pUL94 connects the capsid with the Golgi-derived vesicles by interaction with Golgi-network associated pUL99 to enable secondary envelopment (Figure 5).

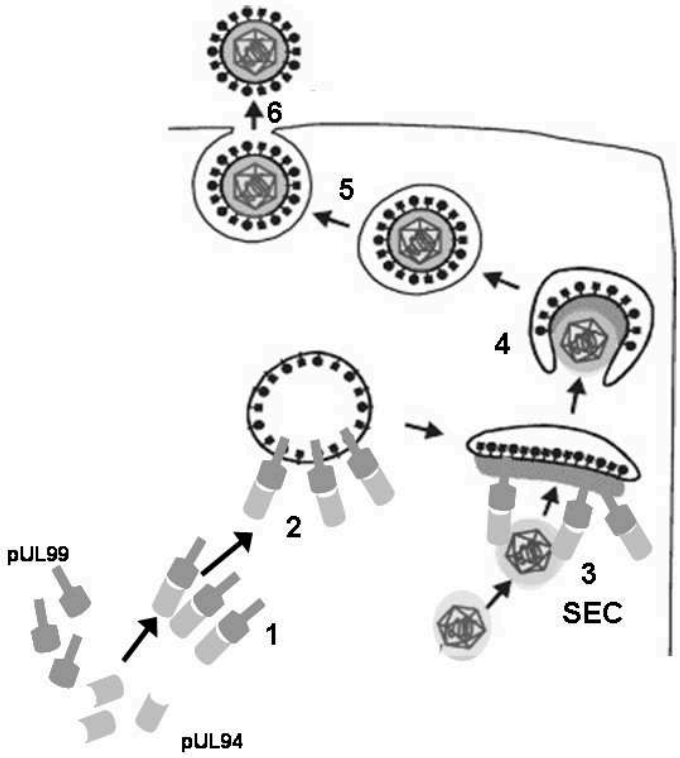

Figure 5: Model for the role of pUL94 and pUL99 in the secondary envelopment process. pUL94 interacts with pUL99 (1) (membrane association not shown) and directs pUL99 to trans-Golgi derived vesicles harbouring several viral tegument and glycoproteins (black) (2). pUL94 acts as a linking protein by interacting with the naked, pre-tegumented capsids. This configuration forms the secondary envelopment complex (SEC) (3). The capsid gets enveloped by budding into the vesicles (4). The vesicles are transported to the cytoplasmic membrane (5) where virions are released upon fusion (6) (Figure modified from (Mettenleiter, 2004)).

Amino acids 22-43 of pUL99 were identified as being responsible for its binding with pUL94, while no linear motif could be found within pUL94 (Liu et al., 2009). However, in the MCMV homolog pM94 a dominant-negative mutant with a small 5 aa insertion in the N-terminus of the protein was described not to form a detectable complex with pM99 (Maninger et al., 2011). Furthermore, a pUL94 mutant was recently described harbouring a point mutation in the C-terminus of the protein which totally lost co-localization to pUL99 (Liu et al., 2012). Due to these observations, there is evidence that a small molecule inhibitor targeting this interaction can be found which acts as an antiviral against HCMV in blocking secondary envelopment.

1.4 Monitoring protein-protein interactions

Classical methods as co-immunoprecipitation and pull down assays, still apply as the gold standard for detection of protein-protein interactions. Both methods are based on affinity purification of the bait protein, which binds to a matrix directly or via an additional tag. Protein

complexes in which the bait protein is part of are specifically retained by the matrix and can be co-purified with the bait. In case of the co-immunoprecipitation assay an antibody against the bait protein replaces the function of a tag. However, both methods are robust and reliable they are not useful for high-throughput screens. A very popular method to monitor and reveal protein-protein interactions for larger scale approaches is the yeast-two hybrid (Y2H) system (Fields and Song, 1989). Low costs, easy handling and *in vivo*-like conditions (e.g. post-translational modifications in yeast) made Y2H a tool for large screen set-ups of interacting proteins, so called interactomes. Recently, a study on evolutionary conserved herpesviral protein interaction networks was published based on the Y2H system (Fossum et al., 2009).
Beside of its many advantages, Y2H suffers from limitations; for example that it is limited to soluble proteins. Furthermore the protein-protein interaction has to take place in the nucleus which is for some proteins not the compartment they originally occur and act. This could lead to abnormal folding and binding properties of the proteins which could influence the result of the screen. Improper folding could also result from aberrant post-translational modifications occurring in yeast which differ from other eukaryotes and the incompatibility of the fusion with the reporter fragment. Therefore, results from Y2H screens always need to be validated by other methods like co-immunoprecipitations and pull-down assays.

1.4.1 Protein fragment complementation assay

Based on the principle of Y2H with the split reporter parts a new method, the so called protein fragment complementation assay (PCA), evolved over the last two decades overcoming the certain disadvantages of the original method (see previous chapter).
In the PCA, a protein-protein interaction is measured by fusing each of the proteins partners to complementary fragments of a reporter enzyme that has been dissected into two fragments. The PCA-fragments are designed so that they are non-functional by themselves and cannot bind to each other by their own. The PCA-fragments are brought into proximity through association of the two fused interacting proteins, which aid the folding and reconstitution of the active reporter from the two spited fragments. Depending on the used reporter (enzymes, GFP, luciferase, antibiotic resistance markers), reconstituted reporter activity can be measured for example by a colometric reaction, fluorescence, luminescence or survival rates, respectively. PCAs make it possible to monitor protein-protein interactions in the natural context where they occur in a living cell. Furthermore, they are not restricted to soluble proteins, though even membrane anchored proteins can be studied. The first example of a PCA was described by Johnsson and Varshavsky utilizing the C-terminal and N-terminal fragment of ubiquitin fused to the proteins of interest as sensor for protein interaction (Johnsson and Varshavsky, 1994). Interaction leads to reconstitution of the native ubiquitin, which is rapidly cleaved *in vivo* by ubiquitin specific proteases with release of a free

reporter. In the subsequent years the number of reporter proteins increased continuously providing different readouts for the desired applications. Examples for reporter proteins allowing in time readout and quantification by substrate application are the dihydrofolate reductase (DHFR) (Pelletier, 1997; Pelletier, Campbell-Valois, and Michnick, 1998), β-galactosidase and the TEM-1 β-lactamase (Galarneau et al., 2002; Pelletier, 1997; Wehrman et al., 2002). PCAs using fluorescent reporter proteins like GFP (Ghosh et al., 2000) and colour and behavioural variants (Hu, Chinenov, and Kerppola, 2002; Remy and Michnick, 2004; Ueyama et al., 2008) allowing direct readout without additional substrate addition and are also known as bimolecular fluorescence complementation (BiFC).

The uses of PCAs are increasing, spanning different areas such as the study of biochemical networks, screening for protein inhibitors and determination of drug effects. PCAs were used for example to identify the interaction partners of the protein kinase PKB/Akt (Remy and Michnick, 2004) and also to elucidate Wnt/β-catenin signalling pathways including a library screen to identify compounds that induce β-catenin nuclear accumulation (Verkaar et al., 2010). The applications of PCAs are not limited to cellular context. Hashimoto and colleagues (Hashimoto et al., 2009) describe an *in vitro* PCA in which fusion proteins are produced by wheat germ cell-free protein synthesis system and combined in a high-throughput format to screen for protein-protein interaction inhibitors. In our lab, we recently established a cell-free TEM-1 β-lactamase based PCA setting using partially purified proteins for the pUL50/pUL53 interaction of HCMV (Schnee et al., 2012).

1.4.2. Beta-lactamase as reporter enzyme in PCA

The TEM-1 β-lactamase is the product of the ampicilin resistance gene (ampr) of *E.coli* and fulfils the essential criteria as reporter enzyme in a PCA. It is small and monomeric, non-toxic and can be expressed in prokaryotic as well as in eukaryotic cells (Matagne, Lamotte-Brasseur, and Frere, 1998; Philippon et al., 1998). In its natural context it is secreted in the periplasmic space due to a signal peptide in the first 23 aa (Kadonaga et al., 1984). In PCA a 29 kDA isoform of TEM-1 β-lactamase (Bla) is used which lacks the secretory signal sequence (Zlokarnik et al., 1998). Since no orthologs of β-lactamase exist in eukaryotic cells there is no problem of background activity which increases the specificity of the PCA. Furthermore there is a versatile repertory of lactamase substrates available. For Bla based PCAs the fluorescent CCF2/AM (Zlokarnik et al., 1998) and the chromogenic cephalosporin nitrocefin (Figure 6B) (O'Callaghan et al., 1972) are the commonly used substrates for readout and quantitative assessment. Both are membrane permeable allowing to study interactions in intact cells as well as in lysates.

The first Bla based PCA was suggested by Garlaneau and Wehrman (Galarneau et al., 2002; Wehrman et al., 2002). They split the β-lactamase enzyme into a N-terminal (BlaN)

and a C-terminal (BlaC) fragment after aa 197 and fused the parts to some test protein interactions to analyze background and restoration of reporter activity upon interaction (Figure 6A).

In our lab, a cell-based β-lactamase PCA was established to investigate the interaction of the herpesvirus UL31 and UL34 protein homologs (Schnee et al., 2006).

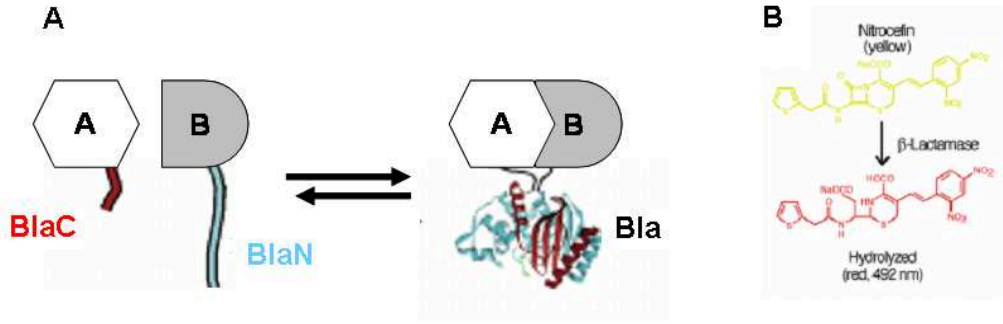

Figure 6: β-Lactamase (Bla) based protein fragment complementations assay (PCA). (A) Schematic representation of the PCA strategy used to study protein-protein interactions. Interaction between protein A and B leads to proximity of the β-lactamase fragments (BlaN and BlaC) allowing correct folding and reconstitution of the enzyme activity. **(B)** Structure of the chromogenic substrate nitrocefin which changes from yellow to red when hydrolyzed by β-lactamase activity (Figures adapted from Garlaneau et al., 2002).

Recently we established a cell-free PCA setting for the pUL50/pUL53 interaction of HCMV (Schnee et al., 2012). The proteins fused to fragments of the β-lactamase are thereby produced in *E.coli* and purified via an introduced His-tag by Ni^{2+}-NTA agarose. This PCA was used so far to further characterize the binding site of pUL53 for pUL50 and to identify inhibitory peptides of this interaction.

1.5 Aims of this work

Since viral protein-protein interactions are attractive drug targets, we aimed to develop a systematic approach by which small molecular inhibitors for essential viral protein-protein interactions can be identified.

We hypothesized that TEM-1 β-lactamase based protein fragment complementation assay may serve as a platform in which a simple cell-based assay can be used to test the feasibility of the PCA and if successful such a PCA can be systematically developed to an *in vitro* assay to screen for inhibitors.

In this work we specifically aimed to establish a screen for specific inhibitors of the pUL50/pUL53 interaction by a high-throughput *in vitro* assay system. This interaction was chosen as potential specific antiviral target because the pUL50 and pUL53 protein families are unique to herpesviruses. Furthermore the interaction domains of pUL50 and pUL53 have been studied and it was shown in MCMV and HCMV that single or small clustered amino acid substitutions in these proteins lead to a strong decrease or a total loss of this heterodimerization (Bubeck et al., 2004; Lotzerich, Ruzsics, and Koszinowski, 2006; Sam et al., 2009) resulting in a failure of virus production (Bubeck et al., 2004) which suggests that a small molecule could also disrupt this interaction.

Therefore, a cell-free assay should be applied in compound library of small molecules to identify inhibitory lead compounds for the pUL50/pUL53 interaction. This included in the first part of this thesis (i) the standardization of the assay conditions for high-throughput screening (HTS), (ii) the HTS of 4,000 small molecules and (iii) characterization of the lead compounds in the cellular and viral context.

A further aim of this work was (iv) to establish a PCA for another essential viral protein-protein interaction which can be used in future HTS screens. Thereby, the interaction of pUL94/pUL99 which plays an essential role during secondary envelopment process of cytoplasmic capsids (Phillips and Bresnahan, 2011a; Silva et al., 2003) was chosen as potential drug target. In our lab, the interaction of the MCMV homologs pM94 and pM99 was previously investigated thereby identifying small insertion mutants of pM94 which lost pM99 binding (Maninger et al., 2011) suggesting a limited binding surface. The interaction was first established for the MCMV and HCMV homologs in the cell-based PCA system to investigate compatibility with the reporter fragment tags, specificity and background before HCMV constructs were transferred to the bacterial expression system.

2. Material

2.1 Chemicals

Except as noted otherwise chemicals were derived from the companies Roche (Mannheim; D), Merck (Darmstadt; D), Roth (Karlsruhe; D), Serva (Heidelberg;D), Sigma-Aldrich (Steinheim; D), Fluka Chemie GmbH (Karlsruhe; D) und Invitrogen (Karlsruhe; D). Lactamase substrate nitrocefin was derived from Oxoid (Wesel; D). Chemical compounds for inhibitor screen were provided from EMC microcollections (Tübingen; D).

2.2 Enzymes

2.2.1 Restriction endonucleases

All used restriction endonucleases were derived from New England Biolabs (NEB) (Frankfurt/Main; D) or Fermentas (St. Leon-Rot; D) and applied referring to the manufacturer's instructions.

2.2.2 Other enzymes

Antarctic Phosphatase	New England Biolabs (NEB)
BP Clonase™ II enzyme mix	Invitrogen, Karlsruhe; D
Klenow fragment	New England Biolabs (NEB)
LR Clonase™ II enzyme mix	Invitrogen, Karlsruhe; D
Proteinase K solution	Invitrogen, Karlsruhe; D
T4-DNA Ligase	New England Biolabs (NEB)
TEM-1 β-lactamase	Abcam, Cambridge; UK

2.3 Devices

Bacterial shaker ISF-1-W	Kühner, Adolf AG, Birsfelden; CH
Centrifuge 5417 R	Eppendorf; D
Confocal microscope Axiovert 200M	Zeiss, Jena; D
Developing machine Optimax TR	MS Laborgeräte, Wieloch; D
Eagle-Eye imaging system	BioRad, München; D
ELISA plate reader (Versamax)	Molecular Devices, CA; USA
Fluorescence microscope 1x71	Olympus, Hamburg; D
Gene Pulser™	BioRad, München; D
Incubator B5050E	Heraeus Instruments, Osterode; D

Mini-PROTEAN3 Cell	BioRad, München; D
Light Cycler	Roche, Mannheim; D
Luminometer	Perkin Elmer, Boston, MA; USA
PCR machine	Roche, Mannheim; D
PerfectBlue™ vertical electrophoresis system	Peqlab, Erlangen; D
Roller mixer SRT	Stuart, Staffordshire; UK
Semi-Dry-Transfer Cell (Trans-BlotSD)	BioRad, München; D
Sonifier 450	Branson, Danbury, CT; USA

2.4 Consumables

Amersham Hybond™-P membrane	GE Healthcare, Buckinghamshire; UK
Cell culture dishes (20 cm^2, 55 cm^2, 145 cm^2)	Becton Dickinson, Heidelberg; D
Cell culture plates (6-, 12-, 24-, 48-, 96-well)	Becton Dickinson, Heidelberg; D
Cell scratcher	Costar, Bodenheim;D
Chemiluminescence film (Hyperfilm™ECL)	GE Healthcare, Buckinghamshire; UK
Electroporation cuvettes	BioRad, München; D
Falcons conical tubes	Becton Dickinson, Heidelberg; D
Pipettes (5 ml, 10 ml, 25 ml)	Sarstedt, Nümbrecht; D
Reaction tubes (1.5 ml, 2 ml)	Eppendorf, Hamburg; D
Whatman paper	Macherey-Nagel, Düren; D

2.5 Commercial kits

Cell Titer 96® Aqueous One Solution Cell Proliferation Assay	Promega, Madison; USA
DNeasy Blood & Tissue Kit	QIAGEN, Hilden; D
ECL plus Western Blotting Detection System	GE Healthcare, Buckinghamshire; UK
Expand High Fidelity PCR system	Roche, Mannheim, D
QIAquick Gel Extraction Kit	QIAGEN, Hilden; D
IllustraTM plasmidPrep Mini Spin Kit	GE Healthcare, Buckinghamshire; UK
Luciferase assay system	Promega, Madison, USA
Nucleobond® Xtra Midi	Macherey-Nagel, Düren; D
QuantiTect SYBR Green PCR Kit	QIAGEN, Hilden; D
QIAquick PCR purification Kit	QIAGEN, Hilden; D

2.6 Antibodies

2.6.1 Primary antibodies

2F12: mouse monoclonal antibody specific for HCMV glycoprotein gB (Biozol, Echingen; D).
CMV pp52 (CH16): mouse monoclonal antibody specific for pp52 (UL44) (Santa Cruz Biotechnology, Heidelberg; D).
cmv: mouse monoclonal antibody specific for HCMV immediate early protein1 (Perkin Elmer, Boston, MA; USA).
3F10: rat monoclonal antibody specific for HA-tag (Roche, Mannheim; D).
A2066: rabbit polyclonal antibody specific for actin (Sigma-Aldrich, Taufkirchen;D).
F3165: mouse monoclonal M2 antibody directed against FLAG-tag (Sigma-Aldrich, Taufkirchen; D).

2.6.2 Secondary antibodies

All secondary antibodies coupled to horseradish peroxidise (HRP) were purchased from Dianova (Hamburg; D).
Anti-mouse IgG (H+L), HRP coupled
Anti-rabbit IgG (H+L), HRP coupled
Anti-rat IgG (H+L), HRP coupled

Anti-rabbit IgG, Alexa 555 conjugate	Invitrogen, Karlsruhe; D
Anti-rat IgG; Alexa 488 conjugate	Invitrogen, Karlsruhe; D

2.7 Bacteria

ccdB Survival Cells	Invitrogen, Karlsruhe; D
DH10B (recA$^-$)	Invitrogen, Karlsruhe; D
Pir1	Invitrogen, Karlsruhe; D
BL21-CodonPlus (DE3)-RIL	Stratagene, Amsterdam; Netherlands

2.8 Cells

HFF: Primary human foreskin fibroblast cells	PromoCell, Heidelberg; D
293T: Human kidney carcinoma cells	ATCC CRL-11268
MEF: Mouse embryonic fibroblasts	isolated from BALB/c mice
U2OS: Osteosarcoma from the tibia of	ATCC HTB-96

a human female

2.9 Viruses

TB40-BAC4	wildtype HCMV (Sinzger et al., 2008)
TB40-BAC4ΔUL5-9/Luc (HCMV-luc)	HCMV mutant expressing firefly luciferase under the control of SV40 promotor (Scrivano et al., 2011)

2.10 Oligonucleotides

All used oligonucleotides were synthesized by Metabion (Martinsried; D).

2.10.1 Oligonucleotides for used for cloning

M94del1-13attB-for: GGGGACAAGTTTGTACAAAAAAGCAGGCTTAATCAGTAGGTTCGTCCAG
M94attB-rev: GGGGACCACTTTGTACAAGAAAGCTGGGTACATGTGCTCGAGAACGAT

UL94attB-for: GGGGACAAGTTTGTACAAAAAAGCAGGCTTAATGGCTTGGCGCAGCGGG
UL99attB-rev: GGGGACCACTTTGTACAAGAAAGCTGGGTATTAGTGCACTAGGTTCTT

M94attb-for: GGGGACAAGTTTGTACAAAAAAGCAGGCTTAATGGCGACGTCCAGACTA

UL99attB-for: GGGGACAAGTTTGTACAAAAAAGCAGGCTTAATGGGTGGCGAACTCTGC
UL99attB-rev: GGGGACCACTTTGTACAAGAAAGCTGGGTATTAAAAGGACAAGGGGGC

Acc65I-CUL99del-for:
AGTTCGGTACCACGTCCGGTGAGCCCCTGAAAGGTTCCGACGAAGGGGAGGACGATGA
BlpI-CUL99-rev: CGGCAGTCGCTTAGCCACCA

BglII-UL94-for: GGCGGCGGATCCAGATCTATGGCTTGGCGCAGCGGGCTTT
NotI-UL94-rev: GTGGTGCTCGAGTGCGGCCGCGTGCACTAGGTTCTTAAGC

BamHI-CUL99His-for: GGCGGCGGATCCATGGGTGGCGAACTCTGCAA
NotI-CUL99-rev: GCTCGAGTGCGGCCGCAAAGGACAAGGGGGCGGC

EcoRV-UL50HA-for: ATTCTGCAGATATCATGGAGATGAACAAGGTTCTCCA

NsiI-UL50HA-rev:
GCCCTCTAGATGCATTCAAGCGTAGTCGGGCACGTCGTAGGGGTAGTCGCGGTGTGCGGAGCG
TGTCGG

EcoRV-FlagUL53-for:
ATTCTGCAGATATCATGGATTACAAGGATGACGACGATAAGTCTAGCGTGAGCGGCGTGCGCAC
G
NsiI-FlagUL53-rev: GCCCTCTAGATGCATTCAAGGCGCACGAATGCTGTTGAG

2.10.2 Real time PCR primer

HVIPO1: TCATCTACGGGGACACGGAC
HVIPO2: TGCGCACCAGATCCACG
GAPDH-for: TGGTATCGTGGAAGGACTCA
GAPDH-rev: CCAGTAGAGGCAGGGATGAT

2.11 Plasmids

2.11.1 Commercial available and published plasmids

Litmus28	NEB, Frankfurt/Main; D
pDONR^{TM}221	Invitrogen, Karlsruhe; D
pDONR ^{TM}221-M50	provided by J. Haas
pDONR ^{TM}221-M53	provided by J. Haas
pDONR^{TM}221-M94	provided by J. Haas
pDONR^{TM}221-M99	provided by J.Haas
pEF5/FRT-V5-DEST	Invitrogen, Karlsruhe; D
pEPkan-I-*Sce*I	Tischer et al., 2006
pET24-NUL50-His	Schnee et al., 2012
pET24-CUL53-His	Schnee et al., 2012
pL-HA-N	Schnee et al., 2006
pL-HA-C	Schnee et al., 2006
pO6T-C-M53	Schnee et al., 2006
pO6T-C-UL53	Schnee et al., 2006
pO6T-N-M50DM	Schnee et al., 2006
pO6T-N-UL50	Schnee et al., 2006
pOriR6K-M94i13	Maninger et al., 2011
pOriR6K-M99FLAG	Maninger et al., 2011
pOriR6K-zeo-ie	Bubeck et al., 2004

Bacterial artificial chromosomes (BACs):

TB40-BAC4	Sinzger et al., 2008
pSM3fr	Wagner et al., 1999

2.11.2 Plasmids constructed over the project

pL-HA-N_f and pL-HA-C_f:

pL-HA-C and pL-HA-N were digested with AvrII and AflII and inserted in each case in Litmus28 predigested with AvrII and AflII.

pEF5/FRT-V5-N_f-DEST and pEF5/FRT-V5-C_f-DEST

To create Gateway® compatible BlaN- and BlaC- fusion vectors, respectively, pL-HA-N_f and pL-HA-C_f were digested with AflII, blunted by Klenow and finally digested with XbaI. The inserts were then ligated to the vector backbone of pEF/FRT-V5-DEST which resulted from digestion with Acc65I, fill-in and final cleavage with SpeI.

pDONR 221-UL94

The ORF UL94 in TB40-BAC4 was PCR amplified by the forward primer UL94attB-for and the reverse primer UL94attB-rev. The PCR products were then recombined by BP Clonase™ II enzyme reaction with pDONR 221 resulting in pDONR 221-UL94.

pDONR 221-M94i13

The sequence of the dominant negative M94i13 mutant was PCR amplified from pOriR6K-M94i13 with the primer pair M94attB-for and M94attB-rev. The PCR product was finally recombined by BP Clonase™ II enzyme reaction with pDONR 221 to result in pDONR 221-M94i13.

pDONR 221-UL99

The UL99 ORF of TB40-BAC4 was PCR amplified by the primer pair UL99attB-for and UL99attB reverse and the resulting PCR product was recombined by BP Clonase™ II enzyme reaction with pDONR 221 resulting in pDONR 221-UL99.

pO6T-N_f-M50, pO6T-N_f-M94, pO6T-N_f-M94i13, pO6T-N_f-UL94

To fuse the N-terminal PCA fragment of β-lactamase to the different ORFs, pDONR 221-M50, pDONR 221-M94, pDONR 221-M94i13 and pDONR 221-UL94 were recombined by LR Clonase™ II enyme reaction with pEF5/FRT-V5-N_f-DEST, respectively.

Fusion constructs were further digested with AgeI, blunted by Klenow and finally digested by AflII to create an insert (smaller band) which was subloned in the vector backbone of pO6T-C-M53 which was pre-digested by NsiI, filled-in and then digested with AflII to result in pO6T-N_f-M50, pO6T-N_f-M94, pO6T-N_f-M94i13 and pO6T-N_f-UL94, respectively.

pO6T-C_f-M53, pO6T-C_f-M99, pO6T-C_f-UL99

To fuse the C-terminal PCA fragment of β-lactamase to the different ORFs and mutants pDONR 221-M53, pDONR 221-M99 and pDONR 221-UL99 were recombined by LR Clonase™ II enyme reaction with pEF5/FRT-V5-C_f-DEST, respectively.
Fusion constructs were further digested with AgeI, blunted by Klenow and finally digested by AflII to create an insert (smaller band) which was subloned in the vector backbone of pO6T-C-M53 which was pre-digested by NsiI, filled-in and then digested with AflII to result in pO6T-C_f-M53, pO6T-C_f-M99, pO6T-C_f-UL99, respectively.

pO6T-C_f-UL99del22-43

To have a non-binding control of UL99 for the cell-based PCA a PCR product was generated using the primer pair Acc65I-CUL99del-for and BlpI-CUL99-rev and pO6T-C_f-UL99 as template. As a second step the resulting PCR product and the vector pO6T-C_f-UL99 were digested with Acc65I and BlpI and fused by ligation resulting in pO6T-C_f-UL99del22-43.

pO6T-N_f-M50DM

pO6T-N-M50DM was digested with NarI and AhdI and the smaller fragment was inserted into the pO6T-N_f-M50 vector backbone which was also predigested with the same enzymes to result in pO6T-N_f-M50DM.

pOriR6K-UL50-HA

The UL50 ORF was amplified from TB40-BAC4 with the primer pair EcoRV-UL50HA-for and NsiI-UL50HA-rev. The resulting PCR product was then cleaved with EcoRV and NsiI and inserted in the correspondingly treated pOriR6K-zeo-ie to result in pOriR6K-UL50-HA.

pOriR6K-FLAG-UL53

The UL53 ORF was amplified from TB40-BAC4 with the primer pair EcoRV-FlagUL53-for and NsiI-FlagUL53-rev. The resulting PCR product was the cleaved with EcoRV and NsiI and inserted in the correspondingly treated pOriR6K-zeo-ie to result in pOriR6K-FLAG-UL53.

pET24-N-UL94-His

The ORF of UL94 was amplified from TB40-BAC4 with the primer pair BglII-UL94-for and

NotI-UL94-rev. The resulting PCR product was then cleaved by BglII and NotI and then inserted into the BamHI/NotI treated pET24-N-UL50 to resul in pET24-N-UL94-His.

pET24-C-UL99-His

The ORF of UL99 was amplified with the primer pair BamHI-CUL99His-for/NotI-CUL99-rev. The PCR product was then digested with BamHI and NotI and inserted into BamHI/NotI treated pET24-C-UL53-His.

pET24-C-UL99del22-43-His

The sequence of the deletion mutant of UL99 was amplified from pO6T-C_f-UL99del22-43 by the primer pair BamHI-CUL99His-for and NotI-CUL99-rev. The PCR product was then cleaved by BamHI and and NotI and inserted into BamHI/NotI treated pET24-C-UL53-His.

3. Methods

3.1 Bacterial cell culture

All bacteria were grown either in suspension (LB medium) or on agar-plates (LB agar). For plasmid or BAC selection the growth media comprised the appropriate antibiotics in distinct concentration (see below). Cells harbouring a plasmid were grown at 37 °C, whereas BAC-containing cells were grown at 32 °C to enable slower division and proper replication. Cell density in suspension was determined by measuring the optical density at 600 nm, while 1 unit of OD_{600} corresponds to approximately 1 x 10^8 cells.

LB medium (1 l)	LB agar (500 ml)	Antibiotics
10 g Bacto tryptone	7.5 g agar	ampicillin: 50 µg/ml
5 g Bacto yeast extract	in 500 ml LB medium	chloramphenicol: 25 µg/ml
5 g NaCl		kanamycin: 50 µg/ml
		zeocin: 30 µg/ml

3.1.1 Glycerol stocks of bacteria

To maintain a culture of bacteria bearing the plasmid of interest, glycerol stocks were prepared by adding 500 µl glycerol (50%) to 500 µl bacterial culture. The stocks were stored at -80 °C.

3.1.2 Preparation of chemocompetent bacteria

All preparation and centrifugation steps were done on ice or 4 °C using pre-cooled pipettes and solutions. 150 ml of LB medium was inoculated with 1 ml overnight culture and grown at 37 °C until the suspension reaches an OD_{600} of 0.5. Bacteria were pelleted by centrifugation for 10 min at 6,000 x g and resuspended in 20 ml Tfb I buffer. After 50 min incubation on ice, bacteria were pelleted again, resuspended in 2 ml Tfb II and snap frozen in liquid nitrogen as 100 µl aliquots and stored at -80 °C.

Tfb I (pH 5.2)	Tfb II (pH 7.0)
100 mM $RbCl_2$	10 mM MOPS pH 7.0
50 mM $MnCl_2$	10 mM $RbCl_2$
30 mM KAc	75 mM $MnCl_2$
10 mM $CaCl_2$	15% glycerol

3.1.3 Transformation of chemocompetent bacteria

To introduce plasmids into chemocompetent bacteria, 4 µl of a ligation mix or 30 ng of a plasmid were added to 100 µl chemocompetent bacteria and incubated on ice for 30 min. After that, samples were subjected to a heat-shock of 1 min at 42 °C followed by another 2 min of incubation on ice. Bacteria were suspended in 1 ml antibiotic-free LB medium and shaked at 37 °C for 1 h. 200 µl were plated on LB agar plates containing the appropriate antibiotics and incubated overnight at 37 °C.

3.1.4 Preparation of electrocompetent bacteria

All preparation steps were done on ice or 4 °C using pre-cooled pipettes and solutions. 150 ml of LB medium was inoculated with 1 ml overnight culture and grown at appropriate temperature until the suspension reaches an OD_{600} of 0.5. Cultures were then cooled on ice for 15 min and bacteria were pelleted by centrifugation for 10 min at 6,000 x g. To eliminate salts and medium components, bacteria were washed three times with 100 ml 10% glycerol. Finally, the bacterial pellet was resuspended in 1 ml of 10% glycerol and aliquots of 50 µl were snap frozen and stored at -80 °C.

3.1.5 Transformation of electrocompetent bacteria

For introduction of plasmids into bacteria, 50 µl electrocompetent bacteria were thawed for 5 min on ice. About 4 µl of a ligation mixture or 20 ng of a plamid were pipetted to the bacteria cells and then the mixture was transferred into a pre-cooled Gene Pulser® bulb. After electrotransformation (pulse duration: 4.5 ms, 2.5 kV, 200 Ohm, 25 mFD) the cells were immediately resuspended in 1 ml LB medium without antibiotics and transferred to an 2 ml Eppendorf reaction cup. The cells were incubated in the Thermomixer 1 h at 37°C under permanent shaking. After that, 100 µl of the bacteria suspension was plated on pre-warmed agar culture plates comprising the adequate antibiotics and incubated overnight at 37 °C.

3.2 Isolation and purification of DNA

3.2.1 Small scale preparation of plasmid DNA

For small scale analysis, plasmid DNA from a 5 ml overnight culture was isolated by using the IllustraTM plasmidPrep Mini Spin kit from GE Healthcare following the manufacturer's protocol. The plasmid DNA was eluted from the binding columns with 100 µl distilled water. 10 µl were used for restriction pattern analysis.

3.2.2 Small scale preparation of BAC-DNA

Bacterial pellets from 10 ml overnight cultures were resuspended in 150 µl P1 buffer (Qiagen). Preparations were lysed by addition of 150 µl P2 buffer (Qiagen) and incubation for 5 min at RT before they were neutralized by application of 300 µl P3 buffer (Qiagen). Samples were incubated 10 min on ice and precipitations were pelleted by centrifugation at 20,000 x g for 10 min at 4 °C. Cleared supernatants were transferred to new reaction tubes, mixed with 900 µl phenol/chlorophorm/alcohol (25/24/1), and centrifuged for 5 min at 20,000 x g. The upper phase was transferred to a new reaction tube and comprehending BAC-DNA was precipitated by addition of 900 µl isopropanol and centrifugation at 20,000 x g for 20 min. DNA pellets were washed with 70% ethanol and resuspended in ddH_2O.

3.2.3 Large scale preparation of plasmid and BAC-DNA

Large scale preparations of plasmid and BAC DNA were performed using the Nucleobond® Xtra Midi Kit from Macherey-Nagel. A volume of 200 ml of a bacterial overnight culture was used for DNA isolation according to the manufacturer's protocol. The dried plasmid DNA pellet was resuspended in 200 µl distilled water and further analyzed by restriction enzyme digest or stored at -20 °C.

3.3 Analysis of DNA

3.3.1 Restriction enyme digest

For restriction enzyme digest of DNA restriction endonuncleases from NEB were used according to the manufacturer's instructions. Digests for analytical purposes were performed with 500 ng (plasmid) to 1.5 µg (BAC-DNA) or for preparative applications with 5 µg DNA, respectively, and the reaction was incubated for 1-3 h at the recommended temperature.

3.3.2 Agarose gel electrophoresis

DNA fragments obtained by restriction digest from plasmids were separated and analyzed by gel electrophoresis in a 1-2% agarose/ TAE or for BAC DNA in a 0.8% agarose/TBE gel, respectively. Gels were run 20 min at 120 V or 16 h at 80 V. For detection of the DNA bands the gels comprised ethidium bromide in a final concentration of 1 µg/ml which was added before poring. Stained bands were visualized by UV light in an Eagle-Eye imaging system from BioRad.

50 x TAE buffer (pH 7.3)	10 xTBE buffer	6 x DNA loading buffer
2 M Tris	900 mM Tris	15% Ficoll
0.25 M Na-acetate	900 mM boric acid	Orange G
50 mM EDTA	25 mM EDTA	

3.3.3 Isolation of DNA fragments from agarose gels

To extract the respective DNA fragment for further cloning steps, the stained band was exicised under weak UV light from the agarose gel. The DNA was purified from agarose using the QIAquick Gel Extraction Kit from QIAGEN following the manufacturer's protocol. The purified DNA was eluted with 30 µl distilled H_2O.

3.3.4 Dephosphorylation of DNA fragments

To suppress re-circularization of cleaved, linearized vector DNA, the terminal 5´-phosphate groups were removed by using Antarctic Phosphatase (AP) from NEB.
Per 1 µg DNA in appropriate buffer conditions 1 unit of AP was applied. The reaction mixture was incubated at 37 °C for 30 min and finally heat-inactivated at 65 °C for 10 min.

3.3.5 Blunting of DNA overhangs by Klenow

DNA overhangs were blunted by using the Klenow fragment of NEB. For that, 1 µg DNA was incubated with 5 units of Klenow and 100 µM dNTP in 1 x NEB buffer 2 for 15 min at RT. After this, DNA was immediately purified from the enzyme by using QIAquick PCR purification Kit.

3.3.6 Polymerase Chain Reaction (PCR)

To amplify arbitrary pieces of DNA, a PCR was performed. The reaction was done in a total volume of 50 µl using the Expand High Fidelity PCR system from Roche. A standard PCR reaction mixture is shown below.

PCR reaction mixture
10-50 ng of template DNA
500 nM of each oligonucleotide primer
250 µM dNTPs
Expand High Fidelity Polymerase buffer (1 x)
3.5 units of High Fidelity Polymerase

To reduce non-specific amplification, a touchdown PCR was performed with the following conditions (Table 1). Time is variable in the elongation steps (4. + 7.) depending on the length of the resulting PCR product. For every further 500 bp the polymerase needs another 30 sec for elongation.

	Step	Temperature	Time	Cycles
1.	initial denaturation	94 °C	5 min	
2.	denaturation	94 °C	30 sec	
3.	annealing	62-45 °C	30 sec	
4.	elongation	72 °C	30 sec-2 min	-1 °C every cycle; 17 x back to **2.**
5.	denaturation	94 °C		
6.	annealing	45 °C	30 sec	
7.	elongation	72°C	30sec-2 min	
8.	final elongation	72°C	5 min	18 x back to **5.**
9.	end	4 °C	∞	

Table 1: TD-PCR program.

The obtained PCR products were purified using the QIAquick Purification Kit from QIAGEN following the manufacturer's protocol.

3.3.7 Ligation of DNA fragments

Ligation reactions were performed in a total volume of 20 µl comprising 100 ng vector mixed at a molecular ratio of 1:3 with the insert, 2 units of T4 DNA ligase and T4 ligase reaction buffer. The reaction was incubated overnight at 16 °C or for 2 h at RT and then added to competent bacteria for transformation.

3.3.8 BP reaction (Gateway® system)

A BP reaction was performed to create a Gateway® (Invitrogen) entry clone from an attB-flanked PCR product. Therefore a reaction mixture comprising 15-150 ng attB-PCR product, 150 ng pDONR 221 (150 ng/µl) TE buffer, 2 µl BP Clonase™ II enzyme filled up to 10 µl with TE buffer (pH 8.0) was incubated at RT for 1 h. To terminate the reaction, 1 µl of the Proteinase K solution was added the mix and incubated at 37°C for 10 min. 1 µl from the reaction mix was used for transformation into competent cells.

3.3.9 LR reaction (Gateway® system)

A LR reaction was performed to transfer a gene from a Gateway® entry clone to destination vector. Therefore a reaction mixture comprising 15-150 ng donor vector (pDONR 221-gene), 150 ng destination vector (pEF5/FRT-V5-N_f-DEST and pEF5/FRT-V5-C_f-DEST) and 2 µl LR

Clonase™ II enzyme filled up to 10 µl with TE buffer (pH 8.0) was incubated at RT for 1 h. To terminate the reaction, 1 µl of the Proteinase K solution was added the mix and incubated at 37°C for 10 min. 1 µl from the reaction mix was used for transformation into competent cells.

3.3.10 DNA sequencing

DNA sequencing was performed by GATC (Konstanz; D) and by Sequiserve (Vaterstetten; D). Sequences were aligned and verified using Vector NTI Advance™ software.

3.3.11 Quantitative real-time PCR

In order to quantify viral genomes, total DNA was extracted from infected HFF using the DNeasy Blood & Tissue Kit from QIAGEN according to the manufacturer's instructions. Quantitative real-time PCR was performed on a Light Cycler from Roche using 5 µl of DNA, 15 µl reaction mixture of QuantiTect SYBR Green PCR master mix from QIAGEN and 0.5 µM of the primers in each reaction. For quantification of the viral DNA load, primers amplifying the viral DNA polymerase gene region UL54 (Primers: HVIPO1 and HVIPO2) and primers against GAPDH as endogenous reference (Primers: GAPDH-for, GAPDH-rev) were used. Each sample was analyzed in duplicates. PCRs were subjected to 95 °C hot-start for 10 min, and SYBR Green incorporation was monitored for 45 cycles of 95 °C denaturation for 10 sec, 58 °C annealing for 3 sec, and 72 °C elongation for 10 sec. The data were analyzed using the ΔΔCt method.

3.4 Analysis of proteins

3.4.1 SDS-PAGE

Protein samples were separated by polyacrylamide gel electrophoresis (PAGE). Before loading onto gels, protein samples were heated for 7 min at 95 °C in total lysis buffer. Gels were run in 1 x Laemmli buffer for approximately 1 h at 160 V. After electrophoresis, gels were either applied to Western Blot analysis for protein detection.

4 x Stacking gel buffer
0.5 M Tris
0.4% (v/v) SDS
pH 6.8

4 x Separating gel buffer
1.5 M Tris
0.4% (v/v) SDS
pH 8.8

Stacking gel
2.5 ml Rothiphorese 30
3.75 ml 4 x stacking gel buffer
9.75 ml dH_2O
0.1 ml APS (10%) solution
20 µl TEMED

Separating gel (10%,*12%*)
3.3 ml/ *4 ml* Rotiphorese 30
2.5 ml 4 x separating gel buffer
4.1 ml/*3.4* ml dH_2O
0.1 ml APS (10%) solution
3.3 µl TEMED

1 x Laemmli buffer

50 mM Tris
0.4 M glycine
0.1% (w/v) SDS

3.4.2 Coomasssie Blue Stain

To visualize proteins in SDS gels, gels were incubated with staining solution for 30 min and subsequent treatment with destaining solution for several hours.

Staining solution	Destaining solution
50% (v/v) methanol	50% (v/v) methanol
10% (v/v) acetic acid	10% (v/v) acetic acid
0.1% (w/v) Coomassie blue R350	

3.4.3 Western Blot Analysis

After separation of proteins by SDS-PAGE, proteins were transferred from the gel onto Hybond^{TM}-P membrane (GE Healthcare). For that, the membrane was activated 5 min by methanol and then equilibrated in blotting buffer. For transfer, the gel was placed on the activated membrane and covered on both sides by three layers of Whatman paper soaked in blotting buffer. The transfer was performed in a Semidry blotting apparatus (BioRad) for 30 min at 18 V and room temperature. To block unspecific binding sites, blotted membranes were incubated for 1 h at room temperature with blocking buffer. After that, membranes were incubated with primary antibody diluted in blocking buffer overnight at 4 °C. After five washes with (5 x 10 min) with TBS-T, the membranes were incubated with horseradish-coupled secondary antibody diluted in TBS-T for 1-2 h at room temperature and were subsequently washed as described above. Chemiluminescence detection of bound antibodies was performed using ECL plus Western Blotting Detection System from GE Healthcare according to the manufacturer's instructions.

Blotting buffer	Blocking buffer	TBS-T
25 mM Tris	150mM NaCl	150 mM NaCl
190 mM glycine	10 mM Tris/HCl, pH 8.0	10 mM Tris/HCl, pH 8.0
20% methanol	0.5% Tween 20	0.5% Tween 20
	5% skimmed milk powder (w/v)	

3.4.4 Determination of protein concentration

Protein concentrations were determined by the Bradfort method using Bradfort reagent (BioRad) according to the manufacturer's protocol and a bovine serum albumin standard curve for calculation.

3.4.5 Indirect immunofluorescence

For confocal laser scanning, cells were grown on 8 well *µ*-slides, fixed with 4% PFA and after washing with PBS permeabilized with 0.1% Triton-X-100 in PBS. After further washing, cells were blocked for 1 h at RT with 5% donkey serum in PBS (blocking solution). Primary antibodies were applied for 1 h in blocking solution at RT followed by 3 consecutive washings with PBS. Finally, cells were incubated with Alexa Fluor-conjugated secondary antibody in blocking solution. After a final extensive washing step, preparations were mounted on glass slides with Prolong Gold resin (Invitrogen) and analyzed on a confocal laser scanning microscope.

3.5 Tissue culture

3.5.1 Cultivation of mammalian cells

All mammalian cell lines and primary cells grew adherent and were cultured at 37 °C and 95% humidity in presence of 7% CO_2 in DMEM supplemented with 10% FCS, 0.6% penicillin, 1.3% streptomycin and 0.3 mg/ml L-glutamine. For passaging, the cell monolayers grown to confluency were washed once with PBS and detached from plates or flasks by incubation with 25% trypsin/EDTA solution for 2-5 min at RT. Trypsin reaction was stopped by adding of 12 ml supplemented DMEM, cells were resuspended and the pertinent amount was brought to a plate with fresh medium. For maintenance, 293T cell were passaged every 3-4 days by a 1:6 split, whereas HFF and MEF cells were splitted 1:3 once a week. To ascertain defined cell numbers in a cell suspension and distinguish live and dead cells, cells were stained with trypan blue and transferred in a Neubauer chamber (Brand) for counting. All lines were tested regularly for mycoplasma contamination.

3.5.2 Freezing of cells

To maintain a stock of cells, cells were frozen and stored in liquid nitrogen. For that, cells were grown to a confluency of 90%, detached from the plates by trypsin treatment and pelleted by centrifugation (300 x g, 5 min). The cell pellet was carefully resuspended in freezing medium and transferred as 1 ml aliquots to cryo tubes (nunc). For gently freezing, tubes were transferred in isopropanol isolated cryo-boxes and stored at -80°C (-1 °C per hour). After 48-72 h tubes were stored in a liquid nitrogen tank.

Freezing medium

70% DMEM
20% FCS
10% DMSO

3.5.3 Thawing of cells

Frozen aliquots from the liquid nitrogen tank were rapidly thawed in a 37 °C water bath
As soon as possible, cells were resuspended in 10 ml supplemented fresh medium and centrifuged for 5 min at 300 x g. The pellet was taken up in 12 ml fresh supplemented medium and transferred to cell culture dishes.

3.5.4 Cytotoxicity assay

The influence of the chemical compounds on the viability of fibroblast cells during a 14-day incubation period was evaluated using the CellTiter 96® AQueous One Solution Cell Proliferation Assay (Promega), as described by the manufacturer. The assay depends on the bioreduction of an MTS tetrazolium compound (Owen's reagent) by cells into a coloured formazan product that is soluble in tissue culture medium (Cory et al., 1991). This conversion is accomplished by NADPH or NADH produced by dehydrogenase enzymes in metabolically active cells (Berridge and Tan, 1993).
Briefly, 96-well microtiter plates were seeded with 2 x 10^4 cells/well and incubated overnight. Compounds were added in different concentrations in duplicates while keeping the DMSO concentration constant at 1% throughout the whole plate. Cell viability was checked in two-day intervals after substance application until day 14. Therefore, 20 µl CellTiter 96® AQueous One Solution Reagent was added to each well. After 1 h at 37 °C in a humidified, 5% CO_2 atmosphere, the absorbance at 490 nm was recorded using an ELISA plate reader. Data were normalized to background absorbance.

3.5.5 Transfection of eukaryotic cells by FuGENE® HD

Cells were seeded one day before transfection in 6-well plates or 8 well µ-slides. X µg DNA in 100 µl OptiMEM was mixed carefully with 2.5 x Xµl FuGENE® HD tranfection reagent (Roche) and incubated for 30 min at RT. Then the transfection mix was added drop-wise to the cell culture supernatants and the cells were incubated 24-48 h before they were harvested for further experiments.

3.6 Virus culture

3.6.1 Virus infection of cells

For standard infection assays, cells were seeded on multi-well plates or dishes one day before infection to a confluency of around 90%. To infect, inocula were diluted in supplemented medium and applied to the cells. After incubation for 1.5 h at 37 °C inocula

were replaced by supplemented fresh medium and cells were incubated at 37 °C for the appropriate time.

3.6.2 Growth curves

The growth kinetics of HCMV in presence and in absence of chemical compounds was compared in multi-step growth conditions. HFF cells were seeded in 24-well plates (1 x 10^5) and were incubated overnight at 37 °C. The next day, cells were infected at an MOI of 0.2 pfu/cell for 1.5 h at 37 °C. After that, cells were washed five times with fresh medium, medium containing chemical compounds in distinct concentrations or DMSO (mock control) (DMSO concentrations were kept constant at 1% in all wells) was added and cells were incubated at 37 °C. In distinct days post infection over a period of 8 days supernatants were harvested, stored at -80 °C and titers were determined.

3.6.3 Titration of virus

Quantification of infectious virus in supernatants was determined by the TCID50 assay (endpoint titration) (Reed, 1938) on fibroblast cells in 96-well plates. Cells were seeded on 96-well plates one day before titration to 100% density. On the next day, cells were infected with serial dilutions of virus supernatant (10^{-1} to 10^{-8} in a volume of 100 µl of supplemented DMEM) in quadruplicates and were incubated for 8 days at 37 °C. To identify plaque positive wells cells were washed once with PBS and then fixed with 1 x crystal violet for 10 min at RT: After 3 consecutive washings with dH_2O, positive and negative wells were counted under the microscope and titer values were calculated according to the Reed and Muench method.

10 x Crystal violet

10% para-formaldehyde in PBS
1% crystal violet (w/v)

3.6.4 Luciferase assay

A luciferase assay was performed using HCMV expressing firefly luciferase (v-TB40-BAC4ΔUL5-9/Luc) to evaluate the influence of the chemical compounds on virus replication. The assay was performed in 96-well microtiter plates. Briefly, cells were infected with luciferase expressing reporter virus at an MOI of 0.01 pfu/cell for 1.5 h at 37 °C. After that, inocula were removed and 100 µl fresh medium, containing chemical compounds in different concentrations (DMSO concentration was kept constant at 1% throughout the plate) were added to the cells. After certain time points post infection, supernatants were removed and cells were directly lysed on the plate by adding 50 µl 1 x cell culture lysis reagent (Promega)

and incubated for 10 min at RT under permanent shaking. 5 µl of the lysates were subsequently transferred to white 96-well plates, mixed with 40 µl firefly substrate per well (Luciferase reporter assay, Promega) and the luciferase activity was measured for 5 sec in a luminometer.

3.7 Bacterial expression

3.7.1 Expression of heterologous proteins

30-100 ng of plasmid DNA of bacterial expression vectors were transformed in chemocompetent BL21-(DE3)RIL (Stratagene) and cultured overnight at 37 °C on agar plates (Kan/Cam). The next day, 50 -100 colonies were scraped from the plate and used to inoculate 50 ml LB medium with appropriate antibiotics for overnight culture at 37 °C. 20 ml of the overnight culture was used to inoculate 2.5 l antibiotics containing LB medium and the bacterial culture was incubated at 37 °C until it reached an OD_{600} of 0.6. To cool down, culture flasks were put on ice for 15 min. Induction of heterologous proteins was induced by adding IPTG to a final concentration of 0.5 mM and cultures were shaked in an incubator at 20 °C overnight. On the next day, cells were harvested by centrifugation (6000 x g, 4 °C, 20 min) and pellets were resuspended in 35 ml lysis buffer, frozen in liquid nitrogen and stored at -80 °C.

Lysis buffer

300 mM NaCl
50 mM Tris (pH 8.0)
10 mM β-Mercaptoethanol

3.7.2 Lysis of bacteria

The bacterial solution was thawed in a 37 °C water bath and sonified by pulses of 1 sec and 70% amplitude for 10 min (Sonifier 450, Branson) using a flat bottom tip. Subsequently, lysates were cleared by centrifugation at 15,000 x g for 30 min at 4 °C and applied to further purification steps or stored at -80 °C.

3.7.3 Purification of His-tagged proteins

All preparation steps were performed in the cold room with pre-cooled buffer solutions containing freshly added β-mercaptoethanol. 1.6 ml Ni-NTA agarose (QIAGEN) were loaded onto a 10 ml plastic column (BioRad) for sedimentation resulting in a bed volume of 800 µl. Agarose was washed two times with 10 ml dH_2O and one time with 10 ml lysis buffer before the supernatant of the bacterial lysis was applied to the column. After loading and complete flow-through, the column was washed two times with 10 ml lysis buffer and one time with 4

ml lysis buffer containing 5 mM imidazole. His-tagged proteins were eluted from the column by application of 3 ml lysis buffer containing 250 mM imidazole, whereas only the first 1.5 ml of the flowthrough was collected. The protein elution was stored at -80 °C in 30% glycerol.

3.8 Biochemical assays

3.8.1 Nitrocefin assay in cell lysates

Bla-fragment tagged constructs were single or co-transfected into 293T cells. After 48 h, cells were scraped from the plates, sedimented by centrifugation (300 x g, 5 min), washed with 800 µl PBS and lysed with 150 µl 1 x luciferase reporter lysis buffer (Promega). After 30 min on ice, lysates were cleared by centrifugation for 10 min at full speed at 4 °C. For determination of β-lactamase activity, 50 µl of the lysates were transferred to a 96 well plate and mixed with 120 µl phosphate buffer (0.1 M, pH 7.0), 15 µl H_2O and 15 µl nitrocefin (500 mg/ml, Oxoid). Nitrocefin hydrolysis was determined as change in absorption at 495 nm in the linear range (milliabsorptions units/min) at a Versamax plate reader.

3.8.2 Nitrocefin assay with purified proteins

Proteins purified by Ni-NTA agarose were tested for Bla reconstitution in the presence of 15 µl nitrocefin (500 mg/ml, Oxoid) filled up to a total volume of 200 µl with phosphate buffer (0.1 M, pH 7.0). Nitrocefin hydrolysis was determined as change in absorption at 495 nm in the linear range (milliabsorptions units/min) in a Versamax plate reader (Molecular Devices).
For the inhibitory screen, 10 µl screening compound (solved in DMSO; 10 µM final concentration) was mixed with the purified Bla-proteins, 15 µl nitrocefin (500 mg/ml, Oxoid) and filled up to a total volume of 200 µl with phosphate buffer (0.1 M, pH 7.0). The reaction was incubated for 40 min at 37 °C before 10 µl of stop solution (potassium clavulanate, 2 µM) was added for reaction termination. Nitrocefin hydrolysis was determined by absorption measurement at 495 nm in a Versamax plate reader (endpoint determination, absorption at 495 nm).

3.8.3 Nitrocefin assay with β-lactamase

To test the influence of the chemical screening compounds on the reporter β-lactamase, 10 µl chemical compound (in DMSO, final screen concentration 10 µM) was mixed with 10 µl β-lactamase enzyme solution (Abcam; 100 µg/ml, 0.1% BSA), 15 µl nitrocefin (500 mg/ml, Oxoid) and filled up to a total volume of 200 µl with phosphate buffer (0.1 M, pH 7.0). The reaction was incubated for 40 min at 37 °C before 10 µl of stop solution (potassium clavulanate, 20 µM stock) was added for reaction termination. Nitrocefin hydrolysis was

determined by absorption measurement at 495 nm in a Versamax plate reader (endpoint determination, absorption at 495 nm).

3.9 Electron microscopy

For electron microscopy, HFF cells were grown on carbon-coated sapphire discs (3 mm in diameter; Engineering Office M. Wohlwend GmbH, Switzerland) and infected at an MOI of 1. At 5 days post infection, the cells were frozen from the living state by high-pressure freezing with an HPF 01 apparatus (Engineering Office M. Wohlwend GmbH) and freeze substituted in acetone containing 0.1% (wt/vol) uranyl acetate, 0.2% (wt/vol) of osmium tetroxide, and 5% (vol/vol) of water, as described previously (Buser et al., 2007). After embedding the samples in Epon, ultrathin sections were prepared on formvar coated single slot grids for transmission electron microscopy (TEM). Samples were imaged with the JEOL JEM-1400 transmission electron microscope at an acceleration voltage of 80 kV.

4. Results

4.1 Optimization of the *in vitro* NEC-PCA for high-throughput screening (HTS)

In this work, a chemical compound library was screened for inhibitors for the interaction of the nuclear egress complex (NEC) proteins pUL50 and pUL53 of HCMV by a high-throughput screen (HTS) approach based on a protein fragment complementation assay (PCA). A cell-based PCA of these two proteins and their homologs in other herpesviruses was established by Margit Schnee (Schnee et al., 2006) to elucidate conservation of this interaction between subfamilies. However, cell-based PCAs in general are not suitable for direct drug screening approaches due their experimental robustness such as dependency on eukaryotic cell transfection and cell lysis procedures for activity measurements. Furthermore, cell-based screening approaches suffer from excluding cytotoxic candidate compounds before screening which could lead to a miss of information about inhibiting structures. Therefore, the β-lactamase based PCA for the pUL50-pUL53 interaction was modified into a cell-free set-up, termed here *in vitro* NEC-PCA. Thereby, Bla-tagged NEC proteins were produced in an *E.coli* expression system and then combined *in vitro*.

The constructs for *E.coli* expression of Bla-tagged NEC fusion proteins were designed and tested for specificity in a previous study (Schnee et al., 2012).

Figure 7A shows a schematic representation of the expression strategy. For the pUL50 PCA construct (NUL50-His), the conserved region of pUL50 in the N-terminus (aa 1-172) was fused N-terminally with HA-tagged BlaN and C-terminally with an His-tag for purification. Between BlaN and pUL50 a 17 aa glycin-serin (GS) spacer was inserted for ensuring flexible connection between the fusion partners. For control reasons a pUL53 non-binding mutant of pUL50 was cloned as a Bla fusion by the same way and was termed NUL50DM-His. It harboured the same features than NUL50-His besides lacking the aa 51-59 of pUL50 essential for binding to pUL53. The pUL53 PCA construct (CUL53-His) contained the variable and the conserved region 1 of pUL53 (aa1-129) which were fused N-terminally with HA-tagged BlaC and the spacer and C-terminally with a His-tag. All constructs were cloned into the pET24b (+) expression vector carrying a T7 promotor and kanamycin as selection marker.

When CUL53-His is mixed in the assay with NUL50-His, protein-protein interaction leads to proximity of the Bla fragments and therefore reconstitution of Bla activity, which can be detected by hydrolysis of nitrocefin (see Figure 7B, Schnee et al., 2012). The construct NUL50DM-His lacks the binding site for pUL53, therefore mixing of NUL50DM-His and

CUL53-His does not result in Bla complementation and thus defines the background of nitrocefin hydrolysis. In presence of an inhibitor for the pUL50/pUL53 interaction, Bla fragments of NUL50-His and CUL53-His can not properly complement in the assay, resulting in a reduced nitrocefin hydrolysis rate.

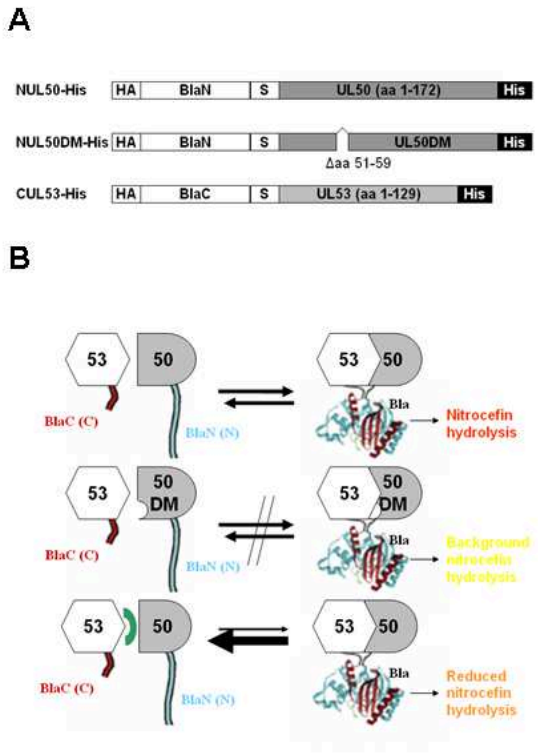

Figure 7: The *in vitro* NEC-PCA.
(A) Schematic representation of the *in vitro* NEC-PCA constructs. The HA-tagged BlaN was fused to the first 172 aa of pUL50 separated by a glycine/serine spacer (S) resulting in NUL50-His. As negative control a BlaN fusion of pUL50 (NUL50DM-His) was constructed, lacking aa 51-59 of pUL50 representing the binding site to pUL53. The HA-tagged BlaC and the spacer were fused to a pUL53 fragment containing the first 129 aa of pUL53 (CUL53-His). All constructs carried a C-terminal His-tag for affinity purification.
(B) Principle of the *in vitro* NEC-PCA. Upper row: Reconstitution of Bla activity when CUL53-His (53) is mixed with NUL50-His (50). Middle row: CUL53-His and NUL50DM-His (50DM) do not interact due to the deletion of the pUL50-pUL53 interaction site. No complementation of the two Bla fragments. (C) Presence of an inhibitor (green) of the pUL50/pUL53 interaction competes Bla complementation when NUL50-His and CUL53-His are mixed.

4.1.1 Propagation and purification of the Bla-tagged constructs

Chemocompetent *E. coli* BL21-CodonPlus (DE3)-RIL were transformed with plasmids coding for the Bla-tagged NEC proteins. After overnight induction of expression by IPTG, the cultures were harvested and proteins were further purified by His-affinity chromatography (see chapter 3.7.3. for details). The bacterial lysates were applied on Ni^{2+}-NTA columns, washed, and the proteins were eluted in three consecutive steps using 0.5 ml lysis buffer containing 250 mM imidazole. The eluates were collected separately (e1, e2, e3). To test the fractions for the presence of the NEC fusion proteins, 10 µl of each elutions were separated by SDS-PAGE and further analyzed by Coomassie staining and Western Blot analysis.
Coomassie stained gels (Figure 8A) showed presence of large amounts of contaminating proteins, which made it difficult to assign the specific protein band. This *E. coli* derived impurity was previously described and had no consequences on specificity and background of the assay (Schnee et al., 2012).
In order to assess the relative quantities of the expressed proteins, we used HA-specific Western Blot analysis. With this method all Bla-tagged proteins were detected at their

predicted sizes of 28 kDa (CUL53-His), 42 kDa (NUL50-His) and 41 kDa (NUL50DM-His) in all three elution fractions (Figure 8B). Therefore eluted fractions were pooled and total protein concentrations were determined by the Bradford method. The pooled CUL53-His elutions constantly led to a total yield of around 1.5 mg protein, while pooled elutions from NUL50-His or NUL50DM-His reproducibly resulted in 7 mg total protein, respectively.

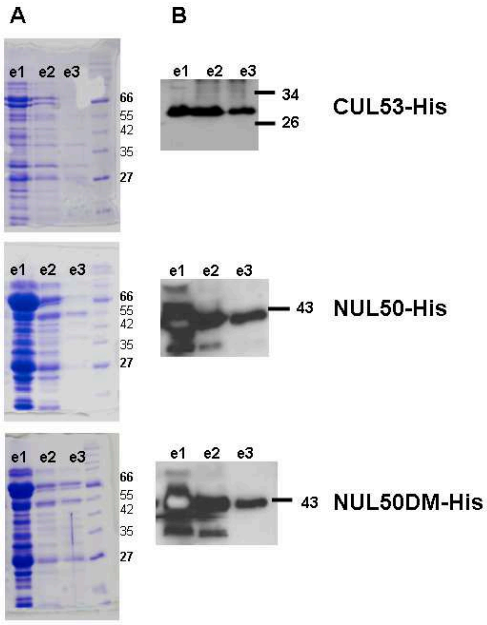

Figure 8: Bacterial expression of the Bla-tagged NEC proteins.
(A) Coomassie stained SDS-PAGE with three consecutive elutions (e1, e2, e3) from Ni^{2+}-NTA purifications of CUL53-His, NUL-His and NUL50DM-His, respectively. 10 µl of each elution was loaded onto a 12 % SDS gel. Numbers on the right indicate marker bands (in kDa). **(B)** HA-specific Western Blots of the protein elutions of CUL53-His, NUL-His and NUL50DM-His. 10 µl of each elution was loaded onto a 12 % SDS gel. Numbers on the right indicate marker bands (in kDa).

4.1.2 Standardization of the assay

To use the *in vitro* NEC-PCA for screening in a chemical compound library, the assay needed to be standardized. It was essential to provide constant and reproducible conditions for the reactions in all screening phases. Furthermore, it was important to determine the optimum capacity (minimal concentration of Bla-tagged proteins in the assay) and to determine an adequate time frame (assay reaction time). Finally, the real-time assay had to be transformed into an endpoint assay enabling multi-plate screening. A counter-screen had to be established to exclude irrelevant inhibitors of the reporter enzyme β-lactamase.

4.1.2.1 Setting up the minimal essential protein concentrations

To optimize the number of possible reactions derived from one protein purification, the minimal concentration of Bla-tagged proteins was determined which is minimally required to deliver specific signal for the interaction. Therefore, same parts of NUL50-His (3.3 µg /µl in 25% glycerole) and CUL53-His (0.6 µg /µl in 25% glycerole) or NUL50DM-His (3.3 µg /µl in 25% glycerole) and CUL53-His (0.6 µg /µl in 25% glycerole), respectively, were premixed (corresponding to dilution 1:1 in Figure 9). The above described ratio of NUL50-His and

CUL53-His eluates (5:1) was established by testing for the highest activity using a setup, in which both components were applied in different amounts and was already described in (Schnee et al., 2012). Serial dilutions of the premixes were prepared using Na-phosphate buffer (pH 7.0). 40 µl of each dilution was then tested in a nitrocefin assay for Bla-activity. Furthermore, the reaction time was measured for each dilution of the NUL50-His/CUL53-His combination, which corresponded to the time until nitrocefin turnover reached the plateau phase.

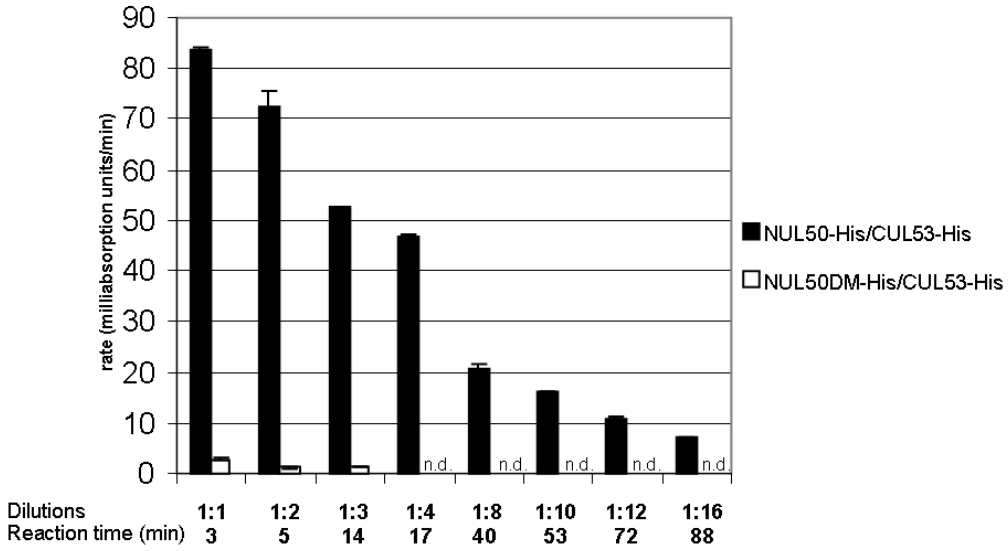

Figure 9: Standardization of the concentration of the Bla-tagged proteins for high-troughput screening (HTS).
NUL50-His (3.3 µg /µl) and CUL53-His (0.6 µg /µl) or NUL50DM-His (3.3 µg /µl) and CUL53-His (0.6 µg /µl), respectively, were premixed (1:1) and diluted to different concentrations with Na-phosphate buffer (pH 7.0). 40 µl of each dilution was then tested in nitrocefin assay (see 3.8.2) for Bla activity. Shown are means of at least 4 independent experiments. Error bars indicate the standard deviation. Numbers at the bottom indicate the time (in min) until the nitrocefin hydrolysis reached its plateau phase.

As expected the signal of NUL50-His/CUL53-His mixtures decreased according to dilution (Figure 9). The NUL50DM-His/CUL53-His mixtures which defined the background activity of each corresponding NUL50-His/CUL53-His mixture showed low Bla activity in the 1:1 to 1:3 dilutions, whereas in higher dilutions no activity could be determined (n.d.) anymore. This defined the signal for the NUL50-His/CUL53-His mixtures in all tested dilutions as specific and theoretically applicable for the library screen. The reaction time of the higher NUL50-His/CUL53-His dilutions (1:12 and 1:16) was over 1 h. In addition, although hydrolysis curves in these dilutions reached a plateau, nitrocefin turnover did not reach 100% (not shown). This indicated that the PCA components started to turn inactive during the prolonged incubation period. Therefore, the Bla-tagged proteins were used in a 1:8 dilution in the screens corresponding to 16.5 µg total protein per well for the NUL50-His preparation and 3 µg for the

CUL53-His, respectively. This protein density corresponded to a hydrolysis rate of around 20 milliabsorption units/min and a reaction time of 40 min.
Based on this, fermentation of 2.5 l volume for each Bla-tagged protein was sufficient to perform more than 400 single assays.

4.1.2.2 DMSO sensitivity of the assay

The chemical compounds from EMC microcollections (Tübingen) were provided prespotted in 96-well plates and were reconstituted in the standard solvent DMSO for 30 min before the PCA was performed. Therefore the influence of DMSO on the PCA was determined implying the maximum tolerable concentration. To this end, the *in vitro* NEC-PCA was performed with the standardized protein amounts and activity (see previous chapter) in presence of different concentrations of DMSO (Figure 10).

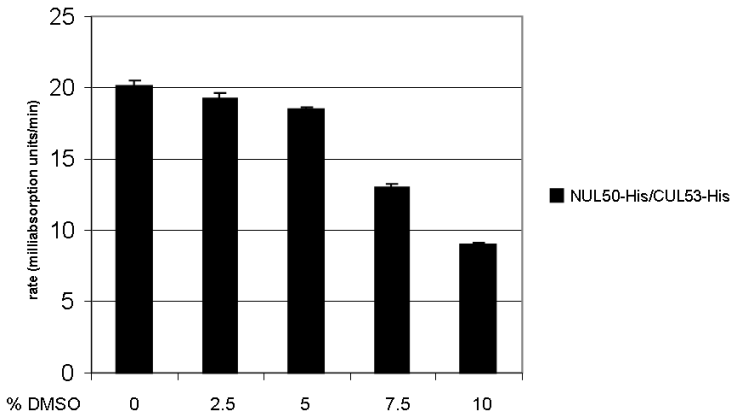

Figure 10: DMSO sensitivity of the *in vitro* NEC-PCA.
The *in vitro* NEC-PCA was performed with standardized protein concentrations (see previous chapter) in presence of different concentrations of DMSO. Nitrocefin hydrolysis rate was determined at 495 nm. Shown are means of 4 independent experiments. Error bars indicate the standard deviation.

The Bla activity decreased only slightly in presence of 2.5% and 5% of DMSO, compared to the 0% control, whereas a strong decrease could be detected in higher concentrations (7.5% and 10%). Therefore, the standardized DMSO concentration was set to 5% in the library screen.

4.1.2.3 Minimal concentration of potassium clavulanate as stop solution

Larger screening trials using the *in vitro* NEC-PCA system demanded an endpoint measurement as final readout. To afford comparable conditions in all tested plates, the reaction should be stopped when the uninfluenced control reaction reached its plateau (40 min reaction time (see chapter 4.1.2.1)). As stop solution, a commercial available β-lactamase inhibitor was tested. In order to determine the minimal concentration of this inhibitor which is necessary to stop the reaction, different concentrations of potassium

clavulante (Sigma) were applied to the standardized *in vitro* NEC-PCA and the nitrocefin turnover (absorption at 495 nm) was measured after 5 and 10 minutes and after 24h.

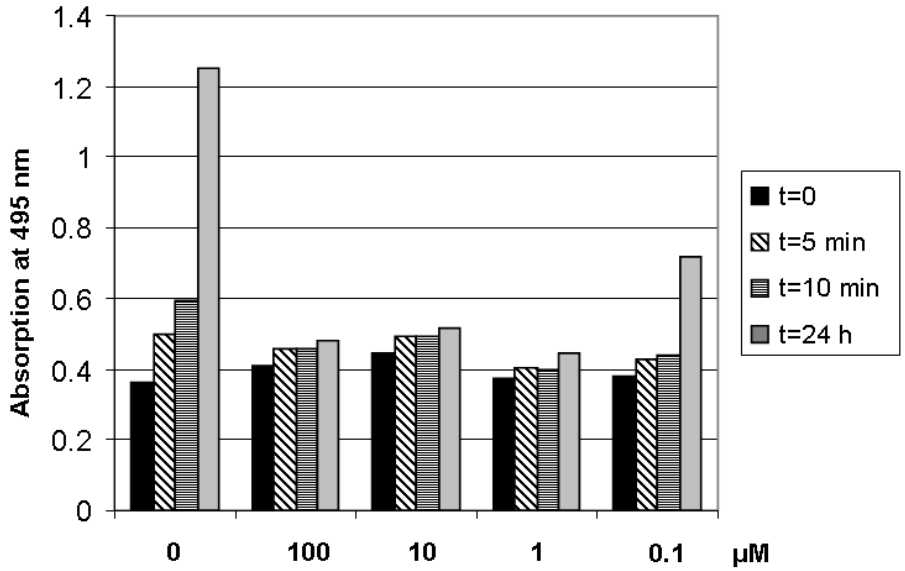

Figure 11: Potassium clavulanate as stop solution in the *in vitro* NEC-PCA.
The *in vitro* NEC-PCA was performed with standardized values. After 20 min of reaction, 10 µl potassium clavulanate solution (Sigma-Aldrich) was added at different concentrations to the 200 µl reaction mixture and absorption at 495 nm was measured immediately after adding (t=0, black bars) and after another 5 min (t=5 min, striped bars) and 10 min (t=10 min, dark gray bars) of incubation at 37 °C. Additionally, the reaction was incubated at 4°C for further 24 h (t=24 h, gray bars) before absorption at 495 nm was measured again. Designations refer to end concentrations of potassium clavulanate after adding to the reaction.

Compared to the mock-control (0 µM) in which the nitrocefin hydrolysis proceeded exponentially, in all tested concentrations of potassium clavulanate the hydrolysis was inhibited, resulting in reduced hydrolysis rates at 5 min after administration (Figure 11). However, the hydrolysis was not stopped completely at any applied concentration indicating a time delay which needed to be considered for the assay setup. This could be observed by comparing the values of 5 min to 10 min after potassium clavulanate administration. In contrast to the small but measurable increase between 0 and 5 min, no further increase of absorption at 495 nm could be measured between 5 to 10 min in concentrations from 100 µM to 1 µM. In the lowest applied concentration a slight increase was still visible. The samples were measured again after 24 h incubation at 4 °C. As expected, all nitrocefin is hydrolyzed in the mock sample, in the 100 µM to 1 µM samples the absorption increased slightly to the 10 min values reflecting the natural decomposition rate of nitrocefin. The signal in the lowest test concentration increased less than the mock control but a residual Bla activity was evident.

Thus, potassium clavulanate at 1 µM end-concentration was used to stop the *in vitro* NEC-PCA for endpoint measurement in the high-throughput screen.

4.1.3 Optimal β-lactamase concentration for HTS counter-screen

Candidate compounds arising from the HTS screen with *in vitro* NEC-PCA need to be tested for Bla inhibitory activity to exclude compounds affecting the reporter enzyme. Therefore, the compounds were tested in a counter-screen with β-lactamase exhibiting the same activity as the fusion proteins in the unaffected *in vitro* NEC-PCA.

To this end, different concentrations of TEM-1 β-lactamase (Abcam) were tested for their nitrocefin hydrolysis activity to find the optimal matching enzyme concentration (Figure 12).

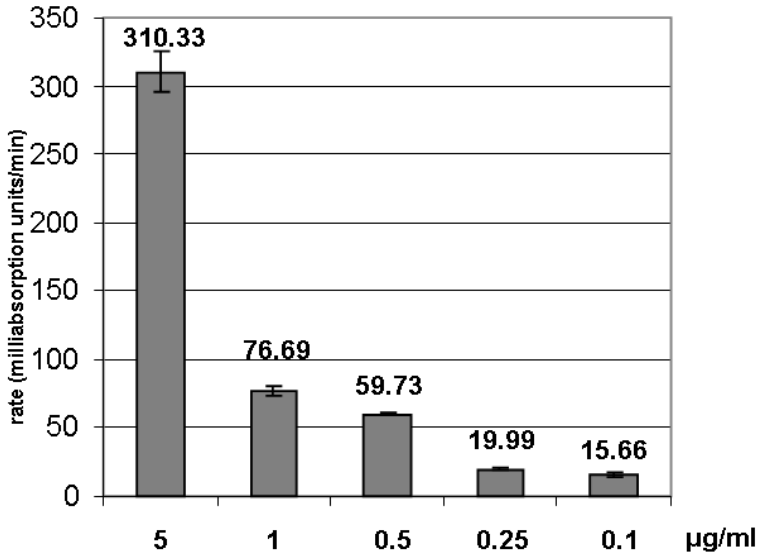

Figure 12: Nitrocefin hydrolysis rate of TEM-1 β-lactamase.
10 µl of different concentrations of TEM-1 β-lactamase (Sigma-Aldrich) were mixed with nitrocefin and Na-phosphate buffer (see Methods 3.8.3) and hydrolysis rate was determined at 495 nm. Designations refer to end concentrations of TEM-1 β-lactamase in the experiment. Shown are means of triplicates. Error bars indicate the standard deviation.

0.25 µg/ml TEM-1 β-lactamase showed a hydrolysis rate of around 20 milliabsorption units/min which is in accordance with the standardized hydrolysis rate of the *in vitro* NEC-PCA (chapter 4.1.2.1). Therefore, this enzyme concentration was used in the counter-screen to test the primary candidate compounds for direct reporter-inhibitory activity.

4.2 The pUL94/pUL99 interaction as potential drug target

We could recently show that our cell-free NEC-PCA (*in vitro* NEC-PCA) was feasible to identify inhibitory peptides for the pUL50/pUL53 protein interaction (Schnee et al., 2012) and that it is suitable to be used in high-throughput screening approaches in small chemical compound libraries (this work). Next, the Bla based PCA system was tested on another essential viral protein-protein interaction to show that our approach is generally applicable.

The herpesviral replication cycle offers a broad spectrum of viral protein-protein interactions. The perinuclear enveloped particles which are formed by budding through inner nuclear membranes (primary envelopment) fuse in a subsequent morphogenesis step with outer nuclear membranes. Unenveloped capsids in the cytoplasm are decorated with tegument proteins and then undergo secondary envelopment by budding into *trans*-Golgi network membranes, producing infectious particles that are secreted from cells (reviewed in (Johnson and Baines, 2011)). Two conserved viral proteins belonging to the pUL16 and pUL11 protein families of herpesviruses were shown to play a crucial role during this process of secondary envelopment. The HCMV representatives pUL94 and pUL99 were shown to interact at the site of capsid budding forming the secondary envelopment complex (SEC) (also see 1.3.2.2). The interaction between the pUL94 and the pUL99 HCMV protein was shown to be essential in viral replication (Phillips et al., 2012), not involved in DNA replication and independent of other viral proteins. Furthermore the linear binding site on pUL99 and non-binding mutants for pUL94 and homologs were already described (Liu et al., 2009; Liu et al., 2012; Maninger et al., 2011). Due to these properties this interaction was an interesting candidate to establish in the PCA system. Similar to the approach taken for the NEC core interaction, first, a cell-based PCA was established on the MCMV homologs pM94/pM99 based on information on their native interaction (Maninger et al., 2011). The homologous proteins of MCMV and HCMV are highly conserved and therefore should behave similarly in the same assay since a characterized non-binding small insertion mutant of pM94 was already described and here can be used to develop controls. Based on the observations on the MCMV proteins a cell-based PCA for the pUL94/pUL99 should be tested. Finally, on the basis of the results of the previous steps, the fusion proteins of the HCMV homologs should be transferred into the bacterial expression system to make the SEC-PCA cell-free and HTS-compatible.

4.2.1 Gateway® compatible Bla-fragment fusion vectors

To construct the new Bla fusion proteins, Gateway® (Invitrogen) compatible fusion plasmids (pEF5/FRT-V5-N_f-DEST and pEF5/FRT-V5-C_f-DEST, see Materials and Methods) were constructed allowing an N-terminal fusion of genes with the Bla fragments for cell-based PCAs in a one-step LR reaction. This platform would allow to integrate other viral interactions into the cell-based PCA system since many herpesvirus ORF libraries including CMV sets existing in Gateway® compatible entry plasmids and have been used for other interaction screens (Fossum et al., 2009; Vizoso Pinto et al., 2011). The general cloning approach is depicted in Figure 13.

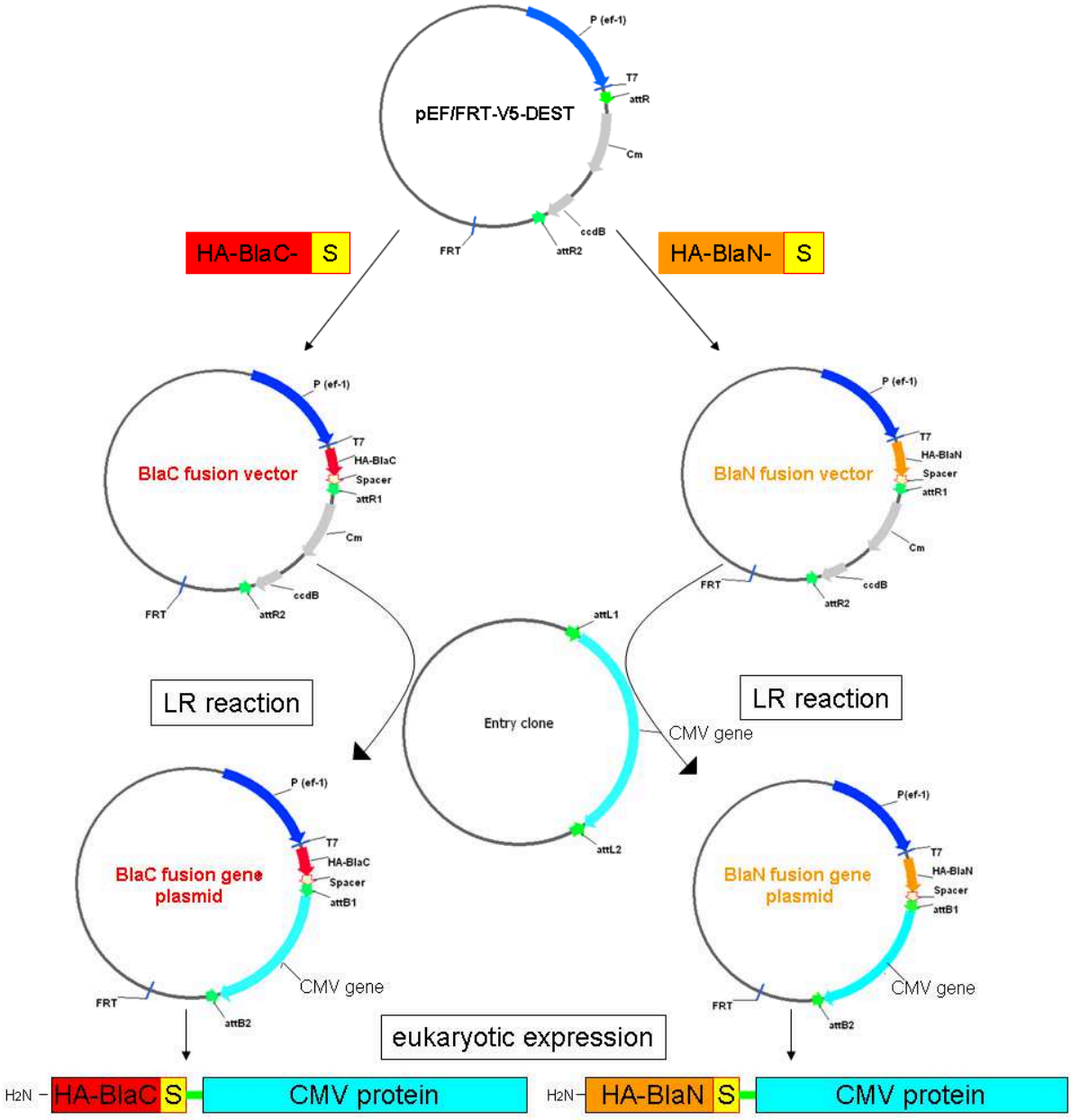

Figure 13: Schematic representation of the Gateway® compatible Bla fusion plasmids. The HA-tagged BlaN (right) and BlaC (left) sequences and a Glycine-Serine spacer sequence (S) were cloned into the Gateway® expression vector pEF/FRT-V5-DEST between promotor (pef-1) and recombination site (attR). CMV gene entry clones with attL recombination sites were recombined with the Bla fusion plasmids in a LR reaction resulting in a plasmid expressing N-terminal Bla fragment tagged CMV proteins.

4.2.2 The pM94/pM99 interaction in the PCA

4.2.2.1 Signal and background of the MCMV SEC-PCA

The M94 gene was fused to the BlaN fragment via the Gateway® compatible fusion vector pEF5/FRT-V5-N_f-DEST and M99 was fused pEF5/FRT-V5-C_f-DEST to the BlaC fragment. Next, both gene fusions were sub-cloned in a pO6T vector backbone resulting in pO6T-N_f-M94 and pO6T-BlaC_f-M99 to generate expression vectors for the cell-based PCA. To determine the background signal of the PCA, the BlaN fragment was fused to a mutant of pM94 (pO6T-N_f-M94i13) which is deficient in binding pM99 (Maninger et al., 2011).
As further control the genes M53 and M50 and a non-binding mutant of M50 were fused to the Bla fragments by the Gateway® fusion vectors (pO6T-C_f-M53, pO6T-N_f-M50 and pO6T-N_f-M50DM). The interaction of these proteins was already characterized by PCA (Schnee et al., 2006) and served as confirmation for the Gateway® fusion system in which the linker between the viral proteins and the Bla fragment had to be modified to fit in the recombination sites.
To test the SEC proteins in PCA, the expression vector pO6T-BlaC_f-M99 was co-transfected into 293T cells with either pO6T-N_f-M94 or pO6T-BlaN_f-M94i13. Furthermore, 293T were transfected with the individual SEC constructs. 24 h after transfection the cells were harvested and lysed. Nitrocefin was added to the cell lysates and the hydrolysis rate was determined by a kinetic readout over 30 min, measuring the absorption at 495 nm every 9 seconds (Figure 14A). For the control interaction, co-expression of N-M50 and C-M53 resulted in hydrolysis rate of around 35 while co-expression of the non-binding mutant N-M50DM with C-M53 resulted in a more than 10 fold lower signal confirming the Gateway derived fusion proteins to be functional also in the PCA.

For the SEC proteins, co-expression of N-M94 and C-M99 led to a hydrolysis rate of around 70, which was more than 20 fold higher than in the lysates of the co-expression of non-binding N-M94i13 with C-M99 or of single expressions. To ensure, that the low signal detected in the PCA with the non-binding M94 mutant was not due to poor protein expression, residual lysates of the co-expressions of the SEC constructs were denatured in total lysis buffer and used for Western Blot analysis probing with HA-specific antibody. The wildtype and the mutant construct of pM94 were detected at the predicted molecular weight of 62 kDA and expressed at the expected level (Figure 14B).

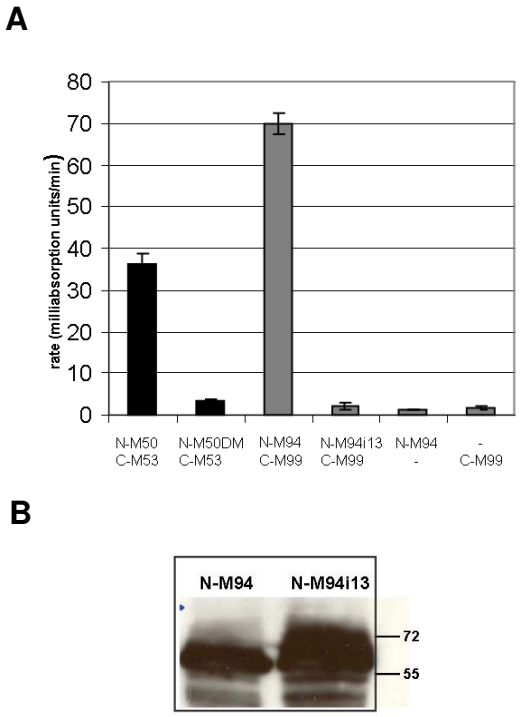

Figure 14: Establishment of the SEC-PCA for MCMV. (A) Bla activity in 293T cell lysates after co- and individual expressions of the Gateway® derived Bla fusion constructs. C-M53 was co-expressed with N-M50 or N-M50DM, respectively. C-M99 was co-expressed with N-M94 or N-M94i13, respectively. Furthermore N-M94, N-M94i13 and C-M99 were single expressed. 24 h post transfection cells were lysed and nitrocefin was added. Mean hydrolysis rates were determined and shown as rate in milliabsorption units/min. Shown are means of at least 4 independent experiments. Error bars indicate the standard deviation. **(B)** Expression levels of N-M94 and N-M94i13 in co-transfection with C-M99 detected by anti-HA specific Western Blot analysis. Numbers on the right indicate the protein marker in kDa.

4.2.2.2 Specificity of the MCMV SEC-PCA

After the establishment of the SEC-PCA in cells the specificity of the assay was tested in the presence of increasing amounts of M99-Flag, which binds N-M94 but does not complement due to the lack of the complementary Bla fragment. If the PCA is dependent on the pM94/pM99 interaction Flag-tagged pM99 would compete with C-M99 for binding, which then should result in the decrease of the PCA signal. Therefore, M99-Flag was expressed by the expression construct pOriR6K-M99FLAG (Maninger et al., 2011). The competitor pOriR6K-M99FLAG was added to the co-transfection mixture (3 µg pO6T-N_f-M94 and 3 µg pO6T-$BlaC_f$-M99) in increasing amounts from 0.5 µg to 2 µg. Transfections mixtures were adjusted to a total amount of DNA of 8 µg by an adequate addition of carrier DNA pOriR6K-zeo-ie. As shown in Figure 15A, the PCA signal decreased in a M99-Flag concentration dependant manner. The initial hydrolysis rate of 37 milliabsorption units/min gradually reduced in presence of increasing amounts of M99-Flag by a third reflecting the relative proportion of Bla-tagged and non-Bla-tagged M99 in the assay. The amounts of N-M94, C-M99 and M99-Flag in the assay were visualized by Western Blots probed for HA- or Flag-tag, respectively (Figure 15B). All proteins were detected at the predicted sizes of 62 kDa (N-M94), 27 kDa (C-M99) and 12 kDa (M99-Flag). Protein amounts of N-M94 and C-M99 were constant in all

samples while a continuous increase of M99-Flag protein amount could be detected relative to transfected pOriR6K-M99FLAG.

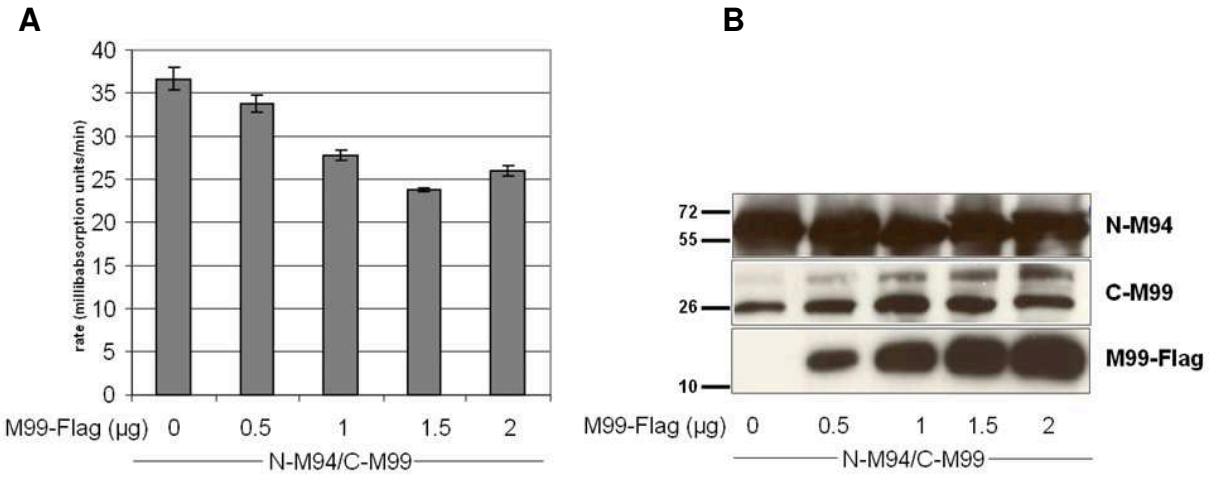

Figure 15: Specificity of the MCMV SEC-PCA. (A) Competition assay. Bla activity in cell lysates after co-expression in 293T cells. N-M94 and C-M99 (3 µg of each DNA) were co-expressed together with increasing amounts of M99-Flag. Total DNA amounts in transfections were kept constant at 8 µg by addition of carrier DNA. Mean hydrolysis rates were determined and shown as rate in milliabsorption units/min. Shown are means of triplicates. Error bars indicate the standard deviation. **(B)** Protein levels of N-M94, C-M99 and M99-Flag in the competition assay. N-M94 and C-M99 were detected by HA-specific antibody, M99-Flag by Flag-specific antibody. Sizes of the marker bands in kDa are indicated on the left.

4.2.3 pUL94 and pUL99 in the PCA

4.2.3.1 Cell-based SEC-PCA of HCMV

Because the interaction of the MCMV proteins pM94 and pM99 could be monitored by cell-based PCA there was interest to establish a HTS approach for inhibitors of the homologous interaction in HCMV. pUL94 and pUL99 were, therefore, tagged with Bla fragments by the Gateway® compatible Bla fusion plasmids as described in 4.2.1 and were subsequently sub-cloned in the pO6T vector backbone for expression. This resulted in plasmids (pO6T-N_f-UL94 and pO6T-C_f-UL99) expressing BlaN-tagged pUL94 (NUL94) and BlaC-tagged (CUL99). To determine the background signal of the PCA, pUL99 mutant lacking the amino acids 22-43 was BlaC-tagged (CUL99del). These amino acids were shown to be crucial in binding pUL94 by previous FRET analysis (Lui et al., 2009).

When NUL94 and CUL99 were co-expressed, the hydrolysis rate of nitrocefin in the cell lysates was around 90 times higher than in cells which expressed NUL94, CUL99 and CUL99del alone. The hydrolysis rate detected after co-expression of NUL94 and CUL99del was around 20% and defined the background of the PCA (Figure 16A). Protein expression levels from co-expression lysates were checked by an anti-HA specific Western Blot. All constructs were detected at their expected molecular weights (NUL94: 62 kDa; CUL99: 36

kDa; NUL99del: 34 kDa). CUL99 and CUL99del were expressed almost to the same level (Figure 16B).

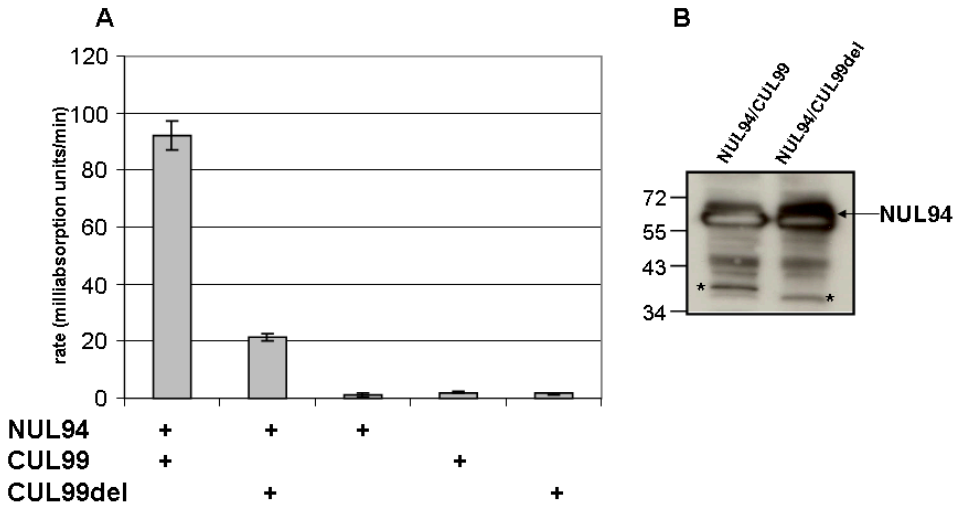

Figure 16: The cell-based SEC-PCA of HCMV. (A) Bla activity in 293T cell lysates after co- and individual expressions of the Gateway® derived Bla fusion constructs. NUL94 was co-expressed with CUL99 or CUL99del, respectively. Furthermore NUL94, CUL99 and CUL99del were single expressed. 24 h post transfection cells were lysed and nitrocefin was added. Mean hydrolysis rates were determined and are shown as rate in milliabsorption units/min. Shown are means of triplicates. Error bars indicate the standard deviation. **(B)** Expression levels of CUL99 or CUL99del (stars) in co-transfection with NUL94 detected by anti-HA specific Western Blot analysis. Numbers on the left indicate the protein marker in kDa.

4.2.3.2 Cross-complementation between the UL16 family members of MCMV and HCMV

There is only little structural information about pUL94 available to date. Soly for its MCMV homolog, pM94, it was previously shown that a small insertion mutation can completely abolish binding to pM99, the homolog of pUL99 (Maninger et al., 2011), indicating a limited interaction site and therefore a potential for small molecules to interfere. The alignment of pUL94 and pM94 (Figure 17B) showed a high sequence homology (48.4% consensus positions, 32.6% identity positions). Therefore it was interesting whether the pM94 can bind to the partner of pUL94, pUL99. Appropriate Bla fusion proteins of both viruses in heterologous pairs were co-expressed to determine their ability to cross-complement in the PCA (Figure 17A).

Co-expression of CUL99 with N-M94 resulted in a 100 times higher nitrocefin hydrolysis rate than co-expression with N-M94i13 and a 10 times higher rate than co-expression of CUL99del with N-M94, indicating that binding site is conserved between the MCMV and HCMV proteins of the pUL16 family.

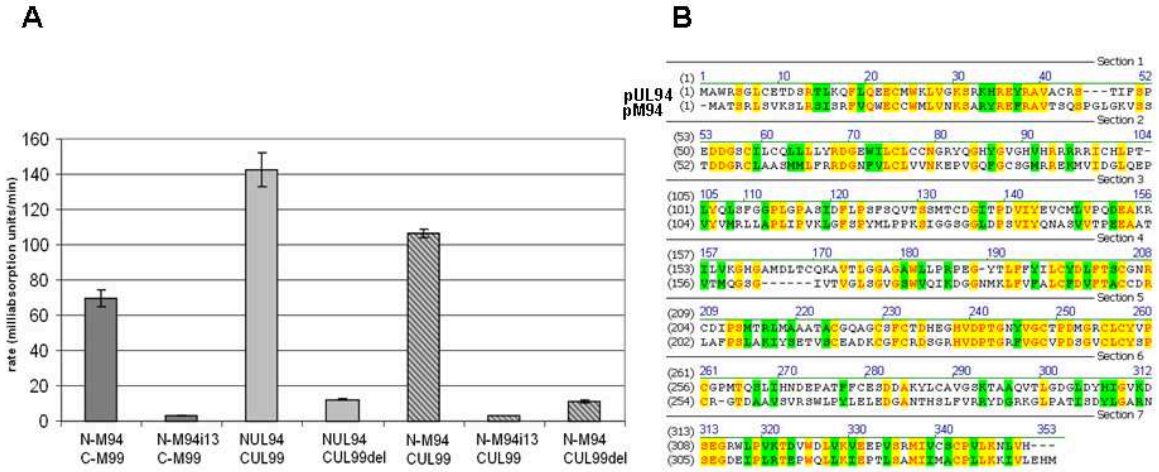

Figure 17: Binding site conservation between pM94 and pUL94. (A) Nitrocefin hydrolysis rates of lysates from homologous and heterologous co-expressions of MCMV and HCMV Bla fusion proteins of the UL16 and UL11 protein families. NUL94 was homologously co-expressed with CUL99 or non-binding mutant CUL99del (light grey bars). N-M94 or N-M94i13 was homologously co-expressed with C-M99 (dark grey bars) and heterologously co-expressed with NUL99 (striped bars). Furthermore N-M94 was heterologously co-expressed with NUL99del (striped bar). Mean nitrocefin hydrolysis rates from lysates were determined at least 4 independent experiments and shown as rate in milliabsorption units/min. Error bars indicate the standard deviation. **(B)** Sequence alignment of pUL94 and pM94. Yellow indicates identical, green similar residues.

4.2.3.3 Bla-complementation by combined single expression lysates of SEC-proteins

The major interest was to establish a PCA which can be used for high-throughput screening of inhibitory molecules for the pUL94/pUL99 interaction. According to the previously established cell-free NEC-PCA (Schnee et al., 2012) in which the complementing fusion proteins were separately expressed, I tested if NUL94 and CUL99 could complement when expressed upon separate transfection and just combined after cell lysis. Therefore, NUL94 and CUL99 were separately expressed in 293T, lysates were prepared and combined in the nitrocefin assay. To verify the background, NUL94 lysates were combined with lysates of single expressed non-binding CUL99del. Furthermore, each construct was combined with lysates of mock-transfected 293T.

Combined lysates of NUL94 and CUL99 resulted in at least 20 times higher nitrocefin hydrolysis rate than the reaction containing non-binding fragments or mock-combinations (Figure 18A). Comparable protein amounts in the lysates and equality of expression in case of CUL99 and CUL99del were verified by HA-specific Western blot (Figue 18B). Remarkably, the SEC-PCA with the combined lysates exhibited 4 times less background compared to the co-expression based SEC-PCA in 4.2.3.1. This background improvement might be a result of reduced spontaneous unspecific β-lactamase folding by the shortened time of encountering of the Bla-tagged proteins under such conditions.

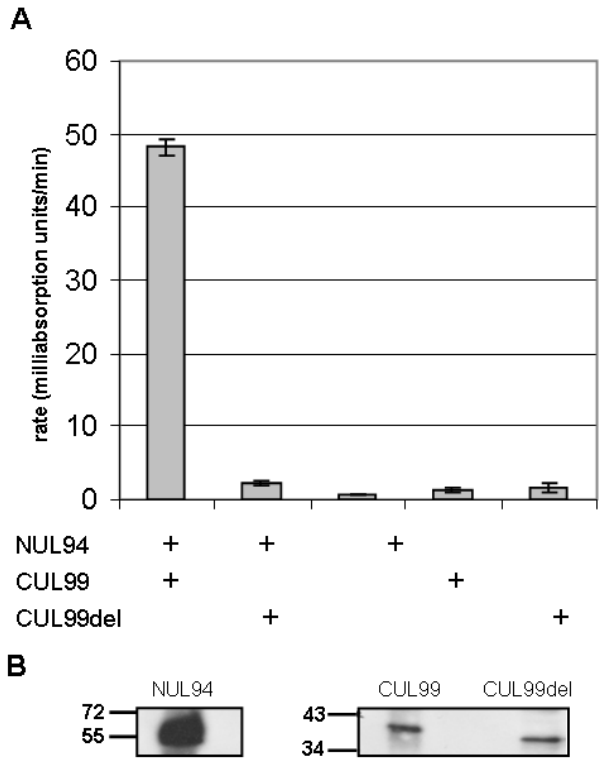

Figure 18: Bla-complementation of combined single expression lysates of SEC-PCA proteins.
(A) NUL94, CUL99 and CUL99del were single expressed in 293T cells. Cells were harvested and cell lysates were prepared as described in 3.8.1 for cell-based PCA. 25 µl of the indicated lysates were tested in combination with each other or with 25 µl of lysates from untreated 293T cells for reconstituted Bla activity. Mean nitrocefin hydrolysis rates were determined in 4 independent experiments and shown as rate in milliabsorption units/min. Error bars indicate the standard deviation.
(B) HA-specific Western Blot analysis of lysates of single expressions of NUL94, CUL99 and CUL99del in 293T. Sizes of the marker bands in kDa are indicated on the left.

4.2.3.4 The bacterial expression constructs of the SEC-PCA

High-throughput screens demand for simple approaches which can be performed in a cost-effective way. The previous experiment showed that NUL94 and CUL99 can complement when the proteins were expressed separately in 293T and lysates were combined in for PCA assay. In accordance to the cell-free NEC-PCA (Schnee et al., 2012) which uses constructs derived from bacterial expression, the components of a SEC-PCA were produced in *E.coli*. Therefore, full-length pUL99 was fused N-terminally with the HA-tagged BlaC and Glycine-Serine spacer and C-terminal with a His-tag for later purification (CUL99-His, Figure 19). As negative control, the pUL99 mutant lacking the 22 amino acids responsible for binding to pUL94 was constructed in a similar way (CUL99del-His). Full-length pUL94 was fused N-terminally to the HA-tagged BlaN fragment and a Glycine-Serine spacer and C-terminally with a His-tag (NUL94-His). All constructs were cloned into pET24 b (+)-expression vector background under T7 promotor.

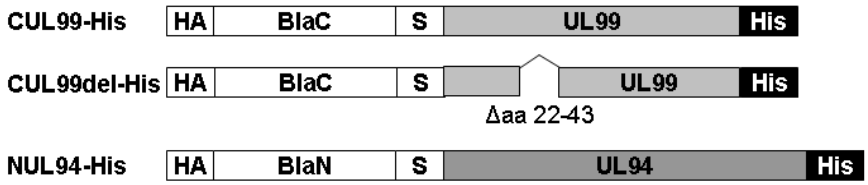

Figure 19: Schematic representation of the *in vitro* SEC-PCA constructs of HCMV. The HA-tagged BlaC was fused to full length pUL99 separated by a glycine/serine spacer (S) resulting in CUL99-His. As negative control a BlaC fusion of pUL99 (CUL99del-His) was constructed, lacking aa 22-43 of pUL99 representing the binding site to pUL94. The HA-tagged BlaN and the spacer were fused to full length pUL94 resulting in NUL94-His. All constructs carried a C-terminal His-tag for affinity purification.

4.2.3.4.1 Purification of Bla-tagged SEC proteins from bacteria

The Bla-tagged SEC-proteins were expressed in BL21-CodonPlus (DE3)-RIL and further processed as described in 3.7.1. Bacterial cultures (2.5 l) were lysed by sonification (3.7.2) and applied to Ni^{2+}-affinity purification for the recombinant proteins (3.7.3). Protein elutions (1.5 ml) were analyzed by Coomassie-stained SDS-PAGE and HA-specific Western blot for purity and protein amounts.

The protein concentration derived from elutions of NUL94-His was about in 2 mg/ml. For the deletion mutant CUL99del-His, the protein yield was around 2 times higher (1.7 mg/ml) than that of the wildtype version CUL99-His (0.8 mg/ml). The Coomassie stained gels showed beside the specific bands for all three recombinant proteins several impurities (Figure 20A). Thereby, contamination of CUL99del-His appeared stronger than of CUL99-His. In the HA-specific Western Blot (Figure 20B), pUL99 constructs were detected at their predicted sizes of 34 kDa (CUL99-His) and 32 kDa (CUL99del-His) in equal amounts, confirming that the difference in protein yields resulted from larger background impurities in CUL99-His elutions. NUL94-His, which was expected at a size of 61 kDa on the Western blot, was detected as a smear between sizes of 50 to 70 kDa, which might reflect some protein degradation.

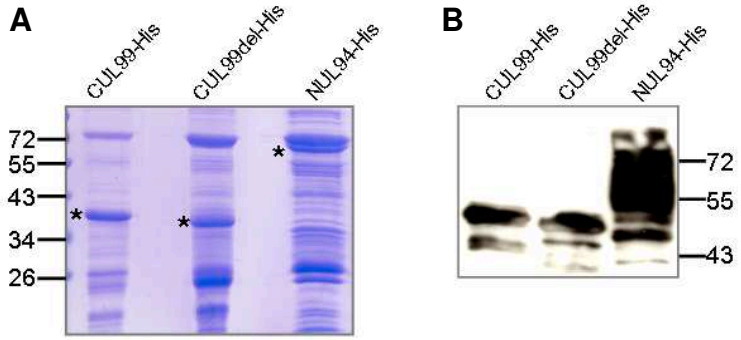

Figure 20: Bacterial expression of Bla-tagged SEC proteins of HCMV. (A) Coomassie stained SDS-PAGE with samples after Ni^{2+}-NTA purification from the expressed CUL99-His, CUL99del-His and NUL94-His. 10 µl of the elutions were loaded on a 12% SDS gel. Black stars mark the positions of the recombinant proteins. Sizes of the marker in kDa are indicated on the left. **(B)** Western Blot analysis of the protein elutions from CUL99-His, CUL99del-His and NUL94-His. 10 µl of each protein elution was separated by SDS-PAGE, blotted and immunodetected with anti-HA specific antibody. Sizes of the marker in kDa are indicated on the right.

4.2.3.4.2 Bla complementation of prokaryotic expressed fusion proteins

In order to determine whether the bacterial derived Bla-tagged fusion proteins could replace eukaryotic expressed in the SEC-PCA, they were tested for Bla complementation in a nitrocefin assay. Therefore, 25 µl of the NUL94 elution were combined with 25 µl of the CUL99-His or CUL99del-His elution, respectively. Furthermore, 25 µl of 293T lysates expressing NUL94, CUL99 or CUL99del were combined with the respective bacterial elutions or with another and nitrocefin hydrolysis was determined (Figure 21).

Combinations including bacterial derived NUL94-His showed no significant difference in nitrocefin hydrolysis when using corresponding fragments for positive and negative binding. However, eukaryotic derived NUL94 could complement with eukaryotic (CUL99) confirming the results described the previous chapter. Interestingly, the BlaC-tagged pUL99 (CUL99-His) derived from prokaryotic expression, showed a significant complementation compared to the non-binding pUL99 controls (CUL99del or CUL99del-His, respectively) when it was combined with NUL94 expressed in eukaryotic cells.

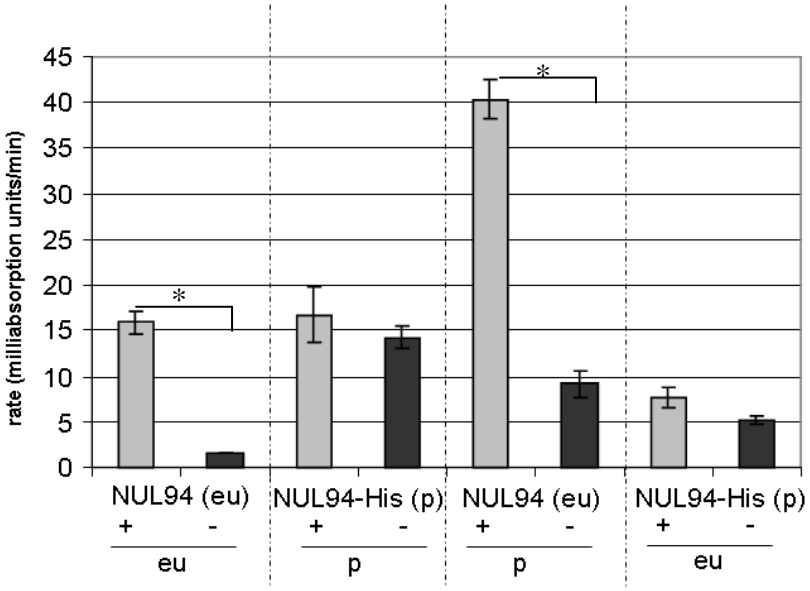

Figure 21: Bla complementation of recombinant expressed SEC-PCA proteins. Bla activity after combing eukaryotic (eu) and prokaryotic (p) expressed SEC-PCA proteins. 25 µl of a lysat from 293T cells expressing NUL94 or 25 µl of NUL94-His elution were combined with 25 µl of lysates or elutions of CUL99 (+eu), CUL99-His (+p), CUL99del (-eu) and CUL99del-His (-p), respectively. Mean nitrocefin hydrolysis rates were determined in at least 5 independent experiments and shown as rate in milliabsorption units/min. Error bars indicate the standard deviation. Significance (*) was calculated by student's t test ($p<0.002$).

These data showed that the PCA approach developed for characterization of the core interaction of the NEC proteins can be transferred to other essential viral protein interactions.

4.3 HTS of a compound library

The HTS to identify inhibitors of the pUL50/pUL53 core interaction was performed with the standardized conditions for the *in vitro* NEC-PCA (iPCA) and the beta-lactamase counter-screen as described in chapter 4.1.2.

Briefly, preplated compounds were reconstituted in 10 µl DMSO for 30 min, before the iPCA was peformed in a total volume of 200 µl with fixed amounts of NUL50-His and CUL53-His proteins (4.1.2.1). The reaction was stopped after 40 min of incubation at 37 °C by addition of potassium clavulante and nitrocefin turnover was determined by absorption measurement at 495 nm. Inhibitory compounds from the iPCA were re-tested in a nitrocefin hydrolysis assay with added β-lactamase exhibiting the same activity as the Bla in the iPCA to exclude direct inhibitors of the reporter enzyme.

4,000 structurally highly diverse potentially non-toxic compounds with pharmacological properties were selected from a small-molecule library containing 30,000 individual heterocyclic structures (Bauer et al., 2011). This library has been already tested for toxicity in different mammalian cell lines (Caco-2, HeLa, A549 and A431) (Bauer et al., 2011) therefore rational selection against highly toxic compounds was possible. This pre-selected library was provided by EMC microcollections (Tübingen). Non-toxic known beta-lactamase inhibitors, however, were not filtered out and provided an internal control in all stages of the subsequent screening. To increase cost- and time-effectiveness, major parts of the library were plated in a first screening round in a compressed format consisting of combinations of 5 compounds per well and different concentrations in 6 different structural groups (Screening scheme is shown in Figure 22A). From this pre-screening results 4,000 compounds were selected for a second screening round of single compounds per well in fixed concentration (10 µM, Figure 22B).

In both screening phases the iPCA was performed in 96-well format. Thereby, 80 wells on each plate were filled with compounds dissolved in 10 µl DMSO, in 14 wells the control reaction was performed (in presence of 10 µl DMSO) and 2 wells harboured potassium clavulanate to reflect total inhibition of the reaction. For evaluation, the absorption at 495 nm in the compound wells (mean values of duplicates in the second phase of screening) was set relative to the mean value of absorption at 495 nm of the 14 control reactions (100%) on the corresponding plate.

99 compounds were identified that displayed >33% signal reduction (Figure 13B). Total inhibition of the reaction by potassium clavulanate resulted in ~80% signal reduction (data not shown). Compounds were tested further in a counter-screen for direct effects on the β-lactamase reporter. 97 compounds showed inhibitory effects including also already known beta-lactamase inhibitors, which confirmed the reliability of the selection schedule. On the other hand, this test confirmed the specificity of two compounds which inhibited the iPCA but not the β-lactamase. Therefore, these two compounds were selected for further analysis of their effective inhibitory concentration on the pUL50/pUL53 interaction in the PCA.

A

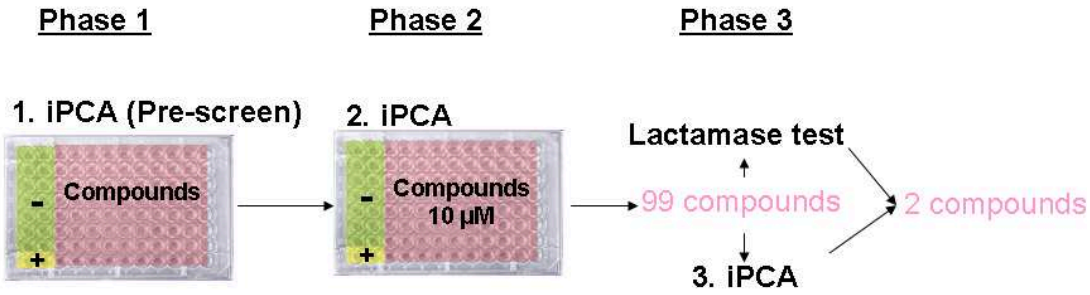

B

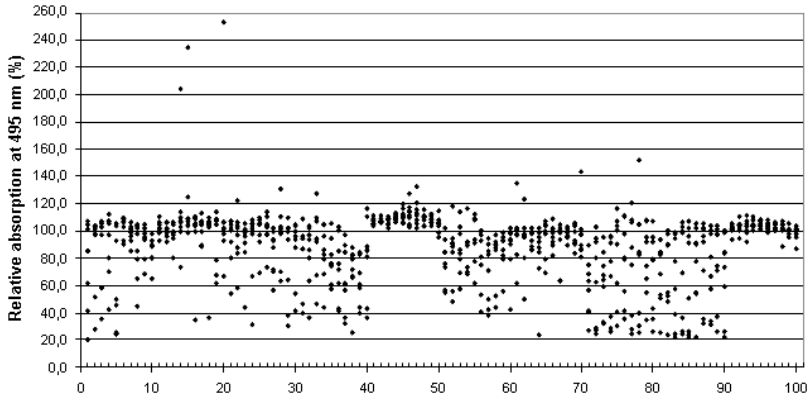

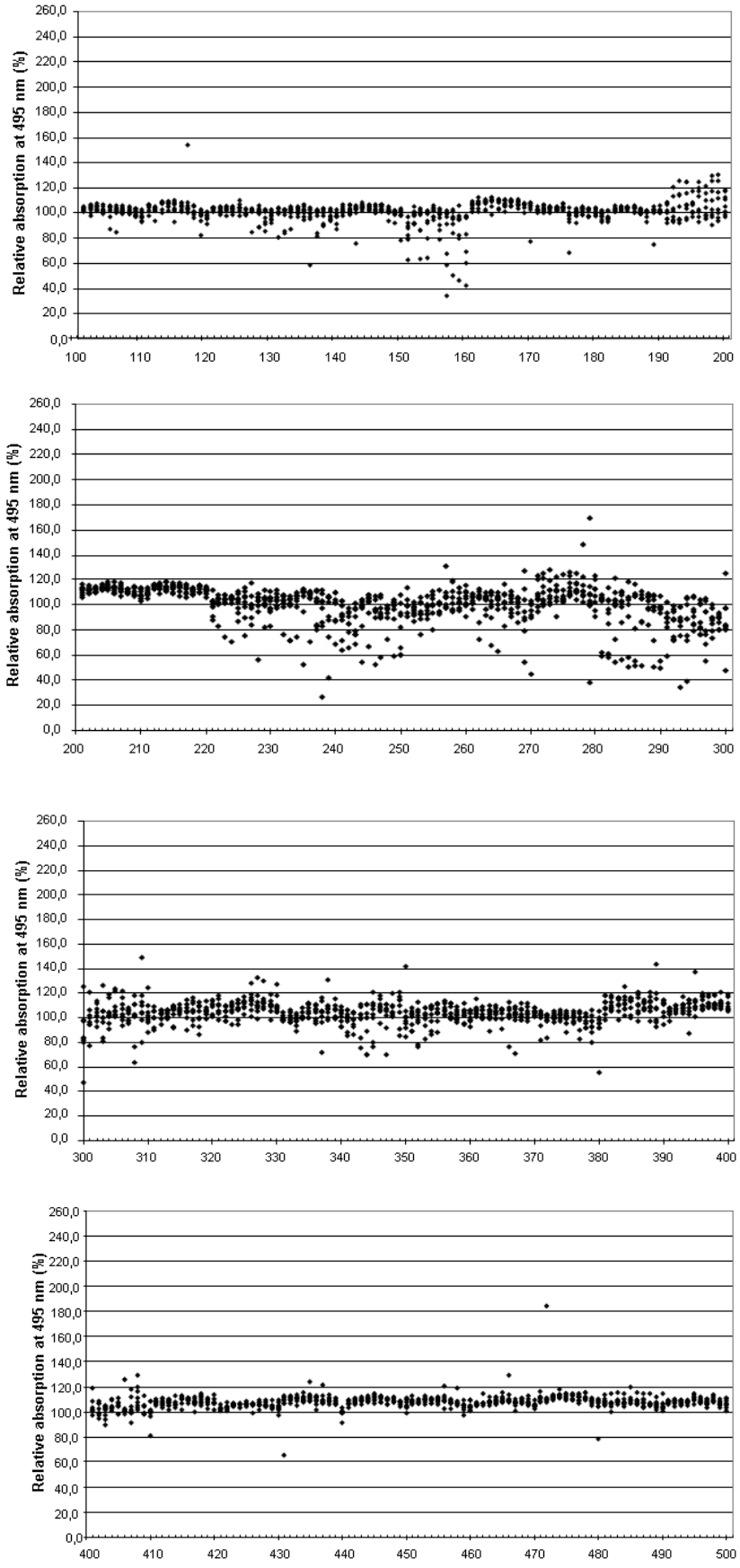

Figure 22: HTS of the *in vitro* NEC-PCA (iPCA) in the compound library. (A) Screening scheme. Compounds were screened in three consecutive phases in 96-well format. In the pre-screen phase,

compound mixes in three different concentrations (50 µM, 10 µM, 5 µM) were tested in duplicates in the iPCA for pre-selection. In the second phase, 4,000 single compounds in 10 µM concentration were tested in the iPCA. The 99 hits from the second phase were counter-screened for β-lactamase inhibition and an iPCA for verification, identifying finally 2 specific inhibitors. (-) indicates wells of the control reaction, (+) indicates wells containing potassium clavulanate (10 µM; 100% inhibition) to reflect total inhibition. **(B)** Scatter blots of the second phase single compound screen with iPCA. Numbers on the x-axis indicate column numbers. Each column reflects values of 8 compounds in the screen. Values are means of independent duplicates and are normalized to the control reaction (100%).

4.3.1 IC_{50} determination of candidate compounds

The chemical structures which were identified as inhibitors of the pUL50/pUL53 core interaction by the HTS are shown in Figure 23A. The two compounds, designated here as 30E06 and 30E07, are structurally related and belong to the same chemical class. To determine IC_{50} values of the two compounds, Bla-activity was measured after application of different compound concentrations to the iPCA in relation to mock control (Figure 23B). Values were fitted into a dose-response curve by the program GraphPad Prism 4.0 and half inhibitory concentration (IC_{50}) was calculated. The IC_{50} of 30E06 was 4.61 µM and the IC_{50} for the 30E07 was 10.29 µM, respectively.

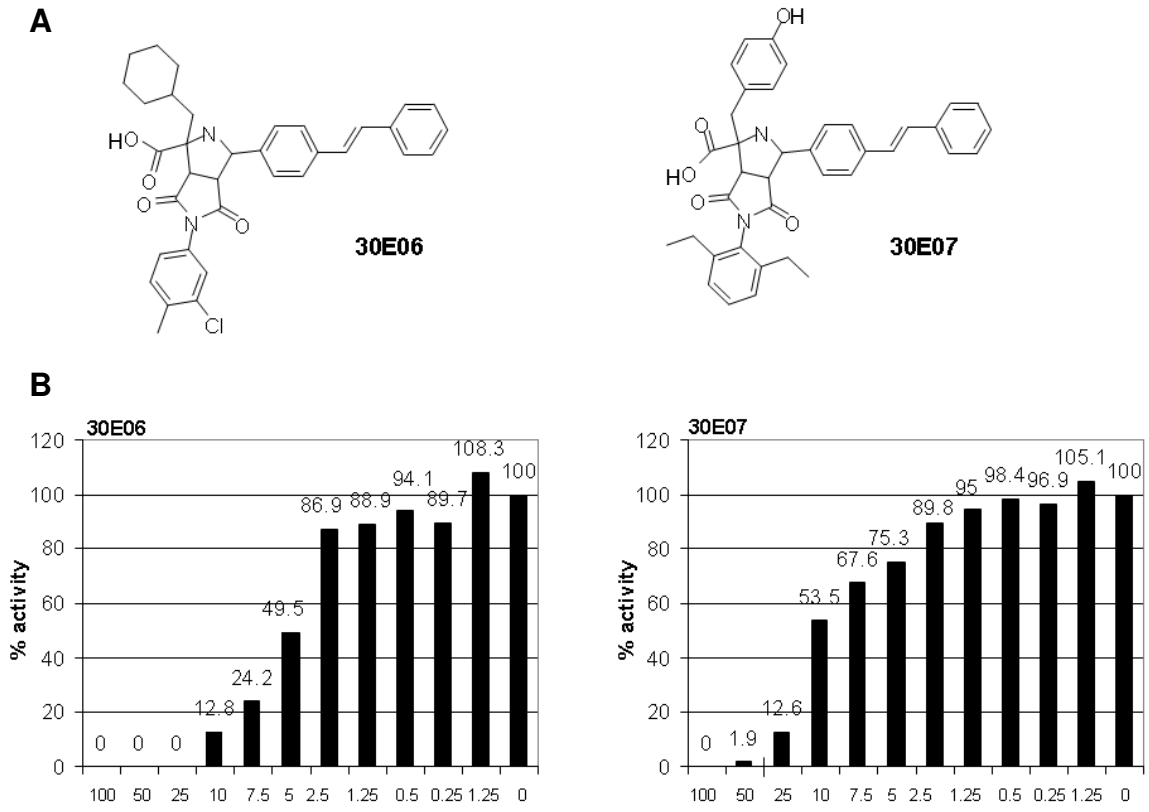

Figure 23: IC_{50} analysis of candidate inhibitors of the pUL50/pUL53 interaction. (A) Chemical structures of the candidate inhibitors designated 30E06 and 30E07 are indicated. **(B)** The standardized *in vitro* NEC-PCA (iPCA) was incubated with different concentrations (in µM) of candidate compounds 30E06 and 30E07 and Bla-activity was measured and set into relation of mock control (100% activity). Shown are means of duplicates.

In this experiment the half-inhibitory concentration of candidate compound 30E06 was about 50% of that of candidate compound 30E07. This assay confirmed that the conditions used in the screen were well chosen and the detailed iPCA test confirmed the inhibitory potential of both compounds.

4.4 Characterization of the inhibitory effect of the HTS-hits in the biological context

4.4.1 Influence of the HTS-hits on the viability of cultured cells

In order to determine the maximal tolerated concentrations of the compounds 30E06 and 30E07 applicable in further experiments, cytotoxicity assays were performed as described in 3.5.4 testing primary MEF and HFF cells (Figure 24) and U2OS and 293T cell lines. The viabilities of the treated cells measured by their reducing potential were compared to the values observed on untreated cells on the corresponding day. As depicted in Figure 15, the 30E06 was non-toxic on MEF and HFF cells up to a concentration of 25 µM, whereas in the highest tested concentration (100 µM) a significant drop of reducing potentials were detected on both cell types. Furthermore, 50 µM 30E06 had a similar effect on MEF cells. For 30E07 differences to untreated cells were not found even in the highest tested concentration of 100 µM either on MEF or HFF cells. The established cell lines we used grew continuously with one doubling a day. Therefore, we measured viability only at one time point spanning about three cell divisions. Since their significantly higher metabolic activity we also expected them to be more vulnerable in the viability assay as primary cells. Accordingly for the U2OS and 293T cell lines, the toxicity was tested after 3 days post application of the compounds. 30E06 was non-toxic on both cell lines only up to concentrations of 10 µM, while 30E07 was non-toxic up to 50 µM concentration (data not shown). This data showed us that 30E07 can be used between in 50-100 µM concentration depending on whether the assay is carried out on primary cells or cell lines, whereas the 30E06 compound could only be used in primary cells up to a concentration of 25 µM.

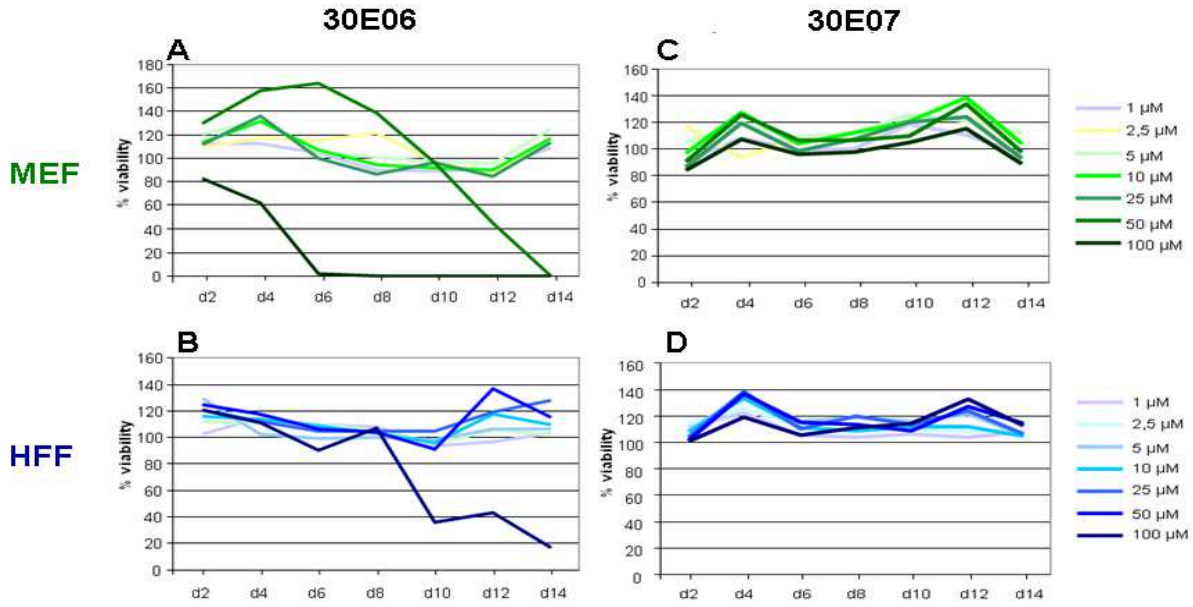

Figure 24: Effects of candidate compounds on viability of primary fibroblasts. Different concentrations of compound 30E06 were incubated on MEF **(A)** or HFF **(B)** and cell proliferation was tested in a two day intervals by application of CellTiter96®Aq_{ueous} One Solution (Promega) and 1 h incubation at 37 °C. Same was done for candidate compound 30E07 (**C** and **D**). DMSO concentration was maintained to 1% in each well. Days (d) post compound application are shown on the x-axis and viability is given in % (normalized mean absorptions at 490 nm of cells with compound/ normalized mean absorptions at 490 nm of mock treated cells) on the y-axis.

4.4.2. Inhibition of pUL50/pUL53 interaction in cell-based assays

Next, HTS-hits were tested for their ability to disrupt the pUL50/pUL53 interaction in the cellular context. Due to its lower cellular toxicity the tests were performed using only 30E07. The minimal cell-toxic concentration of 30E06 was close to its half inhibitory concentration in the NEC-PCA, therefore this compound could not be tested in these assays because its specific effects could not be separated from unspecific toxicity.

4.4.2.1 Candidate compound 30E07 inhibits in the cell-based NEC-PCA

First, 30E07 was tested for its inhibitory potential in a cell-based NEC-PCA which was previously established in our lab (Schnee et al., 2006). In contrast to the cell-free NEC-PCA setting, constructs of the cell-based PCA setting involved the full-length versions of pUL53 and pUL50 and are performed in 293T cells. BlaN-tagged pUL50 (NUL50) was co-expressed with BlaC-tagged pUL53 in 293T cells in absence (+DMSO) and presence of the 50 µM of 30E07 (+30E07). 24 h post transfection Bla activity was determined by the rate of nitrocefin hydrolysis (see Figure 25A). For background determination, single expressions of both fusion proteins were included.

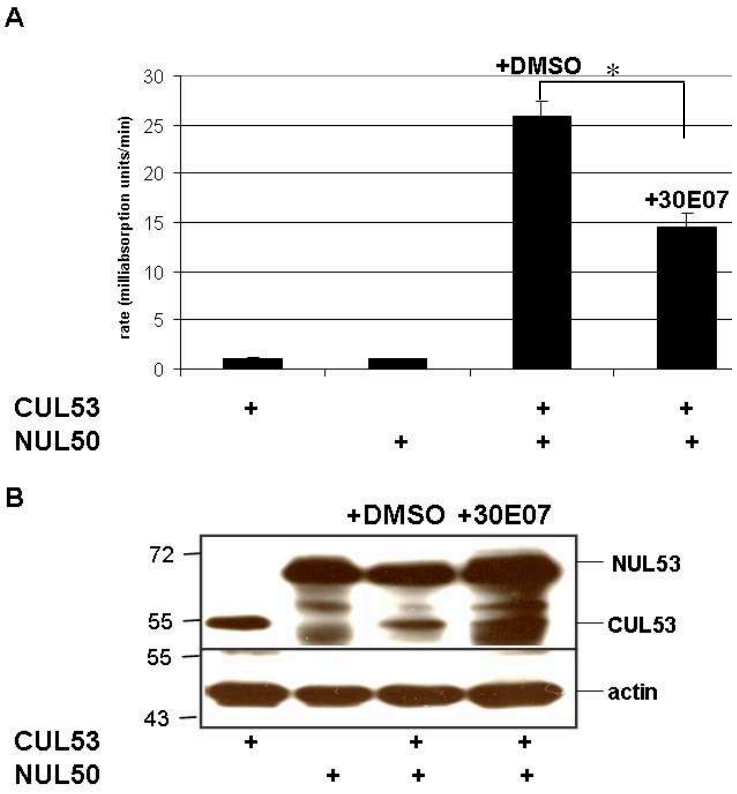

Figure 25: Effect of 30E07 in cell-based NEC-PCA.
(A) Bla activity in cell lysates after single and co-expression in 293T. CUL53 and NUL50 were single and co-expressed in 293T. 6 h post transfection medium was exchanged in the co-expressions to medium containing 50 µM 30E07 (+30E07) or medium containing 0.5% DMSO (+DMSO) as control. After further 16 h of expression, cells were lysed and Bla activity was determined by nitrocefin hydrolysis. Error bars indicate standard deviation. Significance (*) was determined by student's t test ($p<0.02$).
(B) Protein expression levels in the 293T lysates. 5 µl of each lysate was separated by SDS-PAGE (12%), blotted and immunodetected by anti-HA (upper blot) and anti-actin antibody (lower blot).
Numbers on the left indicate the protein marker in kDa.

Background Bla activity in single expressions lysates was low (~4%). Bla activity in lysates from 30E07-treated cells was reduced to around 54% compared to mock-treated co-expressions. In order to exclude signal reduction was due to decreased protein expression, lysates were analyzed by Western Blot specific to the HA-tag present in both fusion proteins (Figure 25B). Thereby, it was shown that expression of the PCA components were not reduced by the drug treatment, suggesting a direct inhibitory effect of 30E07 on protein-protein interation in the cell-based NEC-PCA. On the other hand, these data also confirm the lack of unspecific toxicity after application of 30E07 at 50µM concentration for 293T cells.

4.4.2.2 Candidate compound 30E07 abrogates co-localization of pUL50 and pUL53 in the nucleus

The viral components of any studied NECs are co-localized at the nuclear rim after their co-transfection (Dal Monte et al., 2002; Muranyi et al., 2002). If the core NEC interaction between the pUL50 and pUL53 (or their homologs) is hindered, the pUL53, as its all studied homologs, should de-localize to show a diffuse nucleosolic appearance (Dal Monte et al., 2002; Lotzerich, Ruzsics, and Koszinowski, 2006). In order to determine, if candidate compound 30E07 effects co-localization of pUL50 and pUL53 in the cell, a confocal immnofluorescence analysis was performed. To this end, pUL50 with a C-terminal HA-tag (UL50HA) and pUL53 with an N-terminal Flag-tag (FlagUL53) were co-expressed in U2OS cells in presence and absence of 30E07. As controls, proteins were also expressed alone.

After 24 h of incubation samples were stained for indirect immunofluorescence and the results are shown in Figure 26.

Co-transfection experiments in absence of the candidate compound 30E07 (DMSO) showed the expected co-localization of both proteins at the nulear rim. However, co-expression of both proteins in presence of the candidate compound 30E07 showed homogenous distribution of pUL53 in the nucleus comparable to the result of pUL53 expression in isolation, while pUL50 still located at the nuclear rim.

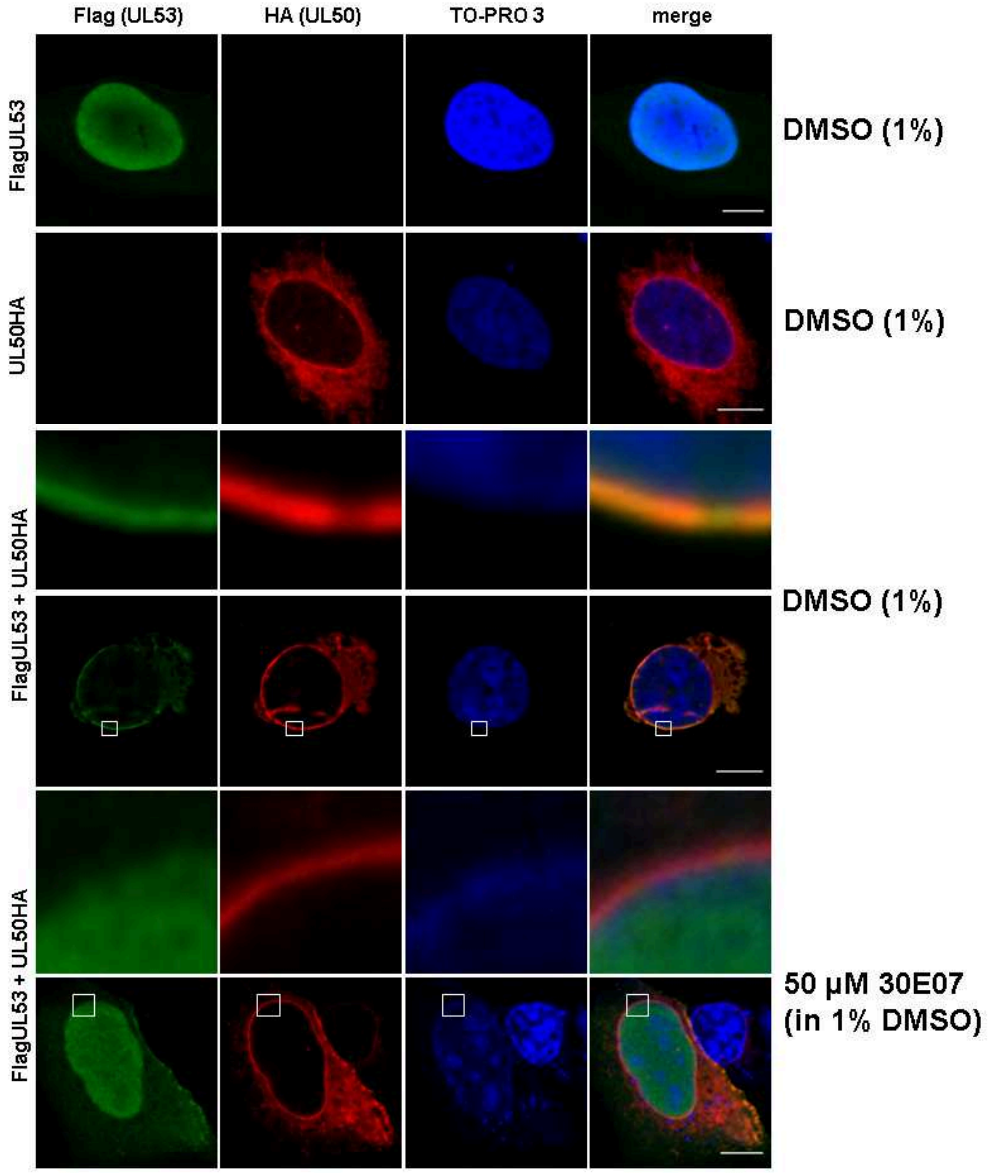

Figure 26: Effect of 30E07 on cellular localization of pUL53 and pUL50. U2OS cells were single (first two columns) or co-transfected with pOriR6K-Flag-UL53 and pOriR6K-UL50-HA on 8 well µ-slides (Ibidi) with FuGene transfection reagent (Roche). 6 h post transfection DMSO (control) or candidate compound 30E07 was added. Cells were further incubated at 37 °C for 18 h before they were fixed and processed for immunofluorescence. Flag specific antibody was used to visualize Flag-tagged pUL53, HA-specific antibody for HA-tagged pUL50. Cell nuclei were counterstained with TOP-PRO 3. Scale bars indicate 10 µm.

We therefore concluded that the compound - similar to the *in vitro* screen - also blocked the pUL50/pUL53 interaction in cells and in the nucleus.

4.4.3 Characterization of the antiviral activity of the screening hits

4.4.3.1 30E06 and 30E07 show dose-dependent antiviral activity against HCMV

To test the screening hits 30E06 and 30E07 for direct antiviral activity we utilised the HCMV-Luc reporter assay (3.6.4). Here, the spread of a Luc expressing recombinant HCMV can be monitored by increase of the Luc expression over time (Scrivano et al., 2011). To this end, HFF cells were infected at a low MOI (0.01 pfu/cell for 1.5 h) with the HCMV reporter virus. The infected cultures were incubated up to 2-8 days with normal medium or medium containing different concentrations of 30E06 and 30E07. Cells were lysed at 2, 4, 6 and 8 days after infection and luciferase activity of the cell extracts was determined by direct luminometery (Figure 27).

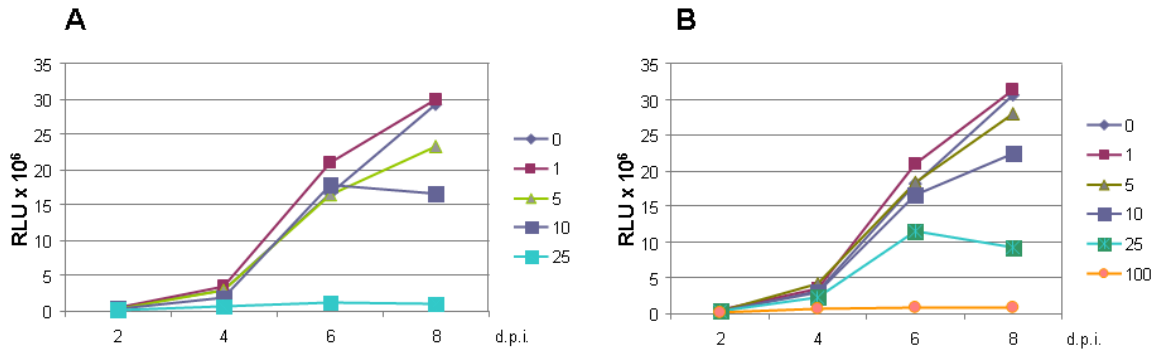

Figure 27: Antiviral effects of 30E06 and 30E07 on HCMV reporter virus. HFF cells were infected with the HCMV reporter virus TB40-Luc expressing the firefly luciferase at an MOI of 0.01 pfu/cell and incubated with different concentrations of **(A)** 30E06 or **(B)** 30E07 for up to 8 days. Luciferase activity was determined every second day in cell lysates on a luminometer. Shown are means of triplicates. Numbers on the right indicate compound concentrations in µM.

Lysates of non-treated infected HFF (0 in Figure 18 A and B) showed the expected increase of luciferase signal over the time. In contrast, no increase of infection induced luciferase activity was observed in the presence of either 30E06 (Figure 27A) or 30E07 (Figure 27B) at the highest non-toxic concentrations resembling a complete block of viral replication. Treatment with lower compound concentrations resulted in a dose-dependent decrease of the slope of the rising luciferase expression indicating dose-dependent limitation of virus spread.

4.4.3.2 30E06 and 30E07 reduce release of infectious virus into supernatants

To verify the antiviral effect of the candidate compounds 30E06 and 30E07 observed in HCMV-Luc reporter assay both compounds were next tested in a plaque reduction assay. To this end, HFF were infected with TB40-BAC4 at an MOI of 0.2 pfu/cell and then treated with the compounds in the highest non-toxic concentrations or with 1% DMSO (mock). Supernatants of the infected cultures were collected distinct days post infection until day 8. The amount of released infectious virions was quantified by plaque assay after titration. Results are shown in Figure 28. As expected, viral titers in supernatants of mock-treated (1% DMSO) infected cells constantly increased over time of infection. Compared to that, around 100 times less infectious virus could be detected in supernatants of 30E06 treated infected cells. Furthermore, no infectious virus could be found in supernatants from infected cells treated with 30E07 implying a complete block of viral replication.

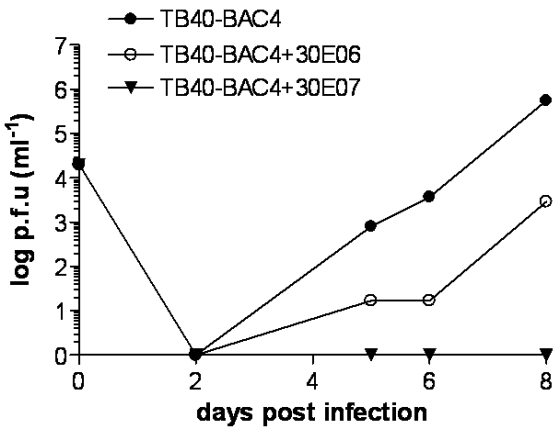

Figure 28: Growth characteristics of HCMV (TB40-BAC4) in presence of candidate compounds. HFF cells were infected with TB40-BAC4 at an MOI of 0.2 for 1.5 h and then treated with medium containing the highest non-toxic doses of 30E06 (final concentration: 25 µM) and 30E07 (final concentration: 100 µM) or DMSO (1%) as control. Supernatants were harvested at indicated days and viral titers were determined by TCID50 assay.

Due to the more desirable toxicity profile of 30E07 (4.4.1), further studies on the lead compounds were performed with 30E07.

4.4.3.3 30E07 moderately reduces expression of viral proteins

To explore the mode of action of 30E07, effects on viral protein expression in general were determined. To this end, HFF cells were infected with HCMV-TB40-BAC4 at an MOI of 0.2. The infection was allowed to proceed in absence (-) and presence (+) of 100 µM 30E07 for 24, 48, 72 and 96h. Infected cells were harvested and processed for Western blotting. Then, the presence of representative virus proteins expressed by immediate-early (IE), early (E) and late (L) kinetics were determined. As depicted in Figure 29, the levels of HCMV IE1 (IE), UL44 (E) and gB (L) proteins were analyzed. The levels of all three viral protein classes were

moderately reduced in the drug treated aliquots. Notably, the levels of IE1 proteins were affected only as late as 72h post infection. These results suggested that 30E07 affected mildly the viral gene expression in general. Alternatively mainly HCMV DNA replication and thus the expression level of late proteins which depend upon DNA replication could be affected. As to be expected from an inhibitory effect on a very specific step in morphogenesis, the extent of the 30E07 induced reduction of the viral protein expression was mild in comparison with the magnitude of the strong plaque reduction induced by the treatment.

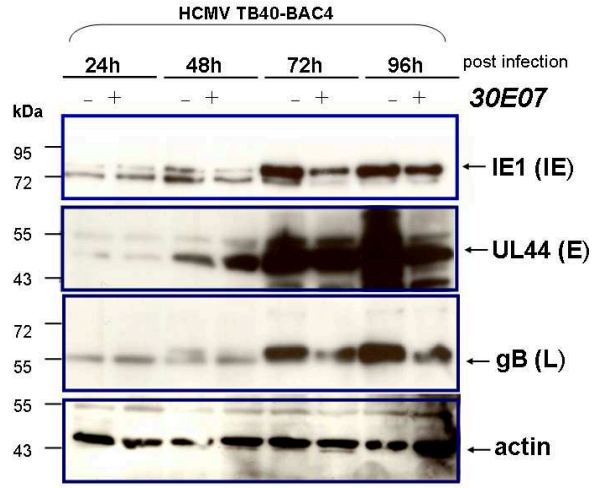

Figure 29: Effect of 30E07 on viral protein expression levels. HFF were infected with TB40-BAC4 at an MOI of 0.2 pfu/cell. The infection was allowed to proceed in absence (-) and presence (+) of 30E07 (100 µM). At different time points cells were harvested and processed for Western blotting. Representative HCMV IE, E or L proteins (right) were visualized using respective antibodies. Cellular β-actin served as a loading control. Numbers on the left indicate the protein marker in kDa.

4.4.3.4 30E07 inhibits viral DNA replication

The moderate reduction of viral protein levels by 30E07 treatment (4.4.3.3) could indicate an effect on DNA synthesis. To test this, the kinetics of viral DNA accumulation after infection was monitored in the presence of 30E07 and compared to samples which were treated with a specific polymerase inhibitor Foscarnet (PAA) or left untreated. Thus, HFF cells were infected with TB40-BAC4 at an MOI of 0.2 and overlaid with medium containing 1% DMSO, PAA (300 µg/ml) or 30E07 (100 µM), respectively. Total DNA was extracted from infected cells at different time points between 6 to 96 h after infection and the copy number of viral DNA was quantified using real-time PCR (3.3.11).

	6 h p.i.	24 h p.i.	48 h p.i.	72 h p.i.	96 h p.i.
DMSO	0.24	0.25	14.25	226.48	582.07
PAA	0.49	0.30	0.48	0.34	0.33
30E07	0.31	0.28	1.70	2.16	1.80

Table 2: Synthesis of HCMV-DNA in presence of PAA or 30E07. HCMV TB40-BAC4-infected cells were treated with DMSO, Foscarnet (PAA), or 30E07. Total intracellular DNA was harvested during a period of 96 h postinfection as indicated, and viral progeny DNA was measured by quantitative real-time PCR (see methods 3.3.11). Values indicate UL54 gene copy numbers in relation to the cellular gene GAPDH copy numbers that served as standard.

As control, the viral DNA polymerase inhibitor PAA exerted, as expected, a strong inhibitory effect on the accumulation of viral DNA between 48-96 h post infection (Table 2). Cells treated with 30E07 showed a less but still quite impressive inhibition of viral DNA synthesis. Thus, the 30E07 induced inhibition of viral protein expression is explained by the inhibitory effect on viral DNA replication.

4.4.3.5 Analysis of ultrastructural phenotypes induced by 30E07

30E07 affected HCMV DNA replication to some extent. However, this alone did not yet explain the complete inhibition of viral particle production at the effective concentration. To analyze the effect of 30E07 on viral morphogenesis, late-stage TB40-BAC4-infected HFF grown in absence and presence of 30E07 by electron microscopy were analyzed. To reduce the effect of 30E07 on DNA replication (see 4.4.3.4) and to make later steps of morphogenesis visible, the drug was added 3 days post infection, at a stage at or beyond the start of viral DNA synthesis.

4.4.3.5.1 30E07 increases number of A-capsids in the nucleus

HFF cells were infected at an MOI 1 with TB40-BAC4 and incubated for 3 days. Then the medium was exchanged to 30E07-containing medium (conc. 100 µM) or medium containing 1% DMSO (control, no drug). Infected cells were further incubated for 2 days and then fixed and prepared for EM (3.9).

To examine 30E07-induced effects on virus capsid maturation and fate, cell nuclei were analyzed for appearing capsid types. As expected, empty A, proteolytically cleaved B-, and DNA-filled C-capsids were readily detected in cells without drug-treatment (Figure 30 and Table 3; for further information (Yu et al., 2005)). In 30E07 treated cells, the number of C-capsids was markedly reduced, while the contingent of A-capsids increased (Figure 30 and

Table 3). The percentage of B-capsids remained constant, indicating a non-disturbed scaffold maturation. Altogether, the proportional increase of A-capsids indicated a defect before or during the cleavage/packaging process (Yu et al., 2005).

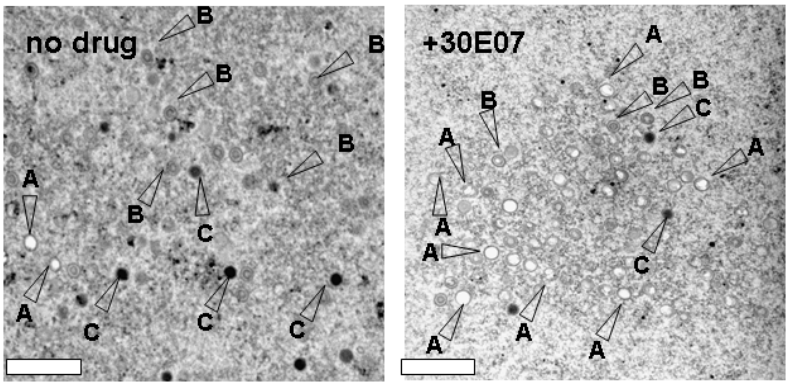

Figure 30: Ultrastructural analysis of effect of 30E07 on nulcear capsid formation. Transmission electron micro-graphs of ultrathin section preparations of TB40-BAC4-infected HFF cells. Medium containing DMSO (no drug) or drug (30E07, 100 µM) was applied 3 days post infection. Cells were fixed 5 days post infection and prepared for electron microscopic analysis. Representative images from the nucleus are shown for both treatments. Arrows indicate A-, B- and C-capsids, respectively. Scale bars: 500 nm.

Virus and treatment	No. of nuclei counted	Capsid type per nucleus (%)		
		A	B	C
TB40-BAC4 alone	7	6	57	37
TB40-BAC4 with 30E07	8	31	57	12

Table 3: Effect of 30E07 on HCMV capsid formation.

4.4.3.5.2 The effect 30E07 on nuclear egress cannot be shown in the viral context

Specific inhibitors of the NEC formation by interfering with the interaction of pUL50/pUL53 or their homologs should mainly provoke a reduced or blocked nuclear particle egress in alpha herpesviruses. A combined effect on DNA cleavage/packaging and on nuclear egress was expected in beta herpesviruses. Therefore the frequency of cytosolic capsids and the ratio between the nuclear and cytosolic capsids were analyzed. Viral assembly complexes in the cytoplasm could be found in treated and untreated cells (Figure 31) indicating that the cytoplasmic maturation machinery (Sanchez et al., 2000) is formed in the presence of the drug.

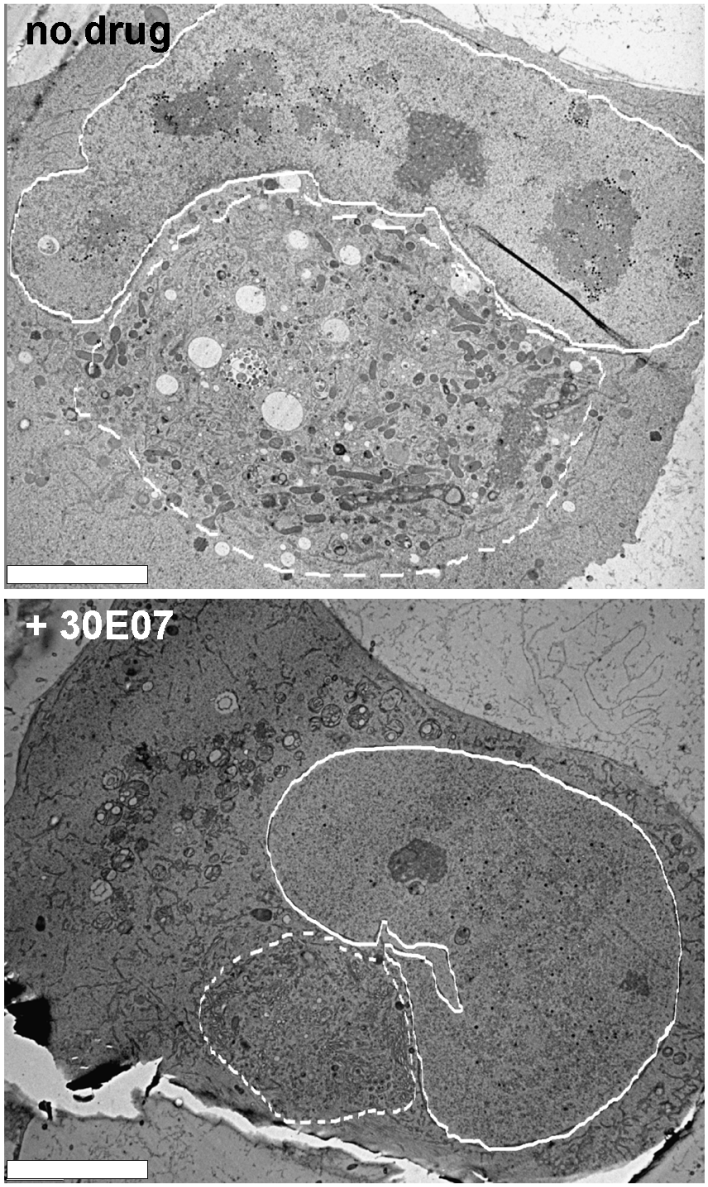

Figure 31: 30E07 does not affect generation of viral assembly compartment in the cytoplasma. Representative electron microscopic images of cytoplasms of DMSO-treated (no drug) and drug-treated (+30E07) TB40-BAC4-infected HFF cells. Continous lines indicate the nucleus, dashed lines the viral assembly compartment. Scale bars: 5 µM.

With respect to total numbers the amount of cytoplasmic capsids was strongly reduced in the presence of 30E07 compared to the untreated HCMV infected cells. The ratio between C-capsids appearing in the cytoplasm (CyC) and C-capsids in the nucleus (NuC) in DMSO and drug-treated cells was quantified from the electron micrographs (Table 4). There was a clear reduction of the total number of capsids in nucleus and cytoplasm. Notably, there was no difference between the treated and untreated cells with respect to the ratio of nuclear and cytosolic capsids. At first sight, these data did not support the notion that 30E07 inhibited export of nuclear capsids. Yet, given that 30E07 was added as late as 3 days post infection, it could not be excluded that these few cytoplasmic capsids may represent stages of morphogenesis prior to the addition of the drug.

TB40-BAC4 infection

no drug		+30E07	
Nuclear C-capsids (NuC)	Cytoplasmic C-capsids (CyC)	Nuclear C-capsids (NuC)	Cytoplasmic C-capsids (CyC)
561	45	23	7
203	25	17	2
82	14	48	2
210	8	49	3
CyC/NuC	8.7 %	CyC/NuC	8.8 %

Table 4: Ultrastructural analysis of effect of 30E07 on egress of nucleocapsids. Quantification of nuclear and cytoplasmic C-capsids in drug treated and untreated HFF cells 5 days post infection. 4 cells were analyzed for each treatment.

4.4.3.5.3 30E07 does not affect secondary envelopment

To investigate potential effects of 30E07 on morphogenesis steps further downstream in the viral replication cycle, the cytoplasm of infected cells untreated and treated with 30E07 were analyzed for cytoplasmic capsid envelopment (Figure 32). The overall number of C-capsids in the cytoplasm was low compared to mock-treated infected cells (also see 4.4.3.5.2). Yet, C-capids which could be found in the cytoplasm of drug-treated cells were regularly enveloped like in non-treated cells, excluding that 30E07 affected the secondary capsid envelopment step.

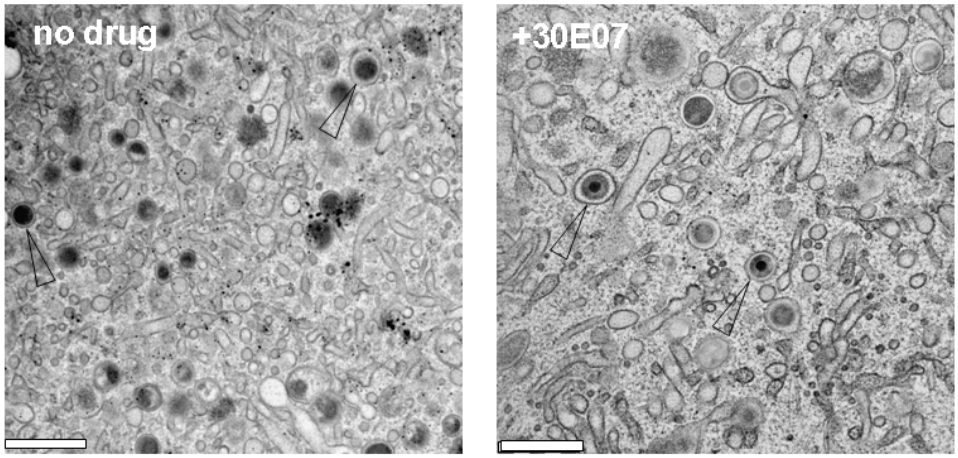

Figure 32: Ultrastructural analysis of effect of 30E07 on cytoplasmic capsid envelopment. Representative electron microscopic images of cytoplasms of DMSO-treated (no drug) and drug-treated (+30E07) TB40-BAC4-infected HFF cells. Arrows indicate secondary enveloped C-capsids. Scale bars: 500 nm.

5. Discussion

Human Cytomegalovirus (HCMV) is an opportunistic pathogen leading to severe morbidity and mortality in immunocompromised patients and represents the major viral cause of birth defects (Britt, 1999). Currently, the most effective way to control CMV infection, given the lack of an effective vaccine, is by antiviral chemotherapy. Almost all anti-HCMV drugs on the market to date are nucleoside analogues inhibiting the viral DNA polymerase. Although these drugs have proved to be successful in management of HCMV disease they suffer from bioavailability and long-term toxicity problems and the development of resistant strains. The similar mode of action in targeting the same protein in the viral machinery implicates furthermore an increased risk of cross-resistance. Therefore, there is an urgent need for new antivirals with different target structure.

In this work there was a focus on small molecular inhibitors in their ability to block essential viral protein-protein interactions governing primary envelopment of intranuclear viral capsids at the nuclear membrane and governing secondary envelopment of cytoplasmic viral capsids in the cytoplasmic virus factories. A HTS platform was set up testing the core interaction of the HCMV NEC. In a second line of this work, a PCA based set-up was established enabling future inhibitory screens for cytoplasmatic envelopment. 4,000 compounds from a library of highly diverse heterocyclic structures (Bauer et al., 2011) were screened by this novel, cell-free approach of target specific protein fragment complementation assay (PCA). Candidate compounds from the screen were further characterized for their mode of action and antiviral effects.

5.1 PCAs as HTS screening tool for inhibitors of protein-protein interactions

In a PCA, two fragments of a reporter enzyme are fused to the proteins of interest. The individual fragments are non-functional; however, interaction of the two proteins brings them into proximity allowing correct folding and reconstitution of functional activity of the reporter. Described PCA applications were performed *in vivo*, in the context of living cells (Michnick et al., 2007). In this setting, proteins can be studied in their natural context, ensuring sub-cellular targeting, post-translational modifications and interactions with other proteins required for folding. Therefore, PCAs were proposed as HTS screening tool for interacting proteins and inhibitors in cell-based assays. Remy and Michnick (Remy and Michnick, 2004) reported about a GFP-PCA based functional cDNA library screen for interaction partners of the protein kinase PKB/Akt. In our lab, such a cell-based PCA was previously used to characterize the core interaction within of the UL31/UL34 family which allowed comparative

studies addressing a comprehensive set of NEC homologs representing all herpesvirus subfamilies (Schnee et al., 2006). However, cell-based assays are not optimal for high-throughput screening approaches for inhibitors. Cell-based assays are complex, either due to the high costs and the preclusion of cytotoxic compounds leading to a lack of information about inhibiting structures in toxic compounds.

In this study, the recently developed cell-free setting based on a β-lactamase (Bla)-PCA was used in which the protein-protein interaction can be studied in isolation (Schnee et al., 2012). PCAs based on Bla are dynamic and reversible, other than those using for example fluorescent reporter proteins like GFP and YFP (Magliery et al., 2005; Nyfeler et al., 2005). They enable to detect interactions in real-time using kinetic detection modes. As an example we have chosen the core interaction of the HCMV-NEC formed by pUL50 and pUL53. It was shown that this protein interaction is essential for viral growth (Bubeck et al., 2004). The interaction of both proteins and their homologs in other herpesviruses were studied by our group and others (Bubeck et al., 2004; Lotzerich, Ruzsics, and Koszinowski, 2006; Sam et al., 2009). The interaction is non-obligatory (De et al., 2005) and direct (Sam et al., 2009). The interactions sites on both proteins were shown to be small and linear and single point mutations in the binding motifs affected or completely abolished the binding (Bubeck et al., 2004; Lotzerich, Ruzsics, and Koszinowski, 2006; Sam et al., 2009). Therefore, it was assumed that a small molecule might inhibit this interaction. Last but not least, as there was no information concerning 3D structures of the proteins allowing a structure-based drug design, a high-throughput screening (HTS) approach was used in this work to identify inhibitors of this interaction.

Therefore, PCA was suitable as a cost effective approach for high-throughput screening (HTS) for small inhibitory compounds of the pUL50/pUL53 interaction.

5.2 Standardization of the *in vitro* NEC-PCA (iPCA)

In this work, the iPCA made use of a chemical compound library to identify inhibitors of the pUL50/pUL53 interaction. First of all, the assay was adapted to high-throughput format. During this process, the minimal amounts of proteins were determined necessary in the assay to give a specific signal. The protein concentration was standardized and minimized to enlarge the number of possible screens which could be performed with one protein purification. At present it is possible to perform more than 400 single assays with purified protein from one 2.5 l bacterial culture. Furthermore, the iPCA was tested for DMSO

tolerance and the readout was changed from real-time to an endpoint measurement by introduction of a stop solution. Compared to the *in vitro* PCA described by Hahimoto and colleagues using mKG fused target proteins (Hashimoto et al., 2009) in which the screening reaction altogether takes 18 h, the total reaction time of the iPCA could be limited to 40 min, a substantial time saving of this assay. Although the PCA in the context of *in vitro* translation is advanced compared to cell-based systems regarding the compartmentalization issues, it suffers from high costs and low yields with respect to protein production.
A counter-screen was developed for excluding compounds having a direct effect on the reporter enzyme β-lactamase. This was necessary because our system utilized a single reporter reaction as readout. Thus, the risk for false positive results could be filtered out. This increase in specificity is demonstrated by the results.

5.3 Towards an inhibitor of the secondary envelopment of HCMV

In the second part of this work, a further essential viral protein-protein was transferred into the iPCA system and a set-up should be established which can be used in future high-throughput inhibitor screens. The interaction built up by the HCMV proteins pUL94 and pUL99 (To et al., 2011) termed here as the secondary envelopment complex (SEC) seemed to be an attractive and suitable platform.

The interaction occurs at late times in infection, when infectious progeny are being produced (Phillips and Bresnahan, 2011a). pUL99 localizes to the viral assembly complex and is essential for secondary envelopment of virions in the cytoplasm (Seo and Britt, 2007; Silva et al., 2003). In the absence of pUL99, partially tegumented but non-enveloped capsids accumulate in the cytoplasm, and no infectious virus is released. Localization of pUL99 to the cytoplasmic assembly complex is essential for virus replication (Seo and Britt, 2006; Seo and Britt, 2007). In this context, pUL94 is suggested to have an essential function in directing pUL99 to the assembly complex, thereby facilitating secondary envelopment of virions (Phillips and Bresnahan, 2011a). The amino acid residues of pUL99 essential for binding to pUL94 are located in a small linear motif (Liu et al., 2009) in the N-terminal half of the protein, while less information is available about pUL94. Binding site analysis by larger deletion mutants always resulted in a complete loss of interaction suggesting a non-linear binding motif and advanced structure required for interaction (Liu et al., 2009). However, recently it was shown that a point mutation in aa 343 in the very C-terminus of the protein disrupts co-localization to pUL99 (Liu et al., 2012). Furthermore, for its MCMV homolog pM94 a 5 aa-insertion mutant in the N-terminus was identified failing to interact with pM99, the homolog of pUL99 (Maninger et al., 2011). The strong effect of these subtle mutations

and the small linear binding motif in pUL99 indicate a limited interface of the pUL94/pUL99 interaction, pointing out the possibility that a small inhibitor might be able to block the SEC formation or stability.

To determine if the pUL94/pUL99 can be monitored by PCA, the interaction was tested in cell-based PCA. Because our lab previously studied extensively on the genetics of the MCMV homolog pM94 (Maninger et al., 2011) and thereby binding deficient mutants to pM99 were already at hand, the study first started on the interaction of the MCMV proteins. To this aim, new Gateway®-based plasmids were created which allow an easy and fast of tagging proteins with the Bla-fragments at the N-terminus. Besides of tagging pM94 and pM99 and the non-binding mutant of pM94 with a 5 aa insertion at position 13 (Maninger et al., 2011), Bla-tagged variants of pM50 and pM53 and the non-binding version of pM50 (Bubeck et al., 2004) were also created. The interaction of pM53 and pM50 was previously shown to be suitable in PCA (Schnee et al., 2006) and should serve here as a control for the Gateway®-tagging approach. The signal to background ratio of the pM50/pM53 interaction monitored by the Bla-tagged constructs derived from Gateway® plasmids was with factor of around 15 comparable to that described by Schnee et al. (Schnee et al., 2006). Consequently, the new cloning platform did not hamper the NEC proteins to interact properly. When N-M94 and C-M99 were co-expressed, the hydrolysis rate of nitrocefin in the cell lysates resulted in 20 fold higher hydrolysis rate than the hydrolysis rates derived from co-expression of N-M94i13 and C-M99 or any single expression of these proteins, respectively. Furthermore, the signal specificity could be confirmed in a competition experiment by co-expression with untagged pM99. These experiments led to two conclusions. First, the successful Bla-tagging via the Gateway® approach allows a fast and easy way of cloning for future studies on viral protein interactions by PCA. Second, the interaction of pM94 and pM99 can be monitored by cell-based PCA. The studies of Maninger et al. created a set of insertion mutants of pM94 with unknown molecular phenotype which were not able to complement in the pM94-deletion background. The insertion mutants can now be categorised in an easy way by testing them in the established pM94/pM99 PCA for their ability in binding pM99. Non-viable mutants still able to bind pM99 would further support the thesis of a second unknown function of the protein (Maninger et al., 2011).

Because the previous studies on the MCMV homologs showed tagging with the Bla-fragments without any sterical constraints, there was an indication that the interaction of the HCMV homologs pUL94 and pUL99 might also be monitored by PCA when proteins were Bla-tagged in a similar way. As control for background a deletion mutant of pUL99 was BlaC-tagged (CUL99del) lacking the responsible residues for binding to pUL94 as predicted by Liu

and colleagues (Liu et al., 2009). Co-expression of NUL94 and CUL99 resulted in a more than 90 times higher nitrocefin hydrolysis rate than in single expression lysates of the tagged constructs showing a specific reconstitution of Bla activity upon co-transfection.

With a working cell-based PCA for the MCMV and HCMV SEC proteins in hands, the conserved properties of the proteins between the different β-herpesviruses should be underlined. The consensus sequence between pUL94 and pM94 accounts for 48%. Therefore it was likely that motifs which are responsible for binding pUL99/pM99 might be conserved between species. This would expand the impact of a potential inhibitor on the HCMV SEC interaction also to MCMV. To analyze this, the Bla-tagged constructs were used in a cross-complementation assay similar to that described for pM50/pM53 interaction described by Schnee and colleagues (Schnee et al., 2006). Thereby, the N-M94 was also able to complement with CUL99, while the N-M94i13 and CUL99del did not. Future studies including the homologous proteins of alpha and gamma herpesviruses in the cell-based PCA might further elucidate the common and specific properties of the UL16 and UL11 protein families.

However, the final interest in the framework of this study was to transfer the interaction to the PCA format in that way that it is possible to screen for inhibitory compounds in larger scale. For this purpose, it was of great benefit that the fusion proteins could interact in the assay when they were produced isolated from each other (Figure 18) indicating that the interaction of pUL94 and pUL99 is non-obligatory.

Next, it was of interest if it was possible to produce one or both fusion proteins in bacteria to further enable a scale-up of the assay. The bacterial derived BlaC-tagged pUL99 could replace the eukaryotic-derived fusion protein. However, the BlaN-tagged pUL94 did not complement with BlaC-tagged pUL99 versions. This might be due to instabilities caused by protein degradation. Liu and colleagues showed that already minor truncations in pUL94 (Liu et al., 2009) always resulted in a total loss of binding properties to pUL99. Accordingly, Western blot analysis of the bacterial derived construct (Figure 20B) lacked a distinct band for NUL94-His and showed a protein pattern indicating degradation. Failures in post-translational protein modification caused by prokaryotic expression or chaperon dependant folding of the protein may also contribute.

Escherichia coli-based cell-free systems are described to underperform in folding of multidomain proteins in comparison to eukaryotic systems (Hirano et al., 2006; Langlais et al., 2007; Zarate et al., 2010). For future larger screens the change to a eukaryotic

expression of pUL94 may be considered. Besides the traditional yeast and baculovirus systems, Kovtun and colleagues recently described a cell-free protein expression system derived from Leishmania enabling the production of eukaryotic proteins in large scale in a rapid and cost-effective way (Kovtun et al., 2011).

Nevertheless, the present system is already suitable for screens with pUL99 (pUL94) derived peptides to further characterize the interaction. Thereby, short peptides mimicking stretches of pUL99 especially in the linear binding region to pUL94 (Liu et al., 2009) appear promising.

5.4 The *in vitro* NEC-PCA (iPCA) in the high-throughput inhibitor screen

A compound library of 4,000 structurally highly diverse potentially non-toxic compounds with pharmacological properties which were selected from a small-molecule library containing 30,000 individual heterocyclic structures (EMC microcollections, Tübingen) was screened with the standardized iPCA. This library has been already tested for toxicity in different mammalian cell lines (Caco-2, HeLa, A549 and A431) (Bauer et al., 2011) and was provided by EMC microcollections (Tübingen). The iPCA would also enable to screen highly cytotoxic compounds, however, this selection allowed a further characterization of the hits in the viral context.

Of almost 100 candidates only 2 were identified showing inhibition in the iPCA but not affecting the β-lactamase in the counter-screen. Both compounds, termed here 30E06 and 30E07, were structurally related suggesting a common mechanism of action.

To further test target specificity, the compounds were tested on primary and continuous cell lines for general cytotoxic effects. 30E07 showed less toxicity than 30E06 and was therefore used for further cell-based assays for the pUL50/pUL53 interaction. 30E07 significantly reduced the nitrocefin hydrolysis rate when applied in the cell-based NEC-PCA (Figure 25) which was established previously in our lab to monitor pUL50/pUL53 interaction in real-time (Schnee et al., 2006). Furthermore, immunofluorescence studies demonstrated that pUL53 delocalizes from the nuclear rim in presence of pUL50 upon drug treatment. The pUL53 was distributed homogenously all over the nucleus like it was described previously for pUL53 in single transfection experiments (Dal Monte et al., 2002; Muranyi et al., 2002). Both findings indicated a direct influence of 30E07 on pUL50/pUL53 interaction. Therefore, the two identified hits acted target specific *in vitro* and in cells.

5.4 Characterization of the antiviral effect of the NEC inhibitors

As a specific inhibition of the NEC formation by of the identified compounds was observed, both candidates were tested for their antiviral activity against HCMV. Interestingly, 30E06 and 30E07 showed a dose-dependant antiviral effect on HCMV when applied in non-toxic concentrations. To elucidate the on target and off target modes of action, the effect of 30E07 on viral gene expression was tested. Thereby, a certain reduction in viral protein expression levels was observed for HCMV infected cells treated with the compound in the highest non-toxic dose. This observation stood in contrast to our expectation that viral protein expression should not be harmed by the drug when affecting the pUL50/pUL53 interaction which acts further downstream in the viral replication cycle. For example, the anti-cytomegalovirus compound AIC246 which acts selectively on capsid packaging and egress and therefore further downstream was described to show no influence on immediate, early and late protein expression levels (Goldner et al., 2011). Deficiency in viral protein expression levels could result from reduced viral DNA replication in herpesviruses. For that reason, an upstream effect of 30E07 on viral DNA synthesis was assumed. To clarify this, 30E07 was tested by quantitative real-time PCR (qPCR) for effects on HCMV genome copy numbers during the first viral replication cycle. A marked inhibition on the *de novo* synthesis of progeny DNA was observed in 30E07 treated infected cells confirming the upstream effect thesis. To elucidate, if the compound also affects other steps in viral morphogenesis late-stage HCMV-infected cells were analyzed in absence and presence of the compound by electron microscopy. The decision which capsid type is formed from the circular pro-capsid depends on the timing of scaffold protein cleavage and recruitment of unit-length viral DNA (Yu et al., 2005). An Increase of either A- or/and B-capsids, which are believed to be non-functional dead-end products, reflects an interference with the process of capsid maturation. Increased numbers of B-capsids are often observed in infected cells treated with drugs targeting the capsid packaging process itself like for the anti-cytomegalovirus compounds AIC246 and benzimidazole-D-ribonucleosides, which were shown to target the viral terminase or the portal protein (Dittmer et al., 2005; Goldner et al., 2011; Krosky et al., 1998). In the case of 30E07 no change in B-capsid number could be observed and therefore it is unlikely that 30E07 affected the capsid packaging process.

However, there was a remarkable increased number of empty A-capsids in the nucleus of drug-treated cells while the number of DNA-filled C-capsids decreased. A-capsids result from a premature cleavage of the scaffold protein before DNA is incorporated into the capsid. Although the drug was applied later in infection (day three post infection), the increased number of A-capsids in drug-treated cells might resulted from the delay in viral DNA synthesis provoked by the drug from the moment of application.

Because the compounds originated from the screen for inhibitors of the pUL50/pUL53 interaction, which is essential in the process of nuclear capsid egress, it was of interest if an effect on nuclear egress could be observed for 30E07. Cytoplasmic capsids and a regular assembly complex could still be found in drug-treated cells, which excluded a complete block of egress. To evaluate if the egress process was anyhow disturbed by the drug, the number of C-capsids appearing in the cytoplasm in relation to C-capsids from the nucleus from untreated and drug-treated cells was quantified. However in both cases, the percentage of cytoplamic C-capsids was around 9%. Furthermore, the cytoplasmic capsids showed regular secondary envelopment, which led to the conclusion that processes downstream of viral DNA synthesis are not harmed by the drug. However, due to the significant decrease of the C-capsids in the drug treated cells and low overall number cytosolic capsids this later findings are only indicative. A final conclusion to this regard requires further studies.

5.4.1 Targeted effect of the screening hits on NEC functions

In summary, we could show that we were able to identify small inhibitory compounds targeting the pUL50/pUL53 interaction of HCMV *in vitro*. The candidate 30E07 from the HTS also showed inhibition on pUL50/pUL53 interaction in cell-based assays. We could clearly show that in co-transfection experiments pUL53 is diffusing homogenously in the nucleus and is not targeted to the nuclear rim to pUL50 in presence of the drug (Figure 26). This strongly argues for a targeted effect of the drugs. Next it should be perhaps tested whether pUL53 is also dissociated in drug-treated cells during infection in the complete viral context.
Furthermore, both identified candidates from the HTS (30E07 and 30E06) exhibited an antiviral effect on HCMV accompanied by an impaired viral protein and DNA synthesis and an inhibition of nuclear capsid maturation. Yet, we could not find any direct evidence that 30E07 inhibits nuclear capsid egress in the viral context.

Do the observed drug effects reflect selectively properties of the targets or do they represent also off target effects? Most of what is currently known about the pUL34/pUL31 of β-herpesviruses originates from studies on dominant-negative (DN) mutants (for more information see (Veitia, 2007)) of both proteins. DNs of pM50 (pUL34 family of MCMV) solely showed a defect in nuclear egress (Bubeck et al., 2004), while pM53 (pUL31 family of MCMV) DNs showed an additional effect on DNA cleavage/DNA capsid packaging and maturation (Popa et al, 2010; Pogoda et al., 2012 in revision). Furthermore, a significant increase of A-capsids reflected an additional effect of pM53 on viral DNA replication which could recently be verified by qPCR studies (Madlen Pogoda, personal communication).
Similarly, in α-herpesviruses, knock-out mutants of pUL31 of HSV-1 showed, besides a defect in nuclear egress, a negative effect on synthesis and packaging of viral DNA (Chang

et al., 2012) and also a delayed expression of viral gene products (Roberts and Baines, 2011). The latter phenotypes were exclusively observed for pUL31- but not for pUL34-null mutants. Studies with knock-out and charge cluster mutations of pUL34 ascribed to the protein a role in proper primary envelopment and lamina alteration as well as a recruitment function of appropriate components to nucleocapsid budding sites (Roller et al., 2010; Wills, Mou, and Baines, 2009). Furthermore, the MCMV homolog pM50 appeared to be crucial to prevent a late stress response by the host cell (Stahl, S. 2012, "Modulation of the Unfolded Protein Response by Murine Cytomegalovirus", *22nd Annual Meeting of the Society for Virology*, Essen (Germany), p. 360) which might lead to disturbance of the late protein synthesis.

Studies on γ-herpesvirus homologs in EBV showed only partial overlapping phenotypes compared to the α- and β-homologs described above. Both protein deletion viruses showed the expected alteration in primary egress. However, the observed abnormal capsid maturation for the pUL31 homolog (BFLF2)-null mutant could not be ascribed to impaired viral DNA synthesis or monomeric genome production (Farina et al., 2005; Granato et al., 2008).
Taking these studies on α- and β-herpesvirus homologs into account gives evidence that the lead compounds generate effects that can be explained by the action on pUL50 and pUL53.
The failure to observe direct effects on nuclear capsid egress might be a result of the experimental set-up in the EM study. We could hardly find any capsid at all when we applied the drug on the day of infection (data not shown). Therefore, to permit some quantification we delayed the drug application to d3 post infection. It has to be assumed that prior to the onset of drug function there were already some C-capsids showing up all known stages, including cytosolic stages. The observed C-capsids in the cytosol at day 5 post infection in drug-treated cells may represent these capsids. The fact that the absolute numbers of C-capsids observed in the cytosol in presence of the drug were very low compared to the wildtype case (see Table 4) supports this notion. We do not know fate and half life of newly synthesized nuclear capsids, which are mainly dead-end products (A- and B-capsids) in drug-treated cells. If we expect a shorter half-life for the dead-end products in the nucleus, this would reduce the overall numbers of the capsids in drug treated cells and would therefore also decrease the ratio of the capsids in- and outside of the nucleus. Future EM studies on the kinetics of morphogenesis could elucidate these questions.

A further aspect we have to consider is that also another protein-protein interaction is blocked by the drugs. Studies on pM53 (Pogoda et al., 2012, in revision) suggest homodimerization of this protein which is abolished in DN mutants of pM53. If the drug

provokes monomeric pUL53 to take a conformation, which is functionally comparable to the DN-properties of the protein mutants (Popa et al. 2010; Pogoda et al., 2012, in revision) phenotypes must occur that go beyond the lack of pUL50 and pUL53 interaction. Such phenotypes may occur at earlier stages of capsid morphogenesis. Studies on pUL53 and pUL50-null mutants have not yet been carried out and would certainly help to complete the picture about the functions of the two proteins in β-herpesviruses.
Future drug studies will have to be performed to specify these effects of 30E07. However, it is might be advantageous to wait with such extensive experimental settings until the lead structure is optimized. Besides the above mentioned studies, ligand binding assays could ascertain a potential interaction (reviewed in (de Jong et al., 2005; Sittampalam, Kahl, and Janzen, 1997)).

5.4.2 Perspectives of the screening hits

Perfect drugs do not emerge from early screens. The identified candidates are leads, which need to be optimized in further studies to get to the point of clinical relevance. Therefore, structure activity relationship (SAR) studies are needed to improve relevant features of the lead compounds. In our special case this would start from the stereospecific synthesis of the compounds 30E07 and 30E06. Both compounds exhibit the same core structure (Figure 23A) holding 3 stereocentres equivalent to 8 possible stereoisomers. The percentage of each stereoisomer in the compound solution used in the screen was not known though 30E06 and 30E07 were synthesized an achiral manner. Therefore, each stereoisomer will have to be produced in an isolated form and retested in the iPCA and cell-based assays for the identification of the active stereoisomer. Further compound modifications will be needed that reduce cellular toxicity and increase target selectivity. X-ray crystallographic studies on the pUL50 and pUL53 proteins would provide useful information for enhanced inhibitor activity. So far, crystallization attempts on these proteins and homologs were not successful due to low solubility of the full-length proteins (Gonnella et al., 2005; Lake and Hutt-Fletcher, 2004). However, Sam and colleagues recently described the production of stable, truncated forms of pUL50 and pUL53 (Sam et al., 2009) still able to interact, which might serve as attractive platform for new efforts.

Altogether, this proof of concept study demonstrated that small-molecule inhibitors can be identified by cell-free NEC-PCA, which can become a useful basis for anti-cytomegalovirus drug development. We believe that future screenings in more extended compound libraries, combined with structure-activity studies will provide an effective small-molecule inhibitor for the interaction of pUL50/pUL53 which would allow to go forward to *in vitro* and *in vivo* testing for activity in CMV disease.

5.5 Concluding remarks

The data presented here show that the β-lactamase based *in vitro* PCA (Schnee et al., 2012) is suitable to be applied in a high-throughput screen for small molecule inhibitors of protein-protein interactions. Furthermore, it was demonstrated that the system is transferable to other protein interactions.

Most importantly, this work proves for the first time that a small molecule is able to inhibit the interaction of pUL50/pUL53. This confirms the assumption of a limited binding site and the suitability of this protein-protein interaction as a potential drug target.

Taken together, this work provides new insights and tools in screening for inhibitors of essential viral protein-protein interactions on the way to new antivirals against HCMV with unique mode of action.

6. References

Adjuik, M., Babiker, A., Garner, P., Olliaro, P., Taylor, W., and White, N. (2004). Artesunate combinations for treatment of malaria: meta-analysis. *Lancet* **363**(9402)**,** 9-17.

Akkarawongsa, R., Pocaro, N. E., Case, G., Kolb, A. W., and Brandt, C. R. (2009). Multiple peptides homologous to herpes simplex virus type 1 glycoprotein B inhibit viral infection. *Antimicrob Agents Chemother* **53**(3)**,** 987-96.

Anand, K., Ziebuhr, J., Wadhwani, P., Mesters, J. R., and Hilgenfeld, R. (2003). Coronavirus main proteinase (3CLpro) structure: basis for design of anti-SARS drugs. *Science* **300**(5626)**,** 1763-7.

Baldick, C. J., Jr., and Shenk, T. (1996). Proteins associated with purified human cytomegalovirus particles. *J Virol* **70**(9)**,** 6097-105.

Bauer, J., Kinast, S., Burger-Kentischer, A., Finkelmeier, D., Kleymann, G., Rayyan, W. A., Schroppel, K., Singh, A., Jung, G., Wiesmuller, K. H., Rupp, S., and Eickhoff, H. (2011). High-throughput-screening-based identification and structure-activity relationship characterization defined (S)-2-(1-aminoisobutyl)-1-(3-chlorobenzyl)benzimidazole as a highly antimycotic agent nontoxic to cell lines. *J Med Chem* **54**(19)**,** 6993-7.

Berridge, M. V., and Tan, A. S. (1993). Characterization of the cellular reduction of 3-(4,5-dimethylthiazol-2-yl)-2,5-diphenyltetrazolium bromide (MTT): subcellular localization, substrate dependence, and involvement of mitochondrial electron transport in MTT reduction. *Arch Biochem Biophys* **303**(2)**,** 474-82.

Bogner, E. (2002). Human cytomegalovirus terminase as a target for antiviral chemotherapy. *Rev Med Virol* **12**(2)**,** 115-27.

Bresnahan, W. A., and Shenk, T. (2000). A subset of viral transcripts packaged within human cytomegalovirus particles. *Science* **288**(5475)**,** 2373-6.

Britt, W. J. (1999). Congenital cytomegalovirus infection. In Sexually Transmitted Diseases and Adverse Outcomes of Pregnancy. *ASM Press***,** 269-281.

Britt, W. J., Jarvis, M., Seo, J. Y., Drummond, D., and Nelson, J. (2004). Rapid genetic engineering of human cytomegalovirus by using a lambda phage linear recombination system: demonstration that pp28 (UL99) is essential for production of infectious virus. *J Virol* **78**(1)**,** 539-43.

Brune, W. (2011). Inhibition of programmed cell death by cytomegaloviruses. *Virus Res* **157**(2)**,** 144-50.

Bubeck, A., Wagner, M., Ruzsics, Z., Lotzerich, M., Iglesias, M., Singh, I. R., and Koszinowski, U. H. (2004). Comprehensive mutational analysis of a herpesvirus gene in the viral genome context reveals a region essential for virus replication. *J Virol* **78**(15)**,** 8026-35.

Buser, C., Walther, P., Mertens, T., and Michel, D. (2007). Cytomegalovirus primary envelopment occurs at large infoldings of the inner nuclear membrane. *J Virol* **81**(6)**,** 3042-8.

Chee, M. S., Bankier, A. T., Beck, S., Bohni, R., Brown, C. M., Cerny, R., Horsnell, T., Hutchison, C. A., 3rd, Kouzarides, T., Martignetti, J. A., and et al. (1990). Analysis of the protein-coding content of the sequence of human cytomegalovirus strain AD169. *Curr Top Microbiol Immunol* **154,** 125-69.

Chou, S., Marousek, G., Auerochs, S., Stamminger, T., Milbradt, J., and Marschall, M. (2011). The unique antiviral activity of artesunate is broadly effective against human cytomegaloviruses including therapy-resistant mutants. *Antiviral Res*.

Coen, D. M., and Schaffer, P. A. (2003). Antiherpesvirus drugs: a promising spectrum of new drugs and drug targets. *Nat Rev Drug Discov* **2**(4)**,** 278-88.

Cory, A. H., Owen, T. C., Barltrop, J. A., and Cory, J. G. (1991). Use of an aqueous soluble tetrazolium/formazan assay for cell growth assays in culture. *Cancer Commun* **3**(7)**,** 207-12.

Craig, J. M., Macauley, J. C., Weller, T. H., and Wirth, P. (1957). Isolation of intranuclear inclusion producing agents from infants with illnesses resembling cytomegalic inclusion disease. *Proc Soc Exp Biol Med* **94**(1)**,** 4-12.

Crough, T., and Khanna, R. (2009). Immunobiology of human cytomegalovirus: from bench to bedside. *Clin Microbiol Rev* **22**(1)**,** 76-98, Table of Contents.

Dal Monte, P., Pignatelli, S., Zini, N., Maraldi, N. M., Perret, E., Prevost, M. C., and Landini, M. P. (2002). Analysis of intracellular and intraviral localization of the human cytomegalovirus UL53 protein. *J Gen Virol* **83**(Pt 5)**,** 1005-12.

Darlington, R. W., and Moss, L. H., 3rd (1968). Herpesvirus envelopment. *J Virol* **2**(1)**,** 48-55.

de Jong, L. A., Uges, D. R., Franke, J. P., and Bischoff, R. (2005). Receptor-ligand binding assays: technologies and applications. *J Chromatogr B Analyt Technol Biomed Life Sci* **829**(1-2)**,** 1-25.

De, S., Krishnadev, O., Srinivasan, N., and Rekha, N. (2005). Interaction preferences across protein-protein interfaces of obligatory and non-obligatory components are different. *BMC Struct Biol* **5,** 15.

Dittmer, A., Drach, J. C., Townsend, L. B., Fischer, A., and Bogner, E. (2005). Interaction of the putative human cytomegalovirus portal protein pUL104 with the large terminase subunit pUL56 and its inhibition by benzimidazole-D-ribonucleosides. *J Virol* **79**(23)**,** 14660-7.

Dunn, W., Chou, C., Li, H., Hai, R., Patterson, D., Stolc, V., Zhu, H., and Liu, F. (2003). Functional profiling of a human cytomegalovirus genome. *Proc Natl Acad Sci U S A* **100**(24)**,** 14223-8.

Efferth, T., Marschall, M., Wang, X., Huong, S. M., Hauber, I., Olbrich, A., Kronschnabl, M., Stamminger, T., and Huang, E. S. (2002). Antiviral activity of artesunate towards wild-type, recombinant, and ganciclovir-resistant human cytomegaloviruses. *J Mol Med (Berl)* **80**(4)**,** 233-42.

Efferth, T., Romero, M. R., Wolf, D. G., Stamminger, T., Marin, J. J., and Marschall, M. (2008). The antiviral activities of artemisinin and artesunate. *Clin Infect Dis* **47**(6)**,** 804-11.

Farina, A., Feederle, R., Raffa, S., Gonnella, R., Santarelli, R., Frati, L., Angeloni, A., Torrisi, M. R., Faggioni, A., and Delecluse, H. J. (2005). BFRF1 of Epstein-Barr virus is essential for efficient primary viral envelopment and egress. *J Virol* **79**(6)**,** 3703-12.

Fields, S., and Song, O. (1989). A novel genetic system to detect protein-protein interactions. *Nature* **340**(6230)**,** 245-6.

Fishman, J. A., and Rubin, R. H. (1998). Infection in organ-transplant recipients. *N Engl J Med* **338**(24)**,** 1741-51.

Fossum, E., Friedel, C. C., Rajagopala, S. V., Titz, B., Baiker, A., Schmidt, T., Kraus, T., Stellberger, T., Rutenberg, C., Suthram, S., Bandyopadhyay, S., Rose, D., von Brunn, A., Uhlmann, M., Zeretzke, C., Dong, Y. A., Boulet, H., Koegl, M., Bailer, S. M., Koszinowski, U., Ideker, T., Uetz, P., Zimmer, R., and Haas, J. (2009). Evolutionarily conserved herpesviral protein interaction networks. *PLoS Pathog* **5**(9)**,** e1000570.

Fuchs, W., Klupp, B. G., Granzow, H., Osterrieder, N., and Mettenleiter, T. C. (2002). The interacting UL31 and UL34 gene products of pseudorabies virus are involved in egress from the host-cell nucleus and represent components of primary enveloped but not mature virions. *J Virol* **76**(1)**,** 364-78.

Galarneau, A., Primeau, M., Trudeau, L. E., and Michnick, S. W. (2002). Beta-lactamase protein fragment complementation assays as in vivo and in vitro sensors of protein protein interactions. *Nat Biotechnol* **20**(6)**,** 619-22.

Ghosh, I. R., Langford, R. M., Nieminen, K., Kari, A., and Takala, J. (2000). Repetitive synchronized cyclical oscillations of multisystem parameters subsequent to high-dose thiopental therapy for status epilepticus secondary to herpes encephalitis. *Br J Anaesth* **85**(3)**,** 471-3.

Goldner, T., Hewlett, G., Ettischer, N., Ruebsamen-Schaeff, H., Zimmermann, H., and Lischka, P. (2011). The novel Anti-Cytomegalovirus Compound AIC246 inhibits HCMV Replication through a Specific Antiviral Mechanism that involves the viral Terminase. *J Virol*.

Gomes, M., Ribeiro, I., Warsame, M., Karunajeewa, H., and Petzold, M. (2008). Rectal artemisinins for malaria: a review of efficacy and safety from individual patient data in clinical studies. *BMC Infect Dis* **8,** 39.

Gonnella, R., Farina, A., Santarelli, R., Raffa, S., Feederle, R., Bei, R., Granato, M., Modesti, A., Frati, L., Delecluse, H. J., Torrisi, M. R., Angeloni, A., and Faggioni, A. (2005). Characterization and intracellular localization of the Epstein-Barr virus protein BFLF2: interactions with BFRF1 and with the nuclear lamina. *J Virol* **79**(6)**,** 3713-27.

Granato, M., Feederle, R., Farina, A., Gonnella, R., Santarelli, R., Hub, B., Faggioni, A., and Delecluse, H. J. (2008). Deletion of Epstein-Barr virus BFLF2 leads to impaired viral DNA packaging and primary egress as well as to the production of defective viral particles. *J Virol* **82**(8)**,** 4042-51.

Harris, S., Ahlfors, K., Ivarsson, S., Lernmark, B., and Svanberg, L. (1984). Congenital cytomegalovirus infection and sensorineural hearing loss. *Ear Hear* **5**(6)**,** 352-5.

Hashimoto, J., Watanabe, T., Seki, T., Karasawa, S., Izumikawa, M., Iemura, S., Natsume, T., Nomura, N., Goshima, N., Miyawaki, A., Takagi, M., and Shin-Ya, K. (2009). Novel in vitro protein fragment complementation assay applicable to high-throughput screening in a 1536-well format. *J Biomol Screen* **14**(8)**,** 970-9.

Hirano, N., Sawasaki, T., Tozawa, Y., Endo, Y., and Takai, K. (2006). Tolerance for random recombination of domains in prokaryotic and eukaryotic translation systems: Limited interdomain misfolding in a eukaryotic translation system. *Proteins* **64**(2)**,** 343-54.

Homman-Loudiyi, M., Hultenby, K., Britt, W., and Soderberg-Naucler, C. (2003). Envelopment of human cytomegalovirus occurs by budding into Golgi-derived vacuole compartments positive for gB, Rab 3, trans-golgi network 46, and mannosidase II. *J Virol* **77**(5)**,** 3191-203.

Hu, C. D., Chinenov, Y., and Kerppola, T. K. (2002). Visualization of interactions among bZIP and Rel family proteins in living cells using bimolecular fluorescence complementation. *Mol Cell* **9**(4)**,** 789-98.

Hudson, J. B. (1979). The murine cytomegalovirus as a model for the study of viral pathogenesis and persistent infections. *Arch Virol* **62**(1)**,** 1-29.

Jacobson, M. A., Sinclair, E., Bredt, B., Agrillo, L., Black, D., Epling, C. L., Carvidi, A., Ho, T., Bains, R., and Adler, S. P. (2006). Antigen-specific T cell responses induced by Towne cytomegalovirus (CMV) vaccine in CMV-seronegative vaccine recipients. *J Clin Virol* **35**(3)**,** 332-7.

Johnson, D. C., and Baines, J. D. (2011). Herpesviruses remodel host membranes for virus egress. *Nat Rev Microbiol* **9**(5)**,** 382-94.

Johnsson, N., and Varshavsky, A. (1994). Split ubiquitin as a sensor of protein interactions in vivo. *Proc Natl Acad Sci U S A* **91**(22)**,** 10340-4.

Jones, T. R., and Lee, S. W. (2004). An acidic cluster of human cytomegalovirus UL99 tegument protein is required for trafficking and function. *J Virol* **78**(3)**,** 1488-502.

Kadonaga, J. T., Gautier, A. E., Straus, D. R., Charles, A. D., Edge, M. D., and Knowles, J. R. (1984). The role of the beta-lactamase signal sequence in the secretion of proteins by Escherichia coli. *J Biol Chem* **259**(4)**,** 2149-54.

Kaptein, S. J., Efferth, T., Leis, M., Rechter, S., Auerochs, S., Kalmer, M., Bruggeman, C. A., Vink, C., Stamminger, T., and Marschall, M. (2006). The anti-malaria drug artesunate inhibits replication of cytomegalovirus in vitro and in vivo. *Antiviral Res* **69**(2)**,** 60-9.

Kimberlin, D. W., Lin, C. Y., Sanchez, P. J., Demmler, G. J., Dankner, W., Shelton, M., Jacobs, R. F., Vaudry, W., Pass, R. F., Kiell, J. M., Soong, S. J., and Whitley, R. J. (2003). Effect of ganciclovir therapy on hearing in symptomatic congenital cytomegalovirus disease involving the central nervous system: a randomized, controlled trial. *J Pediatr* **143**(1)**,** 16-25.

Klupp, B. G., Granzow, H., Fuchs, W., Keil, G. M., Finke, S., and Mettenleiter, T. C. (2007). Vesicle formation from the nuclear membrane is induced by coexpression of two conserved herpesvirus proteins. *Proc Natl Acad Sci U S A* **104**(17)**,** 7241-6.

Klupp, B. G., Hengartner, C. J., Mettenleiter, T. C., and Enquist, L. W. (2004). Complete, annotated sequence of the pseudorabies virus genome. *J Virol* **78**(1)**,** 424-40.

Kovtun, O., Mureev, S., Jung, W., Kubala, M. H., Johnston, W., and Alexandrov, K. (2011). Leishmania cell-free protein expression system. *Methods* **55**(1)**,** 58-64.

Krosky, P. M., Underwood, M. R., Turk, S. R., Feng, K. W., Jain, R. K., Ptak, R. G., Westerman, A. C., Biron, K. K., Townsend, L. B., and Drach, J. C. (1998). Resistance of human cytomegalovirus to benzimidazole ribonucleosides maps to two open reading frames: UL89 and UL56. *J Virol* **72**(6)**,** 4721-8.

Lake, C. M., and Hutt-Fletcher, L. M. (2004). The Epstein-Barr virus BFRF1 and BFLF2 proteins interact and coexpression alters their cellular localization. *Virology* **320**(1)**,** 99-106.

Lambert, D. M., Barney, S., Lambert, A. L., Guthrie, K., Medinas, R., Davis, D. E., Bucy, T., Erickson, J., Merutka, G., and Petteway, S. R., Jr. (1996). Peptides from conserved regions of paramyxovirus fusion (F) proteins are potent inhibitors of viral fusion. *Proc Natl Acad Sci U S A* **93**(5)**,** 2186-91.

Landini, M. P., Severi, B., Furlini, G., and Badiali De Giorgi, L. (1987). Human cytomegalovirus structural components: intracellular and intraviral localization of p28 and p65-69 by immunoelectron microscopy. *Virus Res* **8**(1)**,** 15-23.

Langlais, C., Guilleaume, B., Wermke, N., Scheuermann, T., Ebert, L., LaBaer, J., and Korn, B. (2007). A systematic approach for testing expression of human full-length proteins in cell-free expression systems. *BMC Biotechnol* **7,** 64.

Lischka, P., and Zimmermann, H. (2008). Antiviral strategies to combat cytomegalovirus infections in transplant recipients. *Curr Opin Pharmacol* **8**(5)**,** 541-8.

Liu, Y., Cui, Z., Zhang, Z., Wei, H., Zhou, Y., Wang, M., and Zhang, X. E. (2009). The tegument protein UL94 of human cytomegalovirus as a binding partner for tegument protein pp28 identified by intracellular imaging. *Virology* **388**(1)**,** 68-77.

Liu, Y., Zhang, Z., Zhao, X., Wei, H., Deng, J., Cui, Z., and Zhang, X. E. (2012). Human cytomegalovirus UL94 is a nucleocytoplasmic shuttling protein containing two NLSs and one NES. *Virus Res*.

Loomis, J. S., Bowzard, J. B., Courtney, R. J., and Wills, J. W. (2001). Intracellular trafficking of the UL11 tegument protein of herpes simplex virus type 1. *J Virol* **75**(24)**,** 12209-19.

Lotzerich, M., Ruzsics, Z., and Koszinowski, U. H. (2006). Functional domains of murine cytomegalovirus nuclear egress protein M53/p38. *J Virol* **80**(1)**,** 73-84.

Lowance, D., Neumayer, H. H., Legendre, C. M., Squifflet, J. P., Kovarik, J., Brennan, P. J., Norman, D., Mendez, R., Keating, M. R., Coggon, G. L., Crisp, A., and Lee, I. C. (1999). Valacyclovir for the prevention of cytomegalovirus disease after renal transplantation. International Valacyclovir Cytomegalovirus Prophylaxis Transplantation Study Group. *N Engl J Med* **340**(19)**,** 1462-70.

Maninger, S., Bosse, J. B., Lemnitzer, F., Pogoda, M., Mohr, C. A., von Einem, J., Walther, P., Koszinowski, U. H., and Ruzsics, Z. (2011). M94 is essential for the secondary envelopment of murine cytomegalovirus. *J Virol* **85**(18)**,** 9254-67.

Marschall, M., Marzi, A., aus dem Siepen, P., Jochmann, R., Kalmer, M., Auerochs, S., Lischka, P., Leis, M., and Stamminger, T. (2005). Cellular p32 recruits cytomegalovirus kinase pUL97 to redistribute the nuclear lamina. *J Biol Chem* **280**(39)**,** 33357-67.

Martinez, J., and St Jeor, S. C. (1986). Molecular cloning and analysis of three cDNA clones homologous to human cytomegalovirus RNAs present during late infection. *J Virol* **60**(2)**,** 531-8.

Matagne, A., Lamotte-Brasseur, J., and Frere, J. M. (1998). Catalytic properties of class A beta-lactamases: efficiency and diversity. *Biochem J* **330 (Pt 2),** 581-98.

Meckes, D. G., Jr., Marsh, J. A., and Wills, J. W. (2010). Complex mechanisms for the packaging of the UL16 tegument protein into herpes simplex virus. *Virology* **398**(2)**,** 208-13.

Melnik, L. I., Garry, R. F., and Morris, C. A. (2011). Peptide inhibition of human cytomegalovirus infection. *Virol J* **8,** 76.

Mettenleiter, T. C. (2004). Budding events in herpesvirus morphogenesis. *Virus Res* **106**(2)**,** 167-80.

Michnick, S. W., Ear, P. H., Manderson, E. N., Remy, I., and Stefan, E. (2007). Universal strategies in research and drug discovery based on protein-fragment complementation assays. *Nat Rev Drug Discov* **6**(7)**,** 569-82.

Milbradt, J., Auerochs, S., and Marschall, M. (2007). Cytomegaloviral proteins pUL50 and pUL53 are associated with the nuclear lamina and interact with cellular protein kinase C. *J Gen Virol* **88**(Pt 10)**,** 2642-50.

Miller, W., Flynn, P., McCullough, J., Balfour, H. H., Jr., Goldman, A., Haake, R., McGlave, P., Ramsay, N., and Kersey, J. (1986). Cytomegalovirus infection after bone marrow transplantation: an association with acute graft-v-host disease. *Blood* **67**(4)**,** 1162-7.

Morton, C. C., and Nance, W. E. (2006). Newborn hearing screening--a silent revolution. *N Engl J Med* **354**(20)**,** 2151-64.

Muranyi, W., Haas, J., Wagner, M., Krohne, G., and Koszinowski, U. H. (2002). Cytomegalovirus recruitment of cellular kinases to dissolve the nuclear lamina. *Science* **297**(5582)**,** 854-7.

Murphy, E., Rigoutsos, I., Shibuya, T., and Shenk, T. E. (2003a). Reevaluation of human cytomegalovirus coding potential. *Proc Natl Acad Sci U S A* **100**(23)**,** 13585-90.

Murphy, E., Yu, D., Grimwood, J., Schmutz, J., Dickson, M., Jarvis, M. A., Hahn, G., Nelson, J. A., Myers, R. M., and Shenk, T. E. (2003b). Coding potential of laboratory and clinical strains of human cytomegalovirus. *Proc Natl Acad Sci U S A* **100**(25)**,** 14976-81.

Neuberger, P., Hamprecht, K., Vochem, M., Maschmann, J., Speer, C. P., Jahn, G., Poets, C. F., and Goelz, R. (2006). Case-control study of symptoms and neonatal outcome of human milk-transmitted cytomegalovirus infection in premature infants. *J Pediatr* **148**(3)**,** 326-31.

O'Callaghan, C. H., Morris, A., Kirby, S. M., and Shingler, A. H. (1972). Novel method for detection of beta-lactamases by using a chromogenic cephalosporin substrate. *Antimicrob Agents Chemother* **1**(4)**,** 283-8.

Ornoy, A., and Diav-Citrin, O. (2006). Fetal effects of primary and secondary cytomegalovirus infection in pregnancy. *Reprod Toxicol* **21**(4)**,** 399-409.

Pagliaro, L., Felding, J., Audouze, K., Nielsen, S. J., Terry, R. B., Krog-Jensen, C., and Butcher, S. (2004). Emerging classes of protein-protein interaction inhibitors and new tools for their development. *Curr Opin Chem Biol* **8**(4)**,** 442-9.

Pante, N., and Kann, M. (2002). Nuclear pore complex is able to transport macromolecules with diameters of about 39 nm. *Mol Biol Cell* **13**(2)**,** 425-34.

Pelletier, A. a. M., S.W. (1997). A protein complementation assay for detection of protein-protein interactions *in vivo*. *Protein Eng.* **10,** 89.

Pelletier, J. N., Campbell-Valois, F. X., and Michnick, S. W. (1998). Oligomerization domain-directed reassembly of active dihydrofolate reductase from rationally designed fragments. *Proc Natl Acad Sci U S A* **95**(21)**,** 12141-6.

Philippon, A., Dusart, J., Joris, B., and Frere, J. M. (1998). The diversity, structure and regulation of beta-lactamases. *Cell Mol Life Sci* **54**(4)**,** 341-6.

Phillips, S. L., and Bresnahan, W. A. (2011a). The human cytomegalovirus tegument protein UL94 is essential for secondary envelopment of HCMV virions. *J Virol*.

Phillips, S. L., and Bresnahan, W. A. (2011b). Identification of binary interactions between human cytomegalovirus virion proteins. *J Virol* **85**(1)**,** 440-7.

Phillips, S. L., Cygnar, D., Thomas, A., and Bresnahan, W. A. (2012). Interaction between the human cytomegalovirus tegument proteins UL94 and UL99 is essential for virus replication. *J Virol*.

Plotkin, S. A., Higgins, R., Kurtz, J. B., Morris, P. J., Campbell, D. A., Jr., Shope, T. C., Spector, S. A., and Dankner, W. M. (1994). Multicenter trial of Towne strain attenuated virus vaccine in seronegative renal transplant recipients. *Transplantation* **58**(11)**,** 1176-8.

Popa, M., Ruzsics, Z., Lotzerich, M., Dolken, L., Buser, C., Walther, P., and Koszinowski, U. H. (2010). Dominant negative mutants of the murine cytomegalovirus M53 gene block nuclear egress and inhibit capsid maturation. *J Virol* **84**(18)**,** 9035-46.

Raynor, B. D. (1993). Cytomegalovirus infection in pregnancy. *Semin Perinatol* **17**(6)**,** 394-402.

Reddehase, M. J., Podlech, J., and Grzimek, N. K. (2002). Mouse models of cytomegalovirus latency: overview. *J Clin Virol* **25 Suppl 2,** S23-36.

Reed, L. J. a. M., H. (1938). A simple method of estimating fifty per cent endpoints. *The American Journal of Hygiene* **27,** 493-497.

Remy, I., and Michnick, S. W. (2004). Regulation of apoptosis by the Ft1 protein, a new modulator of protein kinase B/Akt. *Mol Cell Biol* **24**(4)**,** 1493-504.

Reynolds, A. E., Liang, L., and Baines, J. D. (2004). Conformational changes in the nuclear lamina induced by herpes simplex virus type 1 require genes U(L)31 and U(L)34. *J Virol* **78**(11)**,** 5564-75.

Reynolds, A. E., Ryckman, B. J., Baines, J. D., Zhou, Y., Liang, L., and Roller, R. J. (2001). U(L)31 and U(L)34 proteins of herpes simplex virus type 1 form a complex that accumulates at the nuclear rim and is required for envelopment of nucleocapsids. *J Virol* **75**(18)**,** 8803-17.

Rivera, L. B., Boppana, S. B., Fowler, K. B., Britt, W. J., Stagno, S., and Pass, R. F. (2002). Predictors of hearing loss in children with symptomatic congenital cytomegalovirus infection. *Pediatrics* **110**(4)**,** 762-7.

Roberts, K. L., and Baines, J. D. (2011). UL31 of herpes simplex virus 1 is necessary for optimal NF-kappaB activation and expression of viral gene products. *J Virol* **85**(10)**,** 4947-53.

Roller, R. J., Bjerke, S. L., Haugo, A. C., and Hanson, S. (2010). Analysis of a charge cluster mutation of herpes simplex virus type 1 UL34 and its extragenic suppressor suggests a novel interaction between pUL34 and pUL31 that is necessary for membrane curvature around capsids. *J Virol* **84**(8)**,** 3921-34.

Rubin, R. H. (2001). Cytomegalovirus in solid organ transplantation. *Transpl Infect Dis* **3 Suppl 2,** 1-5.

Ryan, D. P., and Matthews, J. M. (2005). Protein-protein interactions in human disease. *Curr Opin Struct Biol* **15**(4)**,** 441-6.

Sainz, B., Jr., Mossel, E. C., Gallaher, W. R., Wimley, W. C., Peters, C. J., Wilson, R. B., and Garry, R. F. (2006). Inhibition of severe acute respiratory syndrome-associated coronavirus (SARS-CoV) infectivity by peptides analogous to the viral spike protein. *Virus Res* **120**(1-2)**,** 146-55.

Sam, M. D., Evans, B. T., Coen, D. M., and Hogle, J. M. (2009). Biochemical, biophysical, and mutational analyses of subunit interactions of the human cytomegalovirus nuclear egress complex. *J Virol* **83**(7)**,** 2996-3006.

Sanchez, V., Greis, K. D., Sztul, E., and Britt, W. J. (2000). Accumulation of virion tegument and envelope proteins in a stable cytoplasmic compartment during human cytomegalovirus replication: characterization of a potential site of virus assembly. *J Virol* **74**(2)**,** 975-86.

Sanchez, V., and Spector, D. H. (2002). Virology. CMV makes a timely exit. *Science* **297**(5582)**,** 778-9.

Schleiss, M. R. (2008). Cytomegalovirus vaccine development. *Curr Top Microbiol Immunol* **325,** 361-82.

Schnee, M., Ruzsics, Z., Bubeck, A., and Koszinowski, U. H. (2006). Common and specific properties of herpesvirus UL34/UL31 protein family members revealed by protein complementation assay. *J Virol* **80**(23)**,** 11658-66.

Schnee, M., Wagner, F. M., Koszinowski, U. H., and Ruzsics, Z. (2012). A Cell Free Protein Fragment Complementation Assay for Monitoring the Core Interaction of the Human Cytomegalovirus Nuclear Egress Complex. *Antiviral Res***,** in press.

Scrivano, L., Sinzger, C., Nitschko, H., Koszinowski, U. H., and Adler, B. (2011). HCMV spread and cell tropism are determined by distinct virus populations. *PLoS Pathog* **7**(1)**,** e1001256.

Shiba, C., Daikoku, T., Goshima, F., Takakuwa, H., Yamauchi, Y., Koiwai, O., and Nishiyama, Y. (2000). The UL34 gene product of herpes simplex virus type 2 is a tail-

anchored type II membrane protein that is significant for virus envelopment. *J Gen Virol* **81**(Pt 10)**,** 2397-405.

Silva, M. C., Yu, Q. C., Enquist, L., and Shenk, T. (2003). Human cytomegalovirus UL99-encoded pp28 is required for the cytoplasmic envelopment of tegument-associated capsids. *J Virol* **77**(19)**,** 10594-605.

Sinzger, C., Hahn, G., Digel, M., Katona, R., Sampaio, K. L., Messerle, M., Hengel, H., Koszinowski, U., Brune, W., and Adler, B. (2008). Cloning and sequencing of a highly productive, endotheliotropic virus strain derived from human cytomegalovirus TB40/E. *J Gen Virol* **89**(Pt 2)**,** 359-68.

Sittampalam, G. S., Kahl, S. D., and Janzen, W. P. (1997). High-throughput screening: advances in assay technologies. *Curr Opin Chem Biol* **1**(3)**,** 384-91.

Sodeik, B., Ebersold, M. W., and Helenius, A. (1997). Microtubule-mediated transport of incoming herpes simplex virus 1 capsids to the nucleus. *J Cell Biol* **136**(5)**,** 1007-21.

Spear, P. G., and Longnecker, R. (2003). Herpesvirus entry: an update. *J Virol* **77**(19)**,** 10179-85.

Speese, Sean D., Ashley, J., Jokhi, V., Nunnari, J., Barria, R., Li, Y., Ataman, B., Koon, A., Chang, Y.-T., Li, Q., Moore, Melissa J., and Budnik, V. (2012). Nuclear Envelope Budding Enables Large Ribonucleoprotein Particle Export during Synaptic Wnt Signaling. *Cell* **149**(4)**,** 832-846.

Stratton, K., Durch, J. and Lawrence, R. (2001). "Vaccines for the 21st century: a tool for decisionmaking." National Academy Press, 1, Washington, DC.

Streblow, D. N. (2006). A Proteomics Analysis of Human Cytomegalovirus Particles. *In* "Cytomegaloviruses" (M. J. Reddehase, Ed.). Caister Academic Press, Norfolk.

To, A., Bai, Y., Shen, A., Gong, H., Umamoto, S., Lu, S., and Liu, F. (2011). Yeast two hybrid analyses reveal novel binary interactions between human cytomegalovirus-encoded virion proteins. *PLoS One* **6**(4)**,** e17796.

Ueyama, T., Kusakabe, T., Karasawa, S., Kawasaki, T., Shimizu, A., Son, J., Leto, T. L., Miyawaki, A., and Saito, N. (2008). Sequential binding of cytosolic Phox complex to phagosomes through regulated adaptor proteins: evaluation using the novel monomeric Kusabira-Green System and live imaging of phagocytosis. *J Immunol* **181**(1)**,** 629-40.

Varnum, S. M., Streblow, D. N., Monroe, M. E., Smith, P., Auberry, K. J., Pasa-Tolic, L., Wang, D., Camp, D. G., 2nd, Rodland, K., Wiley, S., Britt, W., Shenk, T., Smith, R. D., and Nelson, J. A. (2004). Identification of proteins in human cytomegalovirus (HCMV) particles: the HCMV proteome. *J Virol* **78**(20)**,** 10960-6.

Veitia, R. A. (2007). Exploring the molecular etiology of dominant-negative mutations. *Plant Cell* **19**(12)**,** 3843-51.

Verkaar, F., Blankesteijn, W. M., Smits, J. F., and Zaman, G. J. (2010). beta-Galactosidase enzyme fragment complementation for the measurement of Wnt/beta-catenin signaling. *FASEB J* **24**(4)**,** 1205-17.

ViroPharma, I. (2009a). ViroPharma Announces Discontinuation of Maribavir Phase 3 Study in Liver Transplant Patients. *In* "Company press realease". ViroPharma Inc., Exton, PA.

ViroPharma, I. (2009b). ViroPharma Reports Results of Phase 3 Clinical Trial for Maribavir in Bone Marrow Transplant Patients. *In* "Company Press release". ViroPharma, Inc., Exton, PA.

Vizoso Pinto, M. G., Pothineni, V. R., Haase, R., Woidy, M., Lotz-Havla, A. S., Gersting, S. W., Muntau, A. C., Haas, J., Sommer, M., Arvin, A. M., and Baiker, A. (2011). Varicella zoster virus ORF25 gene product: an essential hub protein linking encapsidation proteins and the nuclear egress complex. *J Proteome Res* **10**(12)**,** 5374-82.

Wehrman, T., Kleaveland, B., Her, J. H., Balint, R. F., and Blau, H. M. (2002). Protein-protein interactions monitored in mammalian cells via complementation of beta -lactamase enzyme fragments. *Proc Natl Acad Sci U S A* **99**(6)**,** 3469-74.

Wills, E., Mou, F., and Baines, J. D. (2009). The U(L)31 and U(L)34 gene products of herpes simplex virus 1 are required for optimal localization of viral glycoproteins D and M to the inner nuclear membranes of infected cells. *J Virol* **83**(10)**,** 4800-9.

Wood, L. J., Baxter, M. K., Plafker, S. M., and Gibson, W. (1997). Human cytomegalovirus capsid assembly protein precursor (pUL80.5) interacts with itself and with the major capsid protein (pUL86) through two different domains. *J Virol* **71**(1)**,** 179-90.

Yamauchi, Y., Shiba, C., Goshima, F., Nawa, A., Murata, T., and Nishiyama, Y. (2001). Herpes simplex virus type 2 UL34 protein requires UL31 protein for its relocation to the internal nuclear membrane in transfected cells. *J Gen Virol* **82**(Pt 6)**,** 1423-8.

Yang, H., Xie, W., Xue, X., Yang, K., Ma, J., Liang, W., Zhao, Q., Zhou, Z., Pei, D., Ziebuhr, J., Hilgenfeld, R., Yuen, K. Y., Wong, L., Gao, G., Chen, S., Chen, Z., Ma, D., Bartlam, M., and Rao, Z. (2005). Design of wide-spectrum inhibitors targeting coronavirus main proteases. *PLoS Biol* **3**(10)**,** e324.

Yeh, P. C., Meckes, D. G., Jr., and Wills, J. W. (2008). Analysis of the interaction between the UL11 and UL16 tegument proteins of herpes simplex virus. *J Virol* **82**(21)**,** 10693-700.

Yu, D., Silva, M. C., and Shenk, T. (2003). Functional map of human cytomegalovirus AD169 defined by global mutational analysis. *Proc Natl Acad Sci U S A* **100**(21)**,** 12396-401.

Yu, X., Trang, P., Shah, S., Atanasov, I., Kim, Y. H., Bai, Y., Zhou, Z. H., and Liu, F. (2005). Dissecting human cytomegalovirus gene function and capsid maturation by ribozyme targeting and electron cryomicroscopy. *Proc Natl Acad Sci U S A* **102**(20)**,** 7103-8.

Zarate, X., Henderson, D. C., Phillips, K. C., Lake, A. D., and Galbraith, D. W. (2010). Development of high-yield autofluorescent protein microarrays using hybrid cell-free expression with combined Escherichia coli S30 and wheat germ extracts. *Proteome Sci* **8,** 32.

Zhao, L., and Chmielewski, J. (2005). Inhibiting protein-protein interactions using designed molecules. *Curr Opin Struct Biol* **15**(1)**,** 31-4.

Zlokarnik, G., Negulescu, P. A., Knapp, T. E., Mere, L., Burres, N., Feng, L., Whitney, M., Roemer, K., and Tsien, R. Y. (1998). Quantitation of transcription and clonal selection of single living cells with beta-lactamase as reporter. *Science* **279**(5347)**,** 84-8.

7. Appendix

7.1 List of Figures

7.2 List of Tables

7.3 Abbreviations

aa	amino acid
AIDS	acquired immunodeficiency syndrome
APS	ammonium persulfate
BAC	bacterial artificial chromosome
BiFC	bimolecular fluorescence complementation
Bla	TEM-1 β-lactamase
bp	base-pair
BSA	bovine serum albumin
dpi	days post infection
DMEM	Dulbecco's modified eagle's medium
DMSO	dimethylsulfoxid
dNTP	desoxyribonuleotide
E	early
e	elutions
EM	electron microscopy
FCS	fetal calf serum
FOM	fomivirsen
GCV	ganciclovir
HA	hemagglutinin
HCMV	human cytomegalovirus
HFF	human foreskin fibroblasts
HRP	horseradish peroxidase
HSV	herpes simplex virus
HTS	high-throughput screening
IC	inhibitory concentration
IE	immediate-early
IF	immunofluorescence
IPTG	isopropyl-ß-D-thiogalactopyranosid
iPCA	*in vitro* NEC-PCA
kbp	kilo base-pair
kDa	kilo daltons

L	late
luc	luciferase
MCMV	murine cytomegalovirus
MEF	mouse embryonic fibroblasts
MOI	multiplicity of infection
MW	molecular weight
NEC	nuclear egress complex
ORF	open reading frame
PAA	phosphonoacetic acid
PAGE	polyacrylamide gel electrophoresis
PBS	phosphate buffered saline
PCA	protein fragment complementation assay
PCR	polymerase chain reaction
pfu	plaque-forming unit
qPCR	quantitative real-time PCR
RT	room temperature
SARS	severe acute respiratory syndrome
SDS	sodium dodecyl sulfate
SEC	secondary envelopment complex
TBS-T	TRIS-buffered saline withTween-20
TD-PCR	Touchdown PCR
TEMED	N,N,N′,N′-Tetramethylethan-1,2-diamin
w/v	weight per volume
Y2H	yeast two-hybrid

8. Danksagung

Zuerst möchte ich mich bei Herrn Prof. Koszinowski bedanken, der mir ermöglichte, meine Doktorarbeit in seinen Laboren durchzuführen, und bei Herrn Prof. Hopfner für die Übernahme der Aufgabe des Fachvertreters. Des Weiteren möchte ich mich bei Dr. Zsolt Ruzsics bedanken, der mit viel Leidenschaft und Glaube das Projekt immer wieder vorantrieb und bei Dr. Margit Schnee, die alles auf den Weg brachte und mir mit vielen Tipps und gut geführten Protokollen den Einstieg in das Projekt erleichterte.

Prof. Wiesmüller und Dr. Holger Eickhoff von EMC microcollections danke ich für die Zusammenarbeit und die Bereitstellung der Molekül-Library.

Bei Prof. Paul Walther und Dr. Martin Schauflinger möchte ich mich für die gute Kooperation bei der Erstellung der Elektronenmikroskopie-Aufnahmen bedanken.

Ausserdem möchte ich mich bei allen Virologen im Genzentrum bedanken, im Besonderen bei Madlen Pogoda für die Unterstützung bei der Erstellung der Immunfluoreszenzen, Dr. Lisa Marcinowski für die Zusammenarbeit bei der Real-time PCR, Dr Zsolt Ruzsics, Dr. Laura Scrivano und Dr. Stefan Jordan für das Korrekturlesen meiner Arbeit, Dr. Barbara Adler, dass sie mich an einem erfolgreichen Nebenprojekt teilhaben ließ und meiner gesamten Arbeitsgruppe für die gute Arbeitsatmosphäre.

Last but not least danke ich meinen Eltern für ihre immerwährende Unterstützung.